LAMINAR HEAT TRANSFER WITH VISCOUS DISSIPATION AND FLUID AXIAL HEAT CONDUCTION IN ANNULAR DUCTS

January, 2005

Graduate School of Science and Technology
Nagasaki University

Odgerel Jambal

Contents

ABSTRACT

The present thesis presents accurate numerical solutions obtained by finite difference method for steady laminar heat transfer to annular flows. This work was carried out as a first step toward numerical solutions of extended Graetz problem with the viscous dissipation and fluid axial heat conduction for annular ducts. Thermal processing in annular ducts can regularly be found in heat exchangers, manufacturing process of extrusion and drawing, drilling operations and etc. There is a need for detailed and systematic research regarding heat transfer and fluid flow characteristics of these types of exchangers. In this respect, an extensive literature search is presented for laminar heat transfer to annular flows.

Consideration is given to steady, hydrodynamically developed but thermally developing laminar flows of Newtonian and non-Newtonian fluids in annular ducts. In this study, two configurations of annular ducts, namely, a duct consisting of stationary concentric tubes and, a duct consisting of a stationary outer tube and an axially moving core tube are applied. The fundamental question under investigation in this study was to include the viscous dissipation and the fluid axial heat conduction in the analysis. When the fluid axial heat conduction and the viscous dissipation are taken into account, the energy equation is elliptic and non-homogeneous in nature. The analysis was performed under the three different thermal boundary conditions. The annular duct is subjected to a step-change in wall temperature or in wall heat flux in order to include the fluid axial heat conduction in both the upstream and downstream directions.

The main purpose of this work was to obtain results that may serve as a reliable reference to check the techniques developed for the treatment of more complicated problems associated laminar heat transfer in annular ducts. By assuming constant thermophysical properties and negligible body forces, the momentum equation and the energy equation are uncoupled. First the flow field is solved independently from the temperature field. Then by applying the flow information, the heat transfer problem is solved. The governing partial differential equations are transformed in terms of several dimensionless quantities and controlling parameters of the problem are identified. The transformed equations are then solved by the finite difference method. Numerical analysis has been conducted for radius ratio range of 0.2, 0.5 and 0.8.

In addition to presenting accurate flow and heat transfer results, the effects of rheological parameters, Brinkman number, Peclet number, radius ratio and mov-

ing core velocity on heat transfer are clarified. For validation purposes, numerical results were obtained for the cases of negligible viscous dissipation and fluid axial heat conduction and, for the radius ratio of 0 and 1 showing excellent agreement with those of available in literature. The heat transfer results are interpreted in the context of the thermally developing flow where the viscous dissipation and the fluid axial heat conduction are present. In order to bring out the effects of the viscous dissipation, the fluid axial heat conduction, the rheological parameters, the moving core velocity and the geometry, the values of temperature distributions and the Nusselt numbers at the tube walls are plotted. The radial temperature distributions are given and explanations of the solutions are provided. The Nusselt number solutions are presented as functions of non-dimensional axial distance and the significance of each curve is also discussed.

Chapter 1

Introduction

1.1 Research Objective and Scope

There is a wide range of heat transfer problems related to thermal processing of materials and manufacturing. Research in thermal processing is largely directed at the basic processes, underlying mechanisms, physical understanding of the effects of different transport mechanisms, physical parameters on general behavior and characteristics, and the thermal process undergone by the material. It is usually a long-term effort which leads to a better quantitative understanding of the process under consideration. However, it can also provide input for design and development [1].

The present research is devoted to a basic problem of heat transfer to laminar flows in annular ducts. The author is specially interested in the effects of the viscous dissipation and the fluid axial heat conduction. The overall focus of this theoretical study is to better understand heat transfer and obtain quantitative information on laminar heat transfer in annular ducts. The objectives of the present study are two-fold.

Objective 1 To obtain results that would be useful in the development and validation of models for fluid flow and heat transfer in annular ducts consisting of stationary tubes.

Objective 2 To obtain results that would be useful in the development and validation of models for fluid flow and heat transfer in an annular duct with an axially moving core.

Heat transfer to duct flows has been an active area of research for number of decades due to the many practical situations in which it is encountered. The first

studies of heat transfer to a duct flow were made by Graetz in 1883-1885 and independently by Nusselt in 1910. Solutions to this problem, which is well known as Graetz problem, and its various extensions continue to evoke many research efforts. A comprehensive review of the work on heat transfer in laminar duct flow was compiled by Shah and London [2] in 1978 and by Kakac et al. [3] in 1987. As a part of the present research a detailed survey of the recent relevant literature has been carried out. The survey reveals that the Graetz problem has not been investigated completely. Complete understanding of heat transfer necessitates solving the problem without making a simplifying assumption that viscous dissipation and/or fluid axial heat conduction may be neglected. To the author's knowledge, there is no existing solution for thermally developing flow in annular flow including the viscous dissipation and the fluid axial heat conduction. Therefore the emphasis in this study is on investigating the thermally developing flow in annular ducts by considering the effects of viscous dissipation and axial heat conduction within the fluid. The fluids can exhibit Newtonian as well as non-Newtonian behaviors depending upon the particular application.

The motivation of the present research is to better understand the flow and heat transfer characteristics in annular ducts. A large number of thermal systems used extensively in industrial applications, thermal energy storage systems, cooling of electronic components and transmission cables are described geometrically by an annulus. An annulus is geometrically a region bounded both internally and externally by cylindrical surfaces. Complete geometrical specification of the annulus requires not only the size of the cylinders but the radius ratio, R^*, which is a ratio of the inner core tube radius, R_i, to the outer tube radius, R_o, and some knowledge of the orientation of the axes of the cylinders. The present study is devoted to

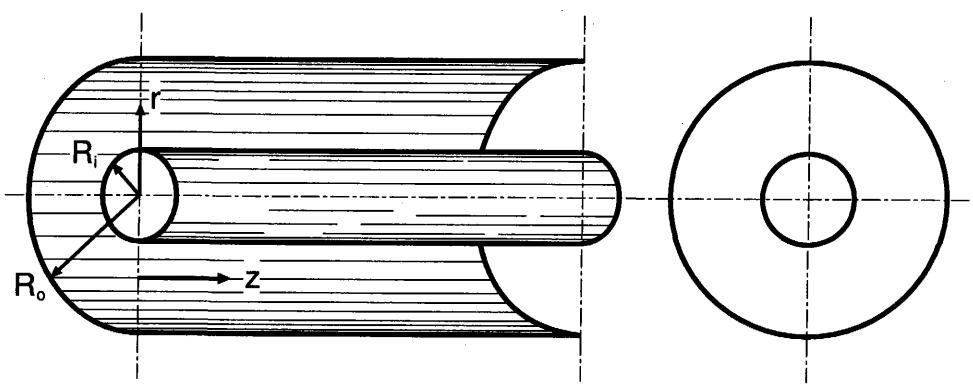

Fig. 1.1: Schematic of a concentric annular duct

concentric annular ducts, in which the axes are coincident. Annular ducts can represent a wide range of geometers including cylindrical ducts (R^*=0) and parallel-plates ducts (R^*=1). Therefore the solution of a problem of heat transfer to annular flows can provide insight into the general problem of laminar heat transfer. In Fig. 1.1, the schematic of a concentric annular duct is shown.

As a main contribution of this investigation, the viscous dissipation and the fluid axial heat conduction are included in the study. The calculation results of the present study demonstrate excellent agreement with those of previous researchers who considered the special cases where the viscous dissipation and/or the fluid axial heat conduction is neglected.

1.2 Previous Works on Heat Transfer in Annular Ducts

The literature on laminar heat transfer in annular duct is very extensive; but it appears that theoretical solution considering the viscous dissipation and the fluid axial heat conduction for thermally developing flow in an annular duct is not available. Similarly, the laminar heat transfer in an annular duct with an axially moving core has been studied so far mainly by neglecting the viscous dissipation and the fluid axial heat conduction. Notably, one finds that the heat transfer in an annular duct with a moving core has not been studied for non-Newtonian fluids. The purpose of this section is to carry out a literature survey for heat transfer in annular ducts.

The present investigation is concerned with the heat transfer of steady laminar flow in smooth concentric annular duct. Accordingly, the papers reviewed here will be restricted to the studies on this particular subject. The literature on heat transfer in annular ducts is vast, particularly for annular ducts with rotating cylinders, turbulent flows and those considered free or mixed convection. Since rotation, turbulence, free convection are beyond the scope of the present work, a review of literature pertaining thereto is unwarranted.

1.2.1 Stationary annular ducts

The literature concerning heat transfer in stationary annular ducts will now be reviewed. The studies of the laminar heat transfer in annular ducts may be divided

into 5 parts, (1) thermally developing but hydrodynamically developed flow of (1.a) Newtonian fluids and (1.b) non-Newtonian fluids, (2) the fluid axial heat conduction included study, (3) the viscous dissipation included study, (4) fully developed flow and (5) simultaneously developing flow.

(1) The heat transfer for thermally developing flow in a concentric annular duct has been investigated extensively in Refs.[4] - [12]. (1.a) Most authors [4] - [9] dealt with laminar forced convection for Newtonian fluids. Hatton and Quarmby [4] reported solutions for the second and third kinds of thermal boundary conditions. Lundberg, et al. [5] - [6] and Worsøe-Schmidt [7] presented solutions for heat transfer in annular ducts for four kinds of thermal boundary conditions. Lee and Kuo [8] presented analytical solutions by using the Galerkin method for an annular duct with specified wall temperature. Buyruk, et al. [9] considered the heat transfer in annular ducts with peripherally varying and axially constant heat flux at the walls. (1.b) Thermally developing flows of non-Newtonian fluids in annular ducts have been investigated in Refs.[10] - [12]. By applying the power-law model to describe the rheological behavior of fluid, Hong and Matthews [10] presented the results for three kinds of thermal boundary conditions. Nascimento, et al. [11] analyzed the heat transfer of Bingham plastics in concentric annular ducts for four types of thermal boundary conditions using a finite transforming technique. Soares, et al. [12] studied the heat transfer to Herschel-Bulkley materials in laminar axial flow through concentric annular ducts and presented an extensive literature survey of recent studies. They applied a finite volume method for the second and third kinds of thermal boundary conditions.

(2) The effect of fluid axial heat conduction on heat transfer of thermally developing flow of Newtonian fluids in annular ducts has been investigated in Refs.[13] - [16]. Hsu [13] investigated the problem analytically for the second kind of thermal boundary condition. He applied two semi-infinite domains bounded by an insulated cylinder and a cylinder with a step change in wall heat flux. Weigand, et al. [14] investigated the fluid axial heat conduction effect on both the laminar and turbulent heat transfer by considering two semi-infinite domains for the third kind of thermal boundary condition and for the condition of cylinder walls maintained at constant temperature. Telles, et al. [15] have proposed a general method to solve the extended Graetz problem depending upon the determination of the asymptotic solution and applied it to solve the steady state heat transfer problem for the thermal entrance regions of parallel-plates, cylindrical and annular ducts. The thermal

boundary conditions were allowed to vary along the axial coordinate. Weigand and Wrona [16] have presented analytical solutions for the heat transfer to laminar and turbulent flows in annular ducts with piecewise constant wall heat flux.

(3) The effect of viscous dissipation in annular flows has been studied in Refs.[17] - [19]. Cox and Macosko [17] have calculated and measured the temperature field of the flow of polymer melts in cylindrical, annular, and slit dies. They noted that the heat due to viscous dissipation results in significant temperature rises in the nozzles of injection molding machines and in the extrusion of polymeric materials. They included the temperature dependency of viscosity in their numerical solution. Winter has considered the temperature fields and the viscous dissipation in polymer flows in Refs.[18] - [19]. In Ref.[19], Winter presented a detailed analysis of the temperature fields caused by viscous heating.

(4) Fully developed steady laminar flow in concentric annular ducts has been investigated for non-Newtonian fluids by Capobianchi and Irvine [20]. They provided numerical solutions of the velocity and temperature fields of non-Newtonian fluids by applying a modified power-law model for the second kind of thermal boundary condition.

(5) Simultaneously developing steady laminar flow of Newtonian fluids in concentric annular ducts has been investigated in Refs.[21] - [22]. Heaton, et al. [21] studied the heat transfer problem for the second kind of thermal boundary condition. Fuller and Samuels [22] numerically investigated the simultaneously developing flow in an annular duct of constant wall temperature by considering the axial heat conduction effect within the fluid.

Extensive literature surveys on the problem of laminar forced convection in concentric and eccentric annular ducts are presented by Manglik and Fang [23]. Also, Shah and London [2] and Kakac, et al. [3] have summarized the laminar convective heat transfer results reported in literature.

1.2.2 Annular duct consisting of moving cylinders

The literature concerning the heat transfer in annular ducts consisting of moving cylinders will be reviewed in this section. Here the literature on heat transfer associated with axially moving cylinders are discussed, while the others associated with rotating cylinders are not included.

The fluid flow and heat transfer in an annular duct with an axially moving core have been studied by neglecting the viscous dissipation and the fluid axial heat

conduction in Refs.[24] - [28]. In these previous studies the Newtonian fluid was under consideration.

In Refs.[24] - [25], the problem of fully developed turbulent flow and heat transfer in a concentric annular duct with a moving core was treated. The velocity profiles and the temperature distributions in annular ducts were predicted for various values of the core velocity for the conditions of (a) a constant heat flux at the core tube wall with the outer tube wall insulated, (b) the outer tube wall heated with the core tube insulated and (c) both of the tube walls heated. The studies have showed that for the equal conditions, increasing the relative velocity of the core causes a decrease in friction factor and an increase in Nusselt number. Also the effect of relative velocity was shown to be diminishing with a decreasing value of the radius ratio. This diminishing effect in the relative velocity was more pronounced for the case of the outer tube heated with the core tube insulated.

In Ref.[26], an analytical investigation of fully developed laminar fluid flow and heat transfer in a concentric annular duct with a moving core has been carried out for the cases of (a) the core tube wall heated with the outer tube wall insulated and (b) the outer tube wall heated with the core tube wall insulated. The assumptions made in this reference were that the tube walls are smooth surfaces, the flow is incompressible and the viscous dissipation and the fluid axial heat conduction are negligible. It was shown that increasing of the relative velocity results in (1) a decrease in friction factor, (2) an increase in Nusselt number for the core tube wall heated case and (3) a decrease in Nusselt number for the outer tube wall heated case.

Thermally developing laminar flow in an annular duct with a moving heated core was analytically studied in Ref.[27] for four kinds of the thermal boundary conditions. The assumptions applied in this reference were the steady and hydrodynamically fully developed flow, constant physical properties and negligible effects of viscous dissipation and fluid axial heat conduction. It was observed that for the equal conditions, increasing relative velocity results in (1) an increase in Nusselt number at the inner core; but a decrease in Nusselt number at the outer tube for all considered thermal boundary conditions and (2) an increase in the value of the thermal entrance length with a maximum at a given relative velocity of the core, $U^* > 0$. The maximum value of the thermal entrance length increases with increasing value of U^* but with smaller values of radius ratio, R^*.

In Ref.[28], fully developed laminar forced convection in an eccentric annular

duct with a moving core has been analyzed under the assumptions of negligible viscous dissipation and fluid axial heat conduction.

The heat transfer in plane Poiseuille-Couette flow, which is a particular case of the annular flow, has been studied recently for non-Newtonian fluids [29] and in this reference a more citation of the published literature on heat transfer for duct flows associated with a moving surface can be found.

Heat transfer to non-Newtonian Couette flow in an annular duct with a moving core was studied by Lin and Hsieh [30] and with a moving outer cylinder by Lin [31]. In their study the fluid was described by the power-law model and the viscous dissipation term was included in the energy equation. They considered a cooling process subject to the boundary conditions of constant wall temperature and the fluid axial heat conduction was neglected.

Jaluria and Choudhury [32] have studied numerically and experimentally the heat transfer associated with the forced convective cooling of a heated cylinder moving axially in a channel. They pointed out that this problem is of interest in several manufacturing processes such as glass fiber drawing, cable coating, extrusion of cylinders and wire drawing. In most of these manufacturing processes, the materials move in a channel of quiescent fluid while in a few of them the forced convection is employed to increase the heat transfer. Aiding and opposing flows were considered for the cases of the channel wall kept at a constant temperature that was (1) lower than the ambient fluid temperature, (2) equal to the ambient fluid temperature, (3) higher than the ambient temperature and, (4) the wall is insulated. The fluids considered were air and water and the rod was made of aluminum or teflon.

Choudhury, et al. [33] have carried out numerical and experimental studies on conjugate problem of a continuesly moving optical fiber in forced flow in a channel. Three different flow configurations namely, (1) aiding (2) opposing and (3) peripheral flows have been considered. It was noted that the solid property variation was found to be insignificant while fluid property variations were quite substantial. The fluids used were pure helium or 50 % (by mass) helium-nitrogen mixture.

Vaskopulos, et al. [34] have numerically and experimentally studied the convective flows in annular ducts with the inner core moving at a constant velocity for conditions applied to the cooling of optical fiber during a drawing process. They pointed out that the natural convection cooling is not adequate for fiber cooling. The results in this reference are appropriate to the cooling of optical fibers by mixed convection.

1.3 Previous Works Considered Both the Viscous Dissipation and the Fluid Axial Heat Conduction

In the present study, the viscous dissipation and the fluid axial heat conduction are included in the problem formulation. When the restrictions of negligible viscous dissipation or fluid axial heat conduction are relaxed, it is known as an extended Graetz problem. It appears that the situations studied in the present research has not been investigated before.

The studies concerning laminar heat transfer with viscous dissipation and fluid axial heat conduction in ducts under uniform wall temperature condition will now be reviewed. The determination of heat transfer rates in the thermal entrance region of ducts has been the subject of numerous investigations and a detailed survey of the abundant relevant literature on the extended Graetz problems can be found in Refs.[2] - [3]. Laminar heat transfer under the effects of both viscous dissipation and fluid axial heat conduction has received rather sparse attention for non-Newtonian fluids inside ducts with uniform wall temperature.

To the author's knowledge, Refs.[35] - [42] had included both the viscous dissipation and the fluid axial heat conduction and these studies are for laminar heat transfer in ducts subjected to uniform wall temperature or (T) thermal boundary condition. In these references, the solutions for temperature distribution have been presented in the form of a finite series and the following two cases were considered.

- Case A: semi-infinite region of $0 \leq z$ with a uniform inlet temperature at $z = 0$, and
- Case B: infinite region of $-\infty \leq z \leq \infty$ with a uniform inlet temperature at $z \rightarrow -\infty$ and a step jump in the wall temperature at $z = 0$.

Singh [35] constructed solutions for Newtonian fluids in a cylindrical duct for Case A. He also included prescribed internal thermal energy generation. However in Ref.[35], the fluid bulk temperature and Nusselt numbers for low Peclet numbers were not presented. Deavours [36] presented an analytical solution for Newtonian flows in a parallel plates duct by decomposing the eigenvalue problem into a system of ordinary differential equations for Case B. Wei and Zhang [37] showed that under fully developed conditions, the solutions obtained for an elliptic energy equation

(with the fluid axial heat conduction term) and for a parabolic one (without the fluid axial heat conduction term) are identical for the boundary condition of uniform wall temperature. Dang [38] developed solutions for power-law fluids in parallel-plates and circular ducts for Case B. Dang included the viscous dissipation effect in the region for $0 < z$, but neglected it for $z \leq 0$. The studies in Ref.[35] - [38] are most relevant to the present study as they consider Newtonian and power-law fluids. However, their mathematical models and solution methods are different from the present work. LeCroy and Eraslan [39] and Lahjomri, et al. [40] treated a thermally developing laminar Hartman flow and Min, et al. [41] and Nield, et al. [42] concerned thermally developing flow of Bingham plastic and porous medium, respectively. From the axial development of Nu reported by Nield, et al. [42], it is seen there is a single fixed point independent of Br in the thermally developing region. Also it can be observed that the value of the Nusselt number corresponding to this fixed point is equal to the Nusselt number value at the fully developed region in the case of non-zero Br.

1.4 Summary of this Thesis

Chapter 1 shows that there is an urgent need for detailed and systematic research regarding the heat transfer and fluid flow characteristics of annular heat exchangers. In this respect, literature search is presented on heat transfer. This chapter specifies the objectives of the present research. The papers reviewed in this chapter are restricted to those particularly relevant to the present study. From the literature surveyed it appears that there have been no reports of studies addressing to the effects of viscous dissipation and fluid axial heat conduction on laminar heat transfer in annular ducts.

Chapter 2 presents the heat transfer characteristics for laminar flow of Newtonian and non-Newtonian fluids in a stationary annular duct where the flow is hydrodynamically fully developed but thermally developing. The viscous dissipation and the fluid axial heat conduction have been included in the formulation. The uncoupled partial differential equations governing the momentum conservation and the energy conservation are solved. First, the velocity fields of the laminar flow are obtained analytically and numerically. Furthermore, the heat transfer study is reported by analyzing the viscous dissipation and the fluid axial heat conduction effects. The study has been accomplished for annular ducts with a step change in the wall temperature or in the wall heat flux. The step change location is designated as the

axial location of $z = 0$ in this study. Three types of thermal boundary conditions have been considered: (1) the downstream part of $z = 0$ or the tube walls at $z > 0$ are kept at an equal and uniform temperature both axially and peripherally (the Ⓣ thermal boundary condition) while the upstream part of $z = 0$ or for $z \leq 0$, the tube walls are kept at the entering fluid temperature, (2) unequal but uniform temperatures at the tube walls for $z > 0$ (the 1st kind of thermal boundary condition) while for $z \leq 0$ the wall temperature at the tube walls are kept at the entering fluid temperature, and (3) for $z > 0$ the outer tube wall insulated with the core tube heated uniformly (the 2nd kind of thermal boundary condition) while for $z \leq 0$ the tube walls are insulated.

The incorporation of the effect of viscous dissipation changes a homogeneous differential equation into a non-homogeneous one. Plus the energy equation including the fluid axial heat conduction term is mathematically an elliptic type equation. Therefore, the study is directed to solve a non-homogeneous, elliptic type differential equation. A special treatment of the infinite region and the boundary condition at the very large axial distance was applied in order to solve the governing equation. The finite difference technique was used to solve the problem in a transformed axial coordinate system. The author made every effort to validate the applied finite difference scheme by calculating special cases which have solutions available in open literature. For all cases compared, a satisfactory agreement is obtained. The present method was able to accurately obtain the results for very small values of the axial location.

The effects of the viscous dissipation characterized by the Brinkman number, the fluid axial heat conduction characterized by the Peclet number, and the shear thinning given by the power-law model, are examined via the friction factor, the Nusselt number, and the fluid temperature for duct of radius ratio ranging from 0 to 1.

The results indicate that when the viscous dissipation is present, the Nusselt number at the core wall decreases for the 1st and 2nd kinds of thermal boundary conditions. Also the study reveals that the consideration of the viscous dissipation for the Ⓣ thermal boundary condition leads a same value for the asymptotic Nusselt number in the fully developed region. An interesting pattern of Nusselt number curves creating a fixed point is observed in the thermal entrance region for the Ⓣ thermal boundary condition. The fixed point location on the Nusselt number curves was checked analytically for a cylindrical duct. This chapter demonstrates

that the occurrence of the fixed points for the (T) thermal boundary condition is entirely a consequence of taking into account the upstream flow in the region $z \leq 0$. The asymptotic Nusselt numbers at the fully developed condition decrease as the flow index increases. In the fully developed region, the results indicate that the Nusselt number at the inner core wall is greater for small radius ratios and that the Nusselt number at the outer cylinder wall is greater for large radius ratios. Comparison of the results with the available data has been done. The shape of the annular plays a significant part in the heat transfer for both thermally developing flows and fully developed flows.

Chapter 3 is devoted to the heat transfer in an annular duct with an axially moving core, which can be commonly seen in continuous casting, extrusion, drawing and wire tube coating etc. For an annular duct with an axially moving core, steady laminar heat transfer of a thermally developing flow has been analyzed numerically by considering the viscous dissipation and the fluid axial heat conduction.

Two types of thermal boundary conditions have been considered: (1) unequal but uniform temperatures at the tube walls for $z > 0$ (the 1st kind of thermal boundary condition) while for $z \leq 0$ the wall temperature at the tube walls is kept at the entering fluid temperature, and (2) for $z > 0$ the outer tube wall is insulated with the core tube heated uniformly (the 2nd kind of thermal boundary condition) while for $z \leq 0$ the tube walls are insulated.

The uncoupled partial differential equations governing the conservation of momentum and energy are solved. First, the velocity fields were obtained. The axial velocity of the core significantly affects the flow characteristics and in turn affects the heat transfer. Therefore, it was important to clarify the effects of the moving core velocity on heat transfer by using an accurate velocity distribution. In this chapter, the fully developed laminar velocity field was obtained by applying the modified power-law model. Then the effects of viscous dissipation and fluid axial heat conduction on the heat transfer for thermally developing flow of non-Newtonian fluids flowing in an annular duct with an axially moving core are investigated. Numerical analysis has been conducted in the following range of parameters: the relative velocity of the core -1, 0 and 1, and radius ratio 0.2, 0.5 and 0.8. The effects of the moving core velocity, flow index of the modified power-law fluid, Brinkman number and Peclet number on the temperature distribution and Nusselt number at the tube walls are discussed.

In Chapter 4, the results obtained in the previous chapters are summarized.

Chapter 2

Stationary Annular Ducts

The present chapter achieves Objective 1 of the present research. This chapter presents the methodology used to reach Objective 1 and it provides the solutions for flow and heat transfer of Newtonian and non-Newtonian fluids. This chapter is organized as follows. In Sections 2.1.1 - 2.1.2, the assumptions, conditions and the boundary conditions are described. In Sections 2.2.1 - 2.2.2, the basic equations and the solutions for the velocity field are presented for Newtonian and non-Newtonian fluids, respectively. In Sections 2.3.1 - 2.4.4, the energy equation and the method of solution are given. In Sections 2.5 - 2.5.2, the laminar heat transfer is considered for the limiting cases of annular geometry or for the parallel-plates and cylindrical ducts. The results for various values of the relevant parameters are presented and discussed in Sections 2.6 - 2.8.5 for the (T) thermal boundary condition, in Sections 2.9 - 2.11.4 for the 1st kind of thermal boundary condition and in Sections 2.12 - 2.14.4 for the 2nd kind of thermal boundary condition. The results are summarized in Section 2.15.

2.1 Problem Formulation

2.1.1 Assumptions and conditions

In formulating the problem mathematically, the following simplifying assumptions and conditions are used in the analysis:

1. The flow under consideration is

   - unidirectional and laminar,
   - hydrodynamically fully developed but thermally developing and

- steady (this requires that both the velocity and the temperature of the flow remain constant in time).

2. The fluid behaviors of non-Newtonian fluids follow the power-law model.
3. No-slip and no-penetration on the tube surfaces or walls.
4. The viscous dissipation is included.
5. The fluid axial heat conduction is included.
6. The thermophysical properties such as thermal conductivity, density, specific heat are constant. In addition, there is no change upon heating or cooling.
7. The body forces are neglected.

As the last assumption suggests, the secondary flow due to buoyancy forces is negligible in this study. Therefore the momentum equation and the energy equation are uncoupled and, the problems of fluid flow and heat transfer can be solved independently [43].

In this study the procedure will be as follows. First, interest lies in obtaining detailed results on velocity fields in annular ducts. Then by applying the velocity information, the results of the temperature fields in the ducts are obtained.

2.1.2 Applied thermal boundary conditions

The thermal boundary conditions, which applied in the study, are described in this section. Reference [2] can be consulted regarding the thermal boundary conditions and in this research three kinds of thermal boundary conditions have been treated.

Figure 2.1 shows, the physical model and the coordinate system for the analysis. The flowing fluid is contained between two infinite circular tubes. This is a two dimensional problem and the cylindrical coordinates are used. The upstream region for $z \leq 0$ is required in order to examine heat transfer by fluid axial heat conduction and of particular importance in including this region is to ensure that the fluid axial heat conduction from downstream to upstream regions would occur [44] - [45]. Further, if viscous dissipation is considered in such analyses, its effect should be also taken into account for $z \leq 0$. Thus, inclusion of the upstream region of $z \leq 0$ in the analysis is needed to exactly account for the preheating of incoming fluid due to viscous dissipation and fluid axial heat conduction.

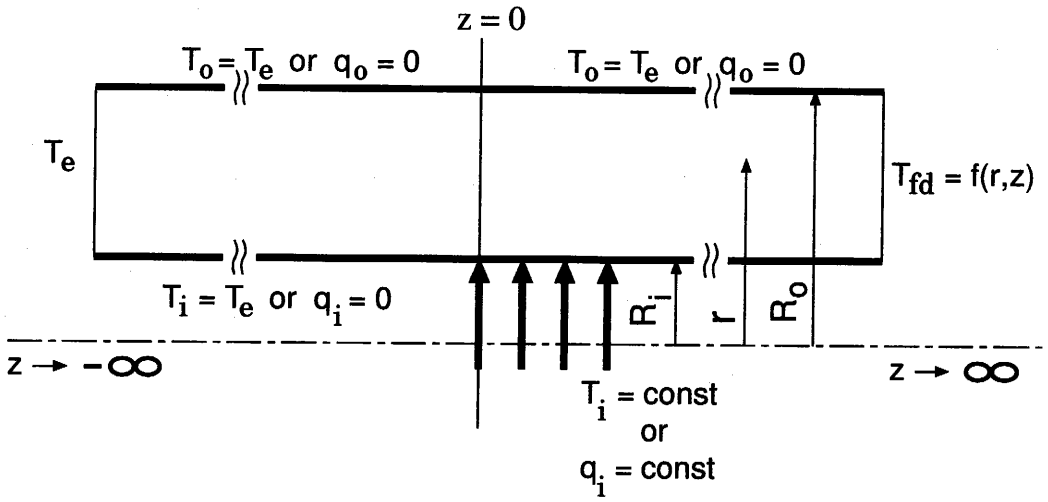

Fig. 2.1: Schematic of the thermal boundary conditions for an annular duct

The energy equation including the fluid axial heat conduction term is an elliptic type partial equation. Elliptic problems require information on all boundaries [22], [46] - [47]. The energy equation, which will be described in Section 2.3.1, is to be solved with the following thermal boundary conditions.

(1) The (T) thermal boundary condition:

$$\begin{cases} T = T_{\mathrm{w}} \quad \text{at} \quad r = R_{\mathrm{i}} \quad \text{for} \quad 0 < z \\ T = T_{\mathrm{w}} \quad \text{at} \quad r = R_{\mathrm{o}} \quad \text{for} \quad 0 < z \\ T = T_{\mathrm{e}} \quad \text{at} \quad r = R_{\mathrm{i}} \quad \text{for} \quad z \leq 0 \\ T = T_{\mathrm{e}} \quad \text{at} \quad r = R_{\mathrm{o}} \quad \text{for} \quad z \leq 0 \\ \lim\limits_{z \to -\infty} \quad T = T_{\mathrm{e}} \quad \text{for} \quad R_{\mathrm{i}} < r < R_{\mathrm{o}} \\ \lim\limits_{z \to \infty} \quad T = T_{\mathrm{fd}}(r, z) \quad \text{for} \quad R_{\mathrm{i}} < r < R_{\mathrm{o}}. \end{cases} \tag{2.1}$$

The boundary conditions in Eq.(2.1) state that the duct walls at the upstream region of $z \leq 0$ are kept at a constant temperature which is equal to the entering fluid temperature, T_{e}. For the downstream of $0 < z$, the walls are at a constant temperature, T_{w}, which may be greater or smaller than the entering fluid temperature, T_{e}.

(2) The 1st kind of thermal boundary condition:

$$\begin{cases} T = T_i & \text{at} \quad r = R_i & 0 < z \\ T = T_e & \text{at} \quad r = R_o & 0 < z \\ T = T_e & \text{at} \quad r = R_i & z \leq 0 \\ T = T_e & \text{at} \quad r = R_o & z \leq 0 \\ \lim\limits_{z \to -\infty} & T = T_e \quad \text{for} \quad R_i < r < R_o & \\ \lim\limits_{z \to \infty} & T = T_{fd}(r, z) \quad \text{for} \quad R_i < r < R_o. & \end{cases} \tag{2.2}$$

The boundary conditions in Eq.(2.2) state that the core and outer cylinder walls are maintained at different temperatures for $0 < z$. But for $z \leq 0$, the walls are kept at the entering fluid temperature.

(3) The 2nd kind of thermal boundary condition:

$$\begin{cases} -k\dfrac{\partial T}{\partial r} = q_i & \text{at} \quad r = R_i & 0 < z \\ k\dfrac{\partial T}{\partial r} = 0 & \text{at} \quad r = R_o & 0 < z \\ k\dfrac{\partial T}{\partial r} = 0 & \text{at} \quad r = R_i & z \leq 0 \\ k\dfrac{\partial T}{\partial r} = 0 & \text{at} \quad r = R_o & z \leq 0 \\ \lim\limits_{z \to -\infty} & T = T_e \quad \text{for} \quad R_i < r < R_o & \\ \lim\limits_{z \to \infty} & T = T_{fd}(r, z) \quad \text{for} \quad R_i < r < R_o. & \end{cases} \tag{2.3}$$

The boundary conditions in Eq.(2.3) state that constant heat flux at the core wall with the outer cylinder wall insulated for $0 < z$. But for $z \leq 0$, both cylinder walls are insulated.

For each of these above thermal boundary conditions, at $z \to -\infty$ the entering fluid temperature T_e is uniform. For large values of the axial location or at $z \to \infty$, the fully developed region is reached. The boundary conditions corresponding to the axial locations of $z \to \infty$ or the values of the temperature profiles, T_{fd}, in Eqs.(2.1) - (2.3) will be obtained in Section 2.4.1.

For convenience in the further discussion, the part of annular duct for $z \leq 0$ is called an unheated wall region and the part for $z > 0$ is called a heated wall region.

2.2 Fluid Flow

In this section, the velocity field information that is necessary for the study on heat transfer is given. This section provides the solutions in analytical and numerical forms for Newtonian and non-Newtonian fluids, respectively. In Ref.[48], an extensive literature survey on laminar annular flows of Newtonian and non-Newtonian fluids can be found.

The conservation equations used for describing a flow may be simplified considerably by making various assumptions with regard to the flow description and the physical properties of the fluid involved. The assumptions applied to the flow study are given in Section 2.1.1 and under these assumptions, the velocity field is independent of the temperature field.

The specific physical situation under consideration is shown in Fig.2.2. Here u denotes the local velocity at the distance r from the center of the annular duct, r is the radial coordinate, R_i is the core tube radius and R_o is the outer tube radius. In order to obtain the velocity distribution inside an annular duct, the related momentum equations are solved. The flow velocity is obtained in dimensionless form as

$$u^* = \frac{u}{u_\mathrm{m}} \tag{2.4}$$

Where u_m is the average velocity given as

$$u_\mathrm{m} = \frac{2}{(R_\mathrm{o}^2 - R_\mathrm{i}^2)} \int_{R_\mathrm{i}}^{R_\mathrm{o}} urdr \tag{2.5}$$

The average velocity, u_m, is used to non-dimensionalize the governing equations as a scaling parameter for velocities.

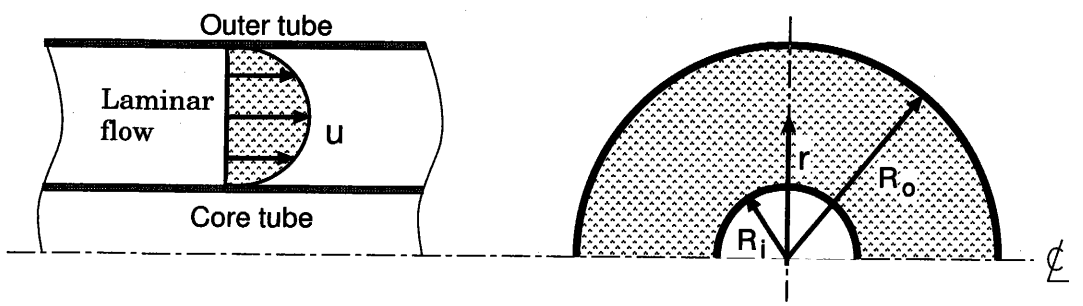

Fig. 2.2: Schematic of a Poiseuille flow in an annular duct

2.2.1 Newtonian fluid flow

The purpose of this section is to describe an analytical solution for a Newtonian fluid flow in an annular duct. The exact solution for a unidirectional laminar flow of a Newtonian fluid can be found in a classical textbook by Bird et al. [49] (pp. 51-54). By applying Bird's solution, the dimensionless velocity, u^*, is obtained in accordance to Eq.(2.4) as follows.

The resulting dimensionless velocity, u^*, and its gradient, du^*/dr^*, for a Newtonian fluid would be:

$$u^* = \frac{2}{M}\left[1-(Nr^*)^2+B\,\ln(Nr^*)\right] \tag{2.6}$$

$$\frac{du^*}{dr^*} = \frac{2}{M}\left(\frac{B}{r^*}-2N^2r^*\right) \tag{2.7}$$

In the above equations, r^* is the dimensionless radius and throughout in the study it is defined as

$$r^* = \frac{r}{D_\mathrm{h}} = \frac{r}{2(R_\mathrm{o}-R_\mathrm{i})} \tag{2.8}$$

D_h is the hydraulic diameter and it is used as a scaling parameter for lengths throughout the study.

B, M and N in Eqs. (2.6) - (2.7) are constants given as

$$B = \frac{R^{*2}-1}{\ln R^*} \tag{2.9}$$

$$M = 1-B+R^{*2} \tag{2.10}$$

$$N = 2(1-R^*) \tag{2.11}$$

Here R^* is the radius ratio. R^* is applied for the geometrical specification of annular ducts.

$$R^* = \frac{R_\mathrm{i}}{R_\mathrm{o}} \tag{2.12}$$

2.2.2 Non-Newtonian fluid flow

As stated in Section 2.1.1, describing the assumptions applied in the study, for non-Newtonian fluids the power-law model is applied. The momentum equation for steady, laminar incompressible fluid flow in cylindrical coordinates with non-slip boundary conditions is

$$\frac{1}{r}\frac{d}{dr}(r\tau) = -\frac{dP}{dz} \qquad \text{and} \qquad \text{B.C.}: \begin{cases} u=0 \quad \text{at} \quad r=R_\mathrm{i} \\ u=0 \quad \text{at} \quad r=R_\mathrm{o} \end{cases} \tag{2.13}$$

According to Assumption 2 given in Section 2.1.1, the fluids are described by the power-law model and the shear stress, τ, in Eq.(2.13) is

$$\tau = -m\left|\frac{du}{dr}\right|^{n-1}\frac{du}{dr}. \tag{2.14}$$

This model is characterized by two parameters: the power-law index, n and the consistency index, m. Equation (2.14) implies that the case where $n = 1$ corresponds to Newtonian fluids, the case where $n < 1$ applies to pseudoplastic fluids and the case where $n > 1$ corresponds to dilatant fluids.

The momentum equation and its boundary conditions are reduced to, in dimensionless form, as follows

$$\frac{1}{r^*}\frac{d}{dr^*}\left(r^*\left|\frac{du^*}{dr^*}\right|^{n-1}\frac{du^*}{dr^*}\right) = -2fRe \tag{2.15}$$

$$\text{B.C.}: \begin{cases} u^* = 0 \quad \text{at} \quad r^* = \dfrac{R^*}{2(1-R^*)} \\ u^* = 0 \quad \text{at} \quad r^* = \dfrac{1}{2(1-R^*)} \end{cases} \tag{2.16}$$

where u^*, r^* and R^* are defined by Eqs.(2.4), (2.8) and (2.12) respectively. f is the friction factor given as

$$f = \frac{D_\mathrm{h}}{2\rho u_\mathrm{m}^2}\left(-\frac{dP}{dz}\right) \tag{2.17}$$

The Reynolds number is defined as

$$Re = \frac{\rho u_\mathrm{m}^{2-n} D_\mathrm{h}^n}{m} \tag{2.18}$$

The dimensionless velocity, u^*, is obtained by solving the momentum equation Eq.(2.15) with Eq.(2.16). For determining the velocity field, u^*, the expression for the average velocity defined by Eq.(2.5) is used. Equation (2.5) can be written in dimensionless form as:

$$\frac{8(1-R^*)}{(1+R^*)}\int_{\frac{R^*}{2(1-R^*)}}^{\frac{1}{2(1-R^*)}} u^* r^* dr^* = 1 \tag{2.19}$$

First, we assume the value of fRe for a given n to solve Eq.(2.15) with Eq.(2.16). Then, Eq.(2.19) is checked by substituting the obtained velocity distribution, u^*, into it. Unless Eq.(2.19) is satisfied within the accuracy of 10^{-5}, a new value of fRe is assumed. This process had been repeated until the correct value of fRe is obtained.

2.3 Heat Transfer

2.3.1 Energy equation

Once the velocity field of the flow is solved, the temperature distribution of the fluid flow can also be determined. With the assumptions described in Section 2.1.1, in two dimensional cylindrical coordinates the energy equation is given as

$$\rho c_p u \frac{\partial T}{\partial z} = k\left[\frac{1}{r}\frac{\partial}{\partial r}\left(r\frac{\partial T}{\partial r}\right) + \frac{\partial^2 T}{\partial z^2}\right] - \tau\frac{du}{dr} \tag{2.20}$$

with c_p noting the specific heat and k the thermal conductivity. The density, ρ, the specific heat, c_p, and the thermal conductivity, k, are assumed to be constants.

In Eq.(2.20), the term in the left is the convection term and the first term on the right-hand side that contains k is the conduction term.

The term containing the shear stress, τ, is the viscous dissipation term, the heat produced by irreversible mechanical energy degradation. Heat generation due to viscous dissipation in flowing fluids acts like a heat source. The temperature increase resulting this way is especially large when either the velocity gradient or the viscosity of the fluid assumes large values. According to a reference by Biermann [50], the viscous dissipation may prevail at a shearing stress higher than about 5×10^4 N/m^2. Tso and Mahulikar [51] pointed out that the relative effect of viscous dissipation may become important in the laminar regime in micro-channels since the steep gradients are maintained there.

The term containing $\partial^2 T/\partial z^2$ is the fluid axial heat conduction term, the heat conduction from downstream to upstream. In order to investigate the fluid axial heat conduction effect, an additional region has to be included in the study. Because in reality the temperature profile at $z = 0$ is not uniform due to the upstream heat penetration through the thermal entrance at $z = 0$; and that the fluid temperature must be considered as uniform far upstream at $z \to -\infty$ [52]. As shown in Fig.2.1 on page 14, the temperature field of the flow is obtained for $-\infty < z < \infty$ in the present study. By applying an additional region i.e. an unheated wall region of $z \leq 0$, it is made sure that a domain is placed upstream of any regions where the axial heat conduction from downstream to upstream would occur.

The solutions for the temperature field are obtained by solving Eq.(2.20) with the thermal boundary conditions described in Section 2.1.2. Then the study has been directed toward the prediction of temperature distribution of the laminar flow in an annular duct, which has a step change in the wall temperature or in the wall

heat flux. Once the temperature distribution is known, the temperature profiles may be integrated to obtain the dimensionless the bulk temperature, T_b, of the fluid flowing within the annular duct as

$$T_b \equiv \frac{\int_{R_i}^{R_o} uTrdr}{\int_{R_i}^{R_o} urdr} = \frac{2}{u_m (R_o^2 - R_i^2)} \int_{R_i}^{R_o} uTrdr. \tag{2.21}$$

The heat transfer coefficients at the tube walls are determined as,
for the (T) thermal boundary condition:

$$h_i \equiv \frac{-k\frac{\partial T}{\partial r}\Big|_{R_i}}{T_w - T_b} \tag{2.22}$$

$$h_o \equiv \frac{k\frac{\partial T}{\partial r}\Big|_{R_o}}{T_w - T_b} \tag{2.23}$$

for the 1st kind of thermal boundary condition:

$$h_i \equiv \frac{-k\frac{\partial T}{\partial r}\Big|_{R_i}}{T_i - T_b} \tag{2.24}$$

$$h_o \equiv \frac{k\frac{\partial T}{\partial r}\Big|_{R_o}}{T_o - T_b} \tag{2.25}$$

for the 2nd kind of thermal boundary condition:

$$h_i \equiv \frac{q_i}{T_i - T_b} \tag{2.26}$$

The Nusselt number at the tube walls, based on the hydraulic diameter of the annulus, D_h, may be written as

$$Nu_i^{(k)} = \frac{h_i^{(k)} \cdot D_h}{k} \tag{2.27}$$

$$Nu_o^{(k)} = \frac{h_o^{(k)} \cdot D_h}{k} \tag{2.28}$$

Where, h is the heat transfer coefficient defined by Eqs.(2.22) - (2.26). The superscript k indicates the thermal boundary condition such as k = T or 1 or 2. k = T corresponds to the (T) thermal boundary condition, $k = 1$ is for the 1st thermal boundary condition, $k = 2$ is for the 2nd kind of thermal boundary condition, respectively.

2.3.2 Non-dimensional formulation

The application of dimensionless groups reduces the number of independent variables. The dimensionless quantities applied in the study are defined below. The dimensionless temperature is given as:

$$\theta^{(T)} = \frac{T - T_e}{T_\mathrm{w} - T_e} \tag{2.29}$$

$$\theta^{(1)} = \frac{T - T_e}{T_\mathrm{i} - T_e} \tag{2.30}$$

$$\theta^{(2)} = \frac{k\,[T - T_e]}{q_\mathrm{i} D_\mathrm{h}} \tag{2.31}$$

The superscripts indicate the thermal boundary conditions.

The calculations of the temperature field in annular ducts are carried out by using the velocity profiles u^* and its gradients du^*/dr^* obtained in Section 2.2 and two dimensionless numbers, namely Peclet number (Pe) and Brinkman number (Br).

The Peclet number, which is the ratio of the heat transport by convection and the heat transport by conduction, is defined as

$$Pe = \frac{\rho c_\mathrm{p} u_\mathrm{m} D_\mathrm{h}}{k} \tag{2.32}$$

The Brinkman number, which is the ratio of the heat production by viscous dissipation and the heat transport by conduction, is defined as

$$Br^{(T)} = \frac{m u_\mathrm{m}^{n+1} D_\mathrm{h}^{1-n}}{k(T_\mathrm{w} - T_\mathrm{e})} \tag{2.33}$$

$$Br^{(1)} = \frac{m u_\mathrm{m}^{n+1} D_\mathrm{h}^{1-n}}{k(T_\mathrm{i} - T_\mathrm{e})} \tag{2.34}$$

$$Br^{(2)} = \frac{m u_\mathrm{m}^{n+1}}{D_\mathrm{h}^{n} q_\mathrm{i}} \tag{2.35}$$

From the analysis, it is obvious that the effect of viscous dissipation is quantitatively significant if the Brinkman number is of appreciable magnitude. Brinkman number clearly depends on fluid properties as well as on the flow conditions and $k\left[T_\mathrm{w}^{(T)} - T_e\right]$ or $k\left[T_\mathrm{i}^{(1)} - T_e\right]$ or q_i. Although Br is usually neglected in low-speed and low-viscosity flows through conventionally sized channels of short lengths, in flows through conventionally sized long pipelines and in micro-channels Br may become important [51].

The axial coordinate is nondimensionlized as

$$z^* = \frac{z}{PeD_\mathrm{h}} \tag{2.36}$$

By employing the relevant definitions for the dimensionless quantities, the dimensionless energy equation is

$$u^* \frac{\partial \theta}{\partial z^*} = \frac{1}{r^*} \frac{\partial}{\partial r^*} \left(r^* \frac{\partial \theta}{\partial r^*} \right) + \frac{1}{Pe^2} \frac{\partial^2 \theta}{\partial z^{*2}} + Br \left| \frac{du^*}{dr^*} \right|^{n-1} \left(\frac{du^*}{dr^*} \right)^2 \tag{2.37}$$

$$\text{in} \quad \frac{R^*}{2(1-R^*)} \leq r^* \leq \frac{1}{2(1-R^*)} \quad \text{and} \quad -\infty \leq z^* \leq \infty$$

The dimensionless energy equation clearly indicates the existence of the fluid axial heat conduction for small Peclet number and of the viscous dissipation for nonzero Brinkman number.

The corresponding thermal boundary conditions are given in the below.

(1) The (T) thermal boundary condition:

$$\begin{cases} \theta = 1 \quad \text{at} \quad r^* = \dfrac{R^*}{2(1-R^*)} & 0 < z^* \\ \theta = 1 \quad \text{at} \quad r^* = \dfrac{1}{2(1-R^*)} & 0 < z^* \\ \theta = 0 \quad \text{at} \quad r^* = \dfrac{R^*}{2(1-R^*)} & z^* \leq 0 \\ \theta = 0 \quad \text{at} \quad r^* = \dfrac{1}{2(1-R^*)} & z^* \leq 0 \\ \theta = 0 \quad \text{at} \quad \dfrac{R^*}{2(1-R^*)} < r^* < \dfrac{1}{2(1-R^*)} & z^* \to -\infty \\ \theta = \theta_{\text{fd}} \quad \text{at} \quad \dfrac{R^*}{2(1-R^*)} < r^* < \dfrac{1}{2(1-R^*)} & z^* \to \infty \end{cases} \tag{2.38}$$

(2) The 1st kind of thermal boundary condition:

$$\begin{cases} \theta = 1 \quad \text{at} \quad r^* = \dfrac{R^*}{2(1-R^*)} & 0 < z^* \\ \theta = 0 \quad \text{at} \quad r^* = \dfrac{1}{2(1-R^*)} & 0 < z^* \\ \theta = 0 \quad \text{at} \quad r^* = \dfrac{R^*}{2(1-R^*)} & z^* \leq 0 \\ \theta = 0 \quad \text{at} \quad r^* = \dfrac{1}{2(1-R^*)} & z^* \leq 0 \\ \theta = 0 \quad \text{at} \quad \dfrac{R^*}{2(1-R^*)} < r^* < \dfrac{1}{2(1-R^*)} & z^* \to -\infty \\ \theta = \theta_{\text{fd}} \quad \text{at} \quad \dfrac{R^*}{2(1-R^*)} < r^* < \dfrac{1}{2(1-R^*)} & z^* \to \infty \end{cases} \tag{2.39}$$

(3) The 2nd kind of thermal boundary condition:

$$\begin{cases} \dfrac{\partial\theta}{\partial r^*} = -1 \quad \text{at} \quad r^* = \dfrac{R^*}{2(1-R^*)} & 0 < z^* \\ \dfrac{\partial\theta}{\partial r^*} = 0 \quad \text{at} \quad r^* = \dfrac{1}{2(1-R^*)} & 0 < z^* \\ \dfrac{\partial\theta}{\partial r^*} = 0 \quad \text{at} \quad r^* = \dfrac{R^*}{2(1-R^*)} & z^* \leq 0 \\ \dfrac{\partial\theta}{\partial r^*} = 0 \quad \text{at} \quad r^* = \dfrac{1}{2(1-R^*)} & z^* \leq 0 \\ \theta = 0 \quad \text{at} \quad \dfrac{R^*}{2(1-R^*)} < r^* < \dfrac{1}{2(1-R^*)} & z^* \to -\infty \\ \theta = \theta_{\text{fd}} \quad \text{at} \quad \dfrac{R^*}{2(1-R^*)} < r^* < \dfrac{1}{2(1-R^*)} & z^* \to \infty \end{cases} \tag{2.40}$$

In the dimensionless form, the bulk temperature is

$$\theta_{\text{b}} \equiv \frac{8(1-R^*)}{1+R^*} \int_{\frac{R^*}{2(1-R^*)}}^{\frac{1}{2(1-R^*)}} u^*\, \theta\, r^*\, dr^* \tag{2.41}$$

Thus, by applying the obtained developing temperature distributions for the each considered thermal boundary condition, according to Eq.(2.22) - Eq.(2.28) the conventional Nusselt numbers are obtained as follows,
for the (T) thermal boundary condition:

$$Nu_{\text{i}} = -\frac{1}{(\theta_{\text{w}} - \theta_{\text{b}})} \frac{\partial\theta}{\partial r^*}\bigg|_{r^*=\frac{R^*}{2(1-R^*)}} \tag{2.42}$$

$$Nu_{\text{o}} = \frac{1}{(\theta_{\text{o}} - \theta_{\text{b}})} \frac{\partial\theta}{\partial r^*}\bigg|_{r^*=\frac{1}{2(1-R^*)}} \tag{2.43}$$

for the 1st kind of thermal boundary condition:

$$Nu_{\text{i}} = -\frac{1}{(\theta_{\text{i}} - \theta_{\text{b}})} \frac{\partial\theta}{\partial r^*}\bigg|_{r^*=\frac{R^*}{2(1-R^*)}} \tag{2.44}$$

$$Nu_{\text{o}} = \frac{1}{(\theta_{\text{o}} - \theta_{\text{b}})} \frac{\partial\theta}{\partial r^*}\bigg|_{r^*=\frac{1}{2(1-R^*)}} \tag{2.45}$$

for the 2nd kind of thermal boundary condition:

$$Nu_{\text{i}} = \frac{1}{\theta_{\text{i}} - \theta_{\text{b}}} \tag{2.46}$$

2.3.3 Governing parameters for the problem

In Section 2.3.2, the governing partial differential equation is transformed by applying several parameters in terms of dimensionless quantities. The problem under consideration contains four independent parameters, which need to be prescribed for the analysis. These are:

- radius ratio, R^* defined by Eq.(2.12), which is the ratio of the inner core radius to the outer tube radius. Since the basic passage cross section in the present study is an annulus, as discussed in Section 1.1, the geometrical parameter R^* characterizes how significant part plays the duct shape in the heat transfer.

- flow index, n, which determines how fast viscous momentum is transferred through the fluid layers in the boundary layer [53]. For shear-thinning or pseudoplastic fluids $n < 1$ whereas, for shear-thickening or dilatant ones $n > 1$. Generally, n depends on the range of shear rates considered [54]. Examples of numerical values of n can be found in Refs.[49] (p. 13), [53] (p. 2840), [54] (p. 78), and [55] (p. 1587). Three values of n are applied for the calculation. They are $n = 1$ (Newtonian fluids), $n = 0.5$ (as an example: carboxymethyl cellulose solution) and $n = 1.5$ (as an example: ethylene oxide in sodium chloride solution).

- Brinkman number, Br, which represents the ratio of overall dissipation to heat conduction from the wall. This number is of remarkable importance in modeling of heat transfer because it establishes the threshold between two contrasting situations: one embracing heat generation due to the viscous dissipation ($Br \neq 0$) and the other implicating negligible heat due to the viscous dissipation ($Br = 0$). For micro-channels, Br is not only a measure of the relative importance of viscous dissipation, but it determines the flow regime in addition to the Reynolds number for flows with heat transfer [56, 57]. In an attempt to investigate the viscous dissipation effect on heat transfer, the Brinkman number, defined by Eqs.(2.33) - (2.35), is used. Negligible viscous dissipation condition is only valid for $Br = 0$. The Brinkman number values can be interpreted directly as representing the viscous dissipation. The more absolute value of the Brinkman number is, the more pronounced effect of viscous dissipation. For a 0.2 % aqueous carbopol solution ($n = 0.26$) flowing in a 30 mm diameter circular duct with average velocity $u_{\mathrm{m}} = 0.0785$ m/s

(an example given in Ref.[54] p. 273), $Br = 8\times10^{-6}$. In this example the temperature difference, $(T_w - T_e)$ in Eq.(2.33) is 65. For oil ($n = 1$) flowing (at an average velocity $u_m = 2$ m/s) in a pipeline ($D_h = 0.3$ m) through a lake (an example given in [58] p. 881), the value of Brinkman is Br = - 1.1. Here the difference $(T_w - T_e)$ in Eq.(2.33) is 20.

- Peclet number, Pe, which characterizes the ratio of heat convection to heat conduction. Pe is applied in modeling the heat transfer as its value determines two different situations: one proposing heat conduction from the downstream (finite Pe) and the other suggesting negligible heat conduction from the downstream within the fluid (infinite Pe). Peclet number, defined by Eq.(2.32), is used to measure fluid axial heat conduction effects. Clearly neglecting the fluid axial heat conduction is acceptable at large values of the Peclet number. Normally, Pe is larger than 100; however, if a high-temperature liquid metal, such as sodium, is flowing slowly the Peclet number value can be as low as 5. In the present study, the case of $Pe \rightarrow \infty$ stands for the negligible fluid axial heat conduction and in order to carry out the calculation for this case the value of $Pe = 10^8$ was applied.

  In Ref.[40], an illustrative example determining the values of Brinkman number and Peclet number can be found.

2.4 Calculation Methodology for the Heat Transfer Study

The incorporation of the terms of viscous dissipation and fluid axial heat conduction changes a homogeneous, parabolic energy equation into a non-homogeneous, elliptic one. The purpose of discussing the type of the governing differential equation is to connect it with the calculation methodology and especially with the key role of the fluid axial heat conduction term.

The governing energy equation does not lend itself to an analytic solution and the author had to resort to numerical methods. The particular numerical scheme adopted is a finite difference method. Two complexities arise for solving the energy equation numerically as an elliptic type problem. One is related with the semi-infinite domain as explained in Section 2.3.1. The other is the necessity of an additional boundary condition since the boundary conditions are needed on all of

the boundaries to solve an elliptic equation [22], [46] - [47]. Therefore, the following 2 aims should be addressed.

1. Obtaining θ_{fd} in Eqs.(2.38) - (2.40) or solving the temperature distributions at $z^* \rightarrow \infty$.

2. Converting the semi-infinite domain, described in Sections 2.1.2 and 2.3.1, into a finite one in order to solve the energy equation by a finite-difference method.

Sections 2.4.1 - 2.4.2 are designated to accomplish these aims. First the temperature distribution at $z^* \rightarrow \infty$ is determined. At a very large value of z^*, the fully developed condition is reached. Therefore the solution for the fully developed flow is applied to calculate the thermally developing flow. Although the primary interest is the thermally developing flow as Section 2.1.1 suggests, the solutions for the heat transfer in the fully developed flow are provided.

2.4.1 Solutions for $z \rightarrow \infty$

As explained immediately above, this section describes the heat transfer in the fully developed flow which would be needed to solve the energy equation. In the preceding three subsections, the temperature fields in the fully developed flows, θ_{fd}, are obtained for the thermal boundary conditions of Ⓣ, 1st kind and 2nd kind respectively.

The Ⓣ T.B.C

For ducts with uniform wall temperature, the temperature of a fully developed flow is a function of r^* alone [15], [37] - [39]. According to this condition, θ_{fd} becomes the particular solution of the following equation.

$$\frac{1}{r^*}\frac{d}{dr^*}\left(r^*\frac{d\theta_{fd}}{dr^*}\right) = -Br\left|\frac{du^*}{dr^*}\right|^{n-1}\left(\frac{du^*}{dr^*}\right)^2 \tag{2.47}$$

$$\text{B.C.}: \begin{cases} \theta = 1 \quad \text{at} \quad r^* = \dfrac{R^*}{2(1-R^*)} \\ \theta = 1 \quad \text{at} \quad r^* = \dfrac{1}{2(1-R^*)} \end{cases} \tag{2.48}$$

By applying the velocity gradient, du^*/dr^*, obtained in Section 2.2, the temperature distribution θ_{fd} is solved. Then θ_{fd} is replaced in Eq.(2.38) to solve the problem of thermally developing flow.

The 1st Kind of T.B.C

For the 1st kind of thermal boundary condition, in the fully developed region the dimensionless temperature is a function of r^* alone.

$$\frac{1}{r^*}\frac{d}{dr^*}\left(r^*\frac{d\theta_{\rm fd}}{dr^*}\right) = -Br\left|\frac{du^*}{dr^*}\right|^{n-1}\left(\frac{du^*}{dr^*}\right)^2 \tag{2.49}$$

$$\text{B.C.}: \begin{cases} \theta = 1 \quad \text{at} \quad r^* = \dfrac{R^*}{2(1-R^*)} \\ \theta = 0 \quad \text{at} \quad r^* = \dfrac{1}{2(1-R^*)} \end{cases} \tag{2.50}$$

By applying the velocity gradient, du^*/dr^*, obtained in Section 2.2, the temperature distribution $\theta_{\rm fd}$ is solved. Then $\theta_{\rm fd}$ is replaced in Eq.(2.39) to solve the problem of thermally developing flow.

The 2nd Kind of T.B.C

For the 2nd kind of boundary condition, in the thermally developed region the energy equation is

$$k\frac{1}{r}\frac{\partial}{\partial r}\left(r\frac{\partial T_{\rm fd}}{\partial r}\right) + m\left|\frac{du}{dr}\right|^{n-1}\left(\frac{du}{dr}\right)^2 = \rho c_{\rm p} u\frac{dT_{\rm b}}{dz} \tag{2.51}$$

$$\begin{cases} -k\dfrac{\partial T_{\rm fd}}{\partial r} = q_{\rm i} \quad \text{at} \quad r = R_{\rm i} \\ k\dfrac{\partial T_{\rm fd}}{\partial r} = 0 \quad \text{at} \quad r = R_{\rm o} \end{cases} \tag{2.52}$$

$dT_{\rm b}/dz$ in Eq.(2.51) is evaluated, from an energy balance as

$$\frac{dT_{\rm b}}{dz} = \frac{2\ R_{\rm i} q_{\rm i}}{\rho c_{\rm p} u_{\rm m}\left(R_{\rm o}^2 - R_{\rm i}^2\right)}\left[1 + \frac{\int_{R_{\rm i}}^{R_{\rm o}} rm\left|\frac{du}{dr}\right|^{n-1}\left(\frac{du}{dr}\right)^2 dr}{R_{\rm i} q_{\rm i}}\right] \tag{2.53}$$

Substitution of the above balance into Eq.(2.51) gives

$$k\frac{1}{r}\frac{\partial}{\partial r}\left(r\frac{\partial T_{\rm fd}}{\partial r}\right) + m\left|\frac{du}{dr}\right|^{n-1}\left(\frac{du}{dr}\right)^2 = \tag{2.54}$$

$$\frac{2uR_{\rm i}q_{\rm i}}{u_{\rm m}\left(R_{\rm o}^2 - R_{\rm i}^2\right)}\left[1 + \frac{\int_{R_{\rm i}}^{R_{\rm o}} rm\left|\frac{du}{dr}\right|^{n-1}\left(\frac{du}{dr}\right)^2 dr}{R_{\rm i} q_{\rm i}}\right]$$

By introducing the relevant dimensionless quantities defined in Section 2.3.2, the above equation becomes

$$\frac{\partial^2\theta_{fd}}{dr^{*2}} + \frac{1}{r^*}\frac{\partial\theta_{fd}}{dr^*} = \frac{4u^*}{(1+R^*)}\left[R^* + 2(1-R^*)\int_{\frac{R^*}{2(1-R^*)}}^{\frac{1}{2(1-R^*)}} V\cdot r^* dr^*\right] - V \tag{2.55}$$

$$\begin{cases} \dfrac{d\theta_{fd}}{dr^*} = -1 \quad \text{at} \quad r^* = \dfrac{R^*}{2(1-R^*)} \\ \dfrac{d\theta_{fd}}{dr^*} = 0 \quad \text{at} \quad r^* = \dfrac{1}{2(1-R^*)} \end{cases} \tag{2.56}$$

where

$$V = Br\left|\frac{du^*}{dr^*}\right|^{n-1}\left(\frac{du^*}{dr^*}\right)^2 \tag{2.57}$$

On the other hand, the following is assumed on the fact that in the thermally fully developed region the temperature solution is a linear function of z^*.

$$\theta_{fd} = Cz^* + \psi(r^*) \tag{2.58}$$

Substitution of Eq.(2.58) into Eq.(2.55) and Eq.(2.56) yields

$$\frac{d^2\psi}{dr^{*2}} + \frac{1}{r^*}\frac{d\psi}{dr^*} = Cu^* - V \tag{2.59}$$

$$\begin{cases} \dfrac{d\psi}{dr^*} = -1 \quad \text{at} \quad r^* = \dfrac{R^*}{2(1-R^*)} \\ \dfrac{d\psi}{dr^*} = 0 \quad \text{at} \quad r^* = \dfrac{1}{2(1-R^*)} \end{cases} \tag{2.60}$$

According to Eq.(2.58)

$$\frac{\partial^2\theta_{fd}}{\partial r^{*2}} = \frac{d^2\psi}{dr^{*2}} \quad \text{and} \quad \frac{\partial\theta_{fd}}{\partial r^*} = \frac{d\psi}{dr^*} \tag{2.61}$$

Thus

$$\frac{d^2\psi}{dr^{*2}} + \frac{1}{r^*}\frac{d\psi}{dr^*} = \frac{4u^*}{(1+R^*)}\left[R^* + 2(1-R^*)\int_{\frac{R^*}{2(1-R^*)}}^{\frac{1}{2(1-R^*)}} V\cdot r^* dr^*\right] - V \tag{2.62}$$

The coefficient C was found by comparing Eq.(2.59) and Eq.(2.62) as

$$C = \frac{4}{(1+R^*)}\left[R^* + 2(1-R^*)\int_{\frac{R^*}{2(1-R^*)}}^{\frac{1}{2(1-R^*)}} V\cdot r^* dr^*\right] \tag{2.63}$$

$\psi(r^*)$ was calculated from Eq.(2.59) with Eq.(2.60) by the finite difference method. θ_{fd} was calculated from Eq.(2.58) and replaced in Eq.(2.40) as a boundary condition to solve the problem.

2.4.2 Coordinate transformation

As stated previously in Section 2.3.1, in order to study the fluid axial heat conduction effect an infinite region is applied in this study. The following relation is employed for transforming the upstream and downstream infinities in Eqs.(2.38) - (2.40) into finite values.

$$z^* = E\tan(\pi z_t^*) \quad \text{or} \quad z_t^* = \frac{1}{\pi}\arctan\left(\frac{z^*}{E}\right) \tag{2.64}$$

where E is a transformation constant taken as unity in this study. The above tangent transverse transformation was employed by Fuller and Samuels [22], Verhoff and Fisher [59], Ku and Hatziavramidis [60] and by Campo and Auguste [61]. By applying the tangent transverse transformation, the upstream infinity at $z^* \to -\infty$ and the downstream infinity at $z^* \to \infty$ are converted to $z_t^* = -0.5$ and $z_t^* = 0.5$, respectively.

2.4.3 Transformed dimensionless energy equation

By introducing the transformed coordinate z_t^* given by Eq.(2.64), the energy equation Eq.(2.37) and the boundary conditions Eqs.(2.38) - (2.40) become

$$l_1\frac{\partial\theta}{\partial z_t^*} = \frac{\partial^2\theta}{\partial r^{*2}} + l_2\frac{\partial^2\theta}{\partial z_t^{*2}} + \frac{1}{r^*}\frac{\partial\theta}{\partial r^*} + Br\left|\frac{du^*}{dr^*}\right|^{n-1}\left(\frac{du^*}{dr^*}\right)^2 \tag{2.65}$$

where

$$l_1 = \frac{\cos^2(\pi z_t^*)}{\pi E}\left[u^* + \frac{1}{Pe^2}\frac{\sin(2\pi z_t)}{E}\right] \tag{2.66}$$

$$l_2 = \frac{1}{Pe^2}\left[\frac{\cos^2(\pi z_t^*)}{\pi E}\right]^2 \tag{2.67}$$

(1) The (T) T.B.C.:

$$\begin{cases} \theta = 1 \ \text{at} & r^* = \dfrac{R^*}{2(1-R^*)} & 0 < z_t^* \\ \theta = 1 \ \text{at} & r^* = \dfrac{1}{2(1-R^*)} & 0 < z_t^* \\ \theta = 0 \ \text{at} & r^* = \dfrac{R^*}{2(1-R^*)} & z_t^* \le 0 \\ \theta = 0 \ \text{at} & r^* = \dfrac{1}{2(1-R^*)} & z_t^* \le 0 \\ \theta = 0 \ \text{at} & \dfrac{R^*}{2(1-R^*)} < r^* < \dfrac{1}{2(1-R^*)} & z_t^* = -0.5 \\ \theta = \theta_{\text{fd}} \ \text{at} & \dfrac{R^*}{2(1-R^*)} < r^* < \dfrac{1}{2(1-R^*)} & z_t^* = 0.5 \end{cases} \tag{2.68}$$

(2) The 1st kind T.B.C.:

$$\begin{cases} \theta = 1 \quad \text{at} \quad r^* = \dfrac{R^*}{2(1-R^*)} & 0 < z_t^* \\ \theta = 0 \quad \text{at} \quad r^* = \dfrac{1}{2(1-R^*)} & 0 < z_t^* \\ \theta = 0 \quad \text{at} \quad r^* = \dfrac{R^*}{2(1-R^*)} & z_t^* \leq 0 \\ \theta = 0 \quad \text{at} \quad r^* = \dfrac{1}{2(1-R^*)} & z_t^* \leq 0 \\ \theta = 0 \quad \text{at} \quad \dfrac{R^*}{2(1-R^*)} < r^* < \dfrac{1}{2(1-R^*)} & z_t^* = -0.5 \\ \theta = \theta_{\text{fd}} \quad \text{at} \quad \dfrac{R^*}{2(1-R^*)} < r^* < \dfrac{1}{2(1-R^*)} & z_t^* = 0.5 \end{cases} \tag{2.69}$$

(3) The 2nd kind T.B.C.:

$$\begin{cases} \dfrac{\partial\theta}{\partial r^*} = -1 \quad \text{at} \quad r^* = \dfrac{R^*}{2(1-R^*)} & 0 < z_t^* \\ \dfrac{\partial\theta}{\partial r^*} = 0 \quad \text{at} \quad r^* = \dfrac{1}{2(1-R^*)} & 0 < z_t^* \\ \dfrac{\partial\theta}{\partial r^*} = 0 \quad \text{at} \quad r^* = \dfrac{R^*}{2(1-R^*)} & z_t^* \leq 0 \\ \dfrac{\partial\theta}{\partial r^*} = 0 \quad \text{at} \quad r^* = \dfrac{1}{2(1-R^*)} & z_t^* \leq 0 \\ \theta = 0 \quad \text{at} \quad \dfrac{R^*}{2(1-R^*)} < r^* < \dfrac{1}{2(1-R^*)} & z_t^* = -0.5 \\ \theta = \theta_{\text{fd}} \quad \text{at} \quad \dfrac{R^*}{2(1-R^*)} < r^* < \dfrac{1}{2(1-R^*)} & z_t^* = 0.5 \end{cases} \tag{2.70}$$

To obtain the temperature field, the transformed energy equation Eq.(2.65) has been solved by applying the velocity fields in stationary concentric annular ducts which were obtained in Section 2.2. The results are discussed in Sections 2.6 - 2.8, 2.9 - 2.11 and 2.12 - 2.14 separately in accordance with the associated thermal boundary conditions.

In the present study, the solution technique to solve the partial differential equation Eq.(2.65), is the finite difference method described in the following section.

2.4.4 Finite difference approximations

The finite difference formulation of the energy equation, Eq.(2.65), along with the associated thermal boundary conditions, Eqs.(2.68) - (2.70), is solved numerically. The dimensionless temperature of the fluid flowing inside an annular duct has been obtained as a result of the finite-difference approach that approximates Eq.(2.65) by transforming into a set of algebraic equations.

Figure 2.3 shows the solution zone, which is axially extended from z_t^* = -0.5 ($z^* \rightarrow -\infty$) to z_t^* = 0.5 ($z^* \rightarrow \infty$). The solution zone is divided into cells and the radial and axial divisions being designated by Δr and Δz_k, respectively. The sub-indices k and m are assigned to the radial and axial directions. Using these notations such as k and m, the derivatives appearing in Eq.(2.65) are converted as follows:

$$\frac{\partial \theta}{\partial z_t^*} \approx \frac{\theta_m^{(k)} - \theta_m^{(k-1)}}{\Delta z_{k-1}} \tag{2.71}$$

$$\frac{\partial^2 \theta}{\partial z_t^{*2}} \approx \frac{\theta_m^{(k+1)} - (1+\sigma^2)\theta_m^{(k)} + \sigma^2 \theta_m^{(k-1)}}{(\Delta z_k)^2} - \frac{(1-\sigma)}{\Delta z_k} \frac{\theta_m^{k+1} - \theta_m^{k-1}}{\Delta z_{k-1} + \Delta z_k} \tag{2.72}$$

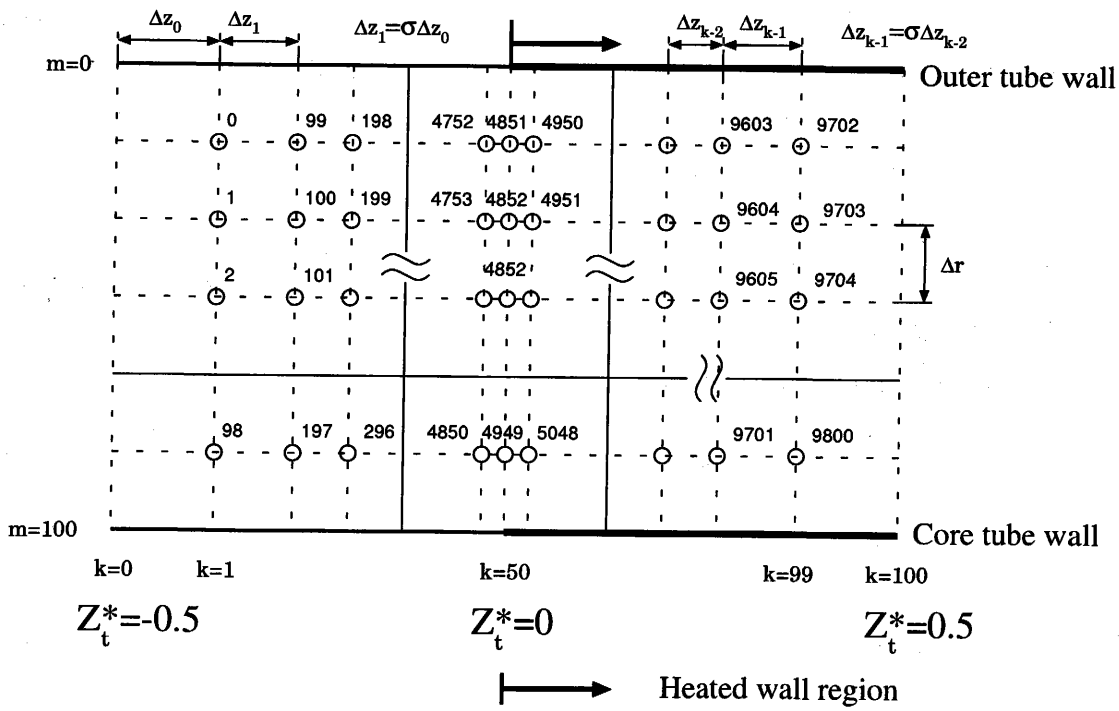

Fig. 2.3: Mesh system applied in the analysis

$$\frac{\partial\theta}{\partial r^*} \approx \frac{\theta_m^{(k)} - \theta_{m-1}^{(k)}}{\Delta r} \tag{2.73}$$

$$\frac{\partial^2\theta}{\partial r^{*2}} \approx \frac{\theta_{m+1}^{(k)} - 2\theta_m^{(k)} + \theta_{m-1}^{(k)}}{(\Delta r)^2} \tag{2.74}$$

Where

$$\sigma = \frac{\Delta z_k}{\Delta z_{k-1}} \tag{2.75}$$

The numerical approach employed for the system equations was based on the Gauss-Seidel method. Mesh sizes of 100×400 consisting of finer grids near $z_t^* = 0$ was applied to allow more accurate representation of the fluid axial heat conduction effect. The mesh sizes along the axial coordinate varies from Δz_{k-1} to Δz_k. In other words, the mesh is updated at each iteration in accordance with Eq.(2.75). The finest mesh is used at the entrance $z^* = 0$ and the mesh spacing is enhanced to both the downstream and the upstream directions by multiplying the foregoing mesh size with a constant σ. Mesh sizes grow denser with the constant degree of σ as they approach to the location of the step change in the wall temperature or in the wall heat flux, i.e., $z_t^* = 0$. Along the r^* direction, equally sized meshes were used. By discretizing the energy equation Eq.(2.65), the final set of finite difference equation becomes:

$$\begin{aligned} l_{1_m}^{(k)} \frac{\theta_m^{(k)} - \theta_m^{(k-1)}}{\Delta z_{k-1}} &= \frac{\theta_{m+1}^{(k)} - 2\theta_m^{(k)} + \theta_{m-1}^{(k)}}{(\Delta r)^2} \\ &+ l_2^{(k)} \left[\frac{\theta_m^{(k+1)} - (1+\sigma^2)\theta_m^{(k)} + \sigma^2\theta_m^{(k-1)}}{(\Delta z_k)^2} - \frac{(1-\sigma)}{\Delta z_k} \frac{\theta_m^{(k+1)} - \theta_m^{(k-1)}}{\Delta z_{k-1} + \Delta z_k} \right] \\ &+ \frac{1}{r_m} \frac{\theta_m^{(k)} - \theta_{m-1}^{(k)}}{\Delta r} + Br \left(\frac{du^*}{dy^*} \right)_m^{n+1} \end{aligned} \tag{2.76}$$

In the numerical computation, the prescribed error ϵ for all the variables was

$$\epsilon = \frac{\sum_{k}^{100} \sum_{m}^{100} \left| \theta_{m.old}^{(k)} - \theta_{m.new}^{(k)} \right|}{\sum_{k}^{100} \sum_{m}^{100} \left| \theta_{m.new}^{(k)} \right|} < 10^{-8} \tag{2.77}$$

The temperature data in annular ducts are extracted from nodal values and the results are discussed in Sections 2.6 - 2.14 separately for each thermal boundary condition.

2.5 Limiting Cases of $R^* = 0$ and $R^* = 1$

This section discusses the heat transfer in cylindrical ($R^* = 0$) and parallel-plates ($R^* = 1$) ducts under the (T) thermal boundary condition. Figure 2.4 shows the physical model and coordinate system. The z axis is taken in the flow direction and passes through the center of the duct designated as (0,0) in Fig.2.4. At $z \rightarrow -\infty$ the fluid enters with a uniform temperature, T_e. The wall temperature is equal to T_e for $z \leq 0$. At $z = 0$ the wall temperature jumps from T_e to T_w. Both T_e and T_w are constants. The flow is assumed to be steady, laminar and hydrodynamically fully developed but thermally developing. Moreover, the properties of the fluid are assumed to be constant and the power-law model is applied to describe the rheological behavior. The velocity fields in cylindrical and parallel-plates ducts were obtained analytically from a momentum balance and given in Ref.[62] as

$$u^* = \frac{1+(2+p)n}{n+1}\left[1-\{(4-2\,p)r^*\}^{\frac{n+1}{n}}\right] \tag{2.78}$$

The dimensionless governing equation for the Graetz problem including both viscous dissipation and fluid axial heat conduction can be represented as

$$u^*\frac{\partial\theta}{\partial z^*} = \frac{1}{r^{*p}}\frac{\partial}{\partial r^*}\left(r^{*p}\frac{\partial\theta}{\partial r^*}\right) + \frac{1}{Pe^2}\frac{\partial^2\theta}{\partial z^{*2}} + Br\left|\frac{du^*}{dr^*}\right|^{n-1}\left(\frac{du^*}{dr^*}\right)^2 \tag{2.79}$$

where $\theta = (T - T_e)/(T_w - T_e)$ is the dimensionless temperature, $z^*=(z/D_h)/Pe$ is the dimensionless axial coordinate, $Pe = \rho c_p u_m D_h/k$ is the Peclet number, $Br = (m u_m^{n+1} D_h^{1-n})/[k(T_w - T_e)]$ is the Brinkman number and $u_m = 2\int_0^R u\ r\ dr/R^2$ or $u_m = 2\int_0^{L/2} u\ dr/L$ is the average velocity of the fluid. The index p in Eqs.(2.78) - (2.79) is equal to 0 for parallel-plates and to 1 for cylindrical ducts .

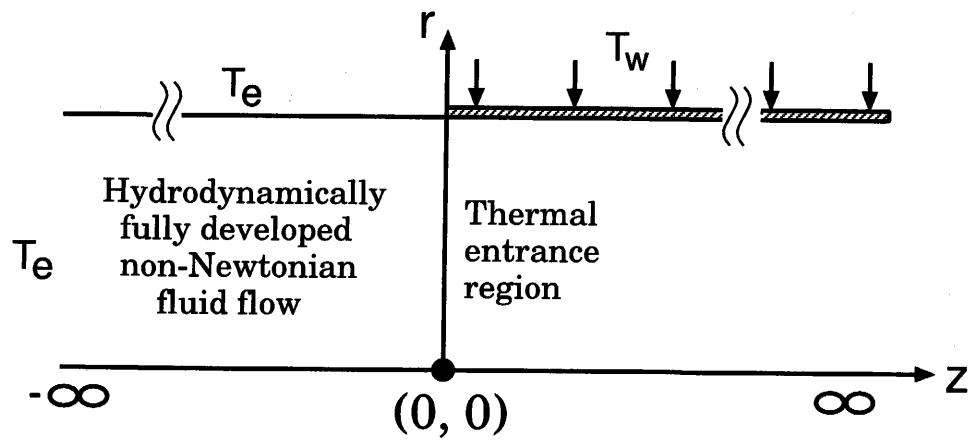

Fig. 2.4: Geometrical configuration

As discussed in Section 2.4, the energy equation is mathematically elliptic and the boundary conditions are needed on all of the boundaries [22, 46, 47]. The boundary conditions for the energy equation are given as

$$\begin{cases} \dfrac{\partial\theta}{\partial r^*} = 0 & \text{at } r^* = 0 \quad \text{for } -\infty < z^* < \infty \\ \theta = 1 & \text{at } r^* = r_w^* \quad \text{for } 0 < z^* \qquad \lim\limits_{z^*\to-\infty} \theta = 0 \quad \text{for } 0 < r^* < r_w^* \\ \theta = 0 & \text{at } r^* = r_w^* \quad \text{for } z^* \le 0 \qquad \lim\limits_{z^*\to\infty} \theta = \theta_{fd}(r^*) \quad \text{for } 0 < r^* < r_w^*. \end{cases} \tag{2.80}$$

Here, θ_{fd}, i.e, the boundary condition of the downstream infinity ($z \to \infty$) is determined for parallel-plates ducts:

$$\theta_{fd} = Br\ 4^{\frac{(n+1)^2}{n}} \left(\frac{2n+1}{n}\right)^n \left(\frac{n}{3n+1}\right) \left[4^{-\frac{3n+1}{n}} - r^{*\frac{3n+1}{n}}\right] \tag{2.81}$$

and for cylindrical ducts:

$$\theta_{fd} = Br\ 2^{\frac{(n+1)^2}{n}} \left(\frac{n}{3n+1}\right)^{1-n} \left[2^{-\frac{3n+1}{n}} - r^{*\frac{3n+1}{n}}\right] \tag{2.82}$$

Once the temperature distribution, θ, is known, the local Nusselt number and the bulk temperature are determined as

$$Nu = \frac{h\ D_h}{k} = \frac{1}{(\theta_w - \theta_b)} \left.\frac{\partial\theta}{\partial r^*}\right|_{r^*=r_w^*}, \qquad \theta_b \equiv (4+4\ p) \int_0^{r_w^*} u^*\ \theta\ r^{*p} dr^* \tag{2.83}$$

The index p is equal to 0 for parallel-plates and to 1 for cylindrical ducts.

References [63] - [69] concerned the laminar heat transfer in cylindrical ducts for the (T) thermal boundary condition and they included the viscous dissipation while neglecting the fluid axial heat conduction. For cases of viscous dissipation included in the energy equation, the conventional Nusselt numbers for laminar flow in ducts subject to uniform wall temperature had been presented for Newtonian fluids in Refs.[63] - [64], for power-law fluids in Refs.[65] - [66], for Bingham plastics in Refs.[67] - [68] and for viscoelastic fluids in Ref.[69].

2.5.1 Temperature distributions and Nusselt numbers for $R^* = 0$ and $R^* = 1$

The temperature distributions of power-law fluids flowing in parallel-plates and cylindrical ducts have been calculated in the axial domain for $-\infty < z^* < \infty$. The computed results are shown graphically and the main features are discussed.

Typical developing temperature profiles in a cylindrical duct are displayed for comparison in Figs. 2.5(a) and 2.5(b). At $z^* = 0$, there is a step change in the wall temperature. In this study, according to the definition of Br, negative Br stands for fluid cooling and positive Br stands for fluid heating.

Figure 2.5(a) illustrates the developments of the local temperature profile for the case of negligible viscous dissipation and fluid axial heat conduction ($Br = 0$ and $Pe \rightarrow \infty$).

Figure 2.5(b) shows the temperature profile for the case of considerable viscous dissipation and fluid axial heat conduction ($Br = 0.1$ and $Pe = 10$). The solid lines in these figures correspond to the region where the wall temperature, θ_w, is 1 ($0 < z^*$). The dotted lines are the temperature profiles for $z^* \leq 0$ where the wall temperature is kept equal to the entering fluid temperature or where the dimensionless wall temperature is 0.

By comparing the temperature developments in Figs.2.5(a) and 2.5(b) it is seen that the fluid temperature is deviated from 0 due to the fluid axial heat conduction and the viscous dissipation before the fluid enters into the heated wall region of $0 < z^*$. The circles show the solutions presented by Olek [70] for the case of negligible viscous dissipation and fluid axial heat conduction and the agreement is reasonably good.

In Fig.2.6, the heat transfer results for a cylindrical duct are illustrated in terms of conventional Nusselt numbers, Nu, against the dimensionless axial coordinate, z^*, in the thermally developing region for Newtonian ($n = 1$), pseudoplastic ($n = 0.5$) and dilatant ($n = 1.5$) fluids with the Peclet number and the Brinkman number as parameters.

In these figures the solid curves stand for $Pe \rightarrow \infty$ and the dotted curves for $Pe = 10$. The figures show that the thermal entrance length increases as Pe decreases.

Another relevant feature on the figures is that when viscous dissipation is considered ($Br \neq 0$) the asymptotic Nu is independent of Br. This behavior has been discussed by previous researchers [63] - [69]. The results in Refs.[63] - [69], demonstrate that two values of Nusselt numbers exist in the fully developed region whether Br value is zero or non-zero. For non-zero Br, the Nusselt number approaches asymptotically to a fully developed value regardless of cooling or heating condition. Nield, et al. [42] explained this behavior of Nusselt numbers in the fully developed region as follows. By changing the Brinkman from zero to non-zero, the homogeneous governing energy equation becomes a non-homogeneous one and the

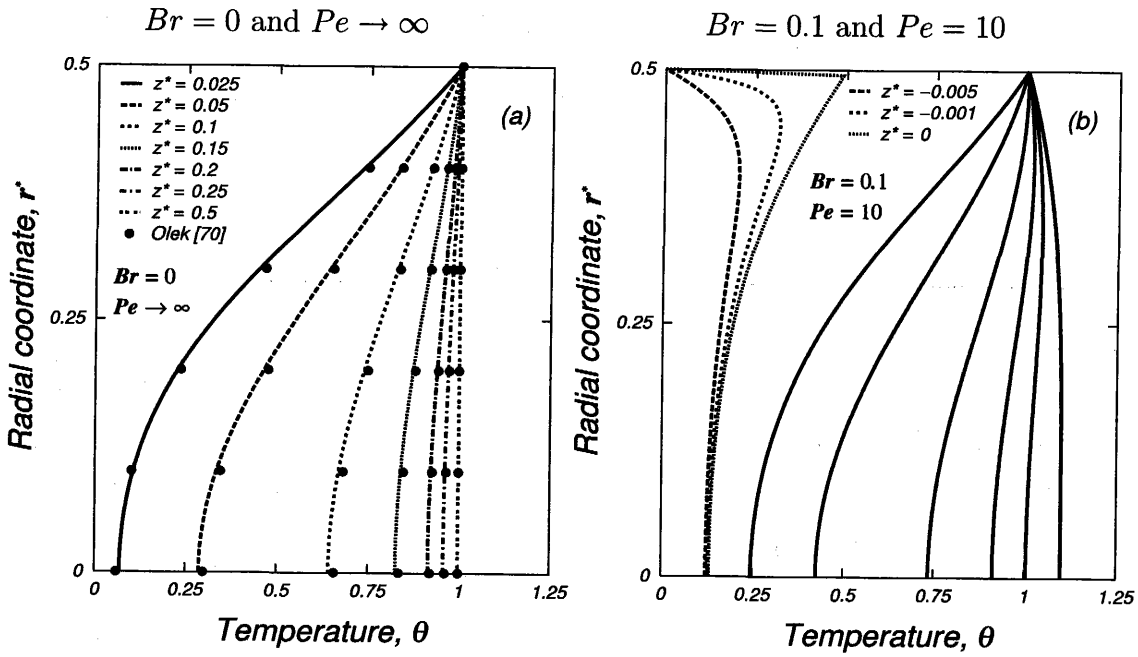

(a) Negligible viscous dissipation and fluid axial heat conduction ($Br = 0$ and $Pe \to \infty$)

(b) Considerable viscous dissipation and fluid axial heat conduction ($Br = 0.1$ and $Pe = 10$)

Fig. 2.5: Developing temperature profiles of a Newtonian fluid ($n = 1$) in a cylindrical duct ($R^* = 0$)

viscous dissipation provides a heat source distribution which persists downstream and changes the nature of the fully developed temperature distribution.

For a Newtonian fluid in a cylindrical duct, $Nu_{fd} = 9.6$ was found by Ou and Cheng [63] and the present solution confirms that. The present study shows that for non-zero Br the asymptotic Nusselt numbers also do not depend on Pe values, whereas for zero Br the asymptotic Nusselt numbers depend on Pe values and the asymptotic Nusselt number increases slightly with a decrease in Pe. The behavior of the Nusselt number variation can be explained from the values of $(\theta_w - \theta_b)$ and $\partial\theta/\partial r^*|_{r^*=1/2}$ (see Eq.(2.83)). As can be seen, for $Br \neq 0$ in the case of heating ($Br > 0$), a minimum value of Nusselt number appears at some axial distance. In the case of cooling ($Br < 0$), Nu attains values of plus and minus infinities in the thermally developing region. These behaviors of the Nusselt number were discussed in [63], [66] and [71]. The numerical values of the asymptotic Nusselt numbers are given in the figures for $Br \neq 0$ and for $Br = 0$.

Laminar heat transfer in cylindrical and parallel-plates ducts has been studied

very extensively in the past. The heat transfer results are compared with the available data in the literature. The circles and triangles show the available data by previous researchers for $Pe \to \infty$ and for $Pe = 10$, respectively. The circles in the thermally developing region show the results by Prusa and Manglik [72] and McKillop [73]. As can be seen, even at small values of z^*, the agreement is excellent. The numerical values of Nu in the fully developed region corresponding to the solid circles shown in Fig.2.6, are the results calculated from the following equation by Dang [38] for non-zero Br as

$$Nu_{\text{fd}} = \frac{2(3n+1)(5n+1)}{n(4n+1)} \tag{2.84}$$

The triangles represent the results reported by Hennecke [47]. Hennecke stated that his results were not intended to be completely valid in the immediate vicinity of $z^* = 0$. This explains the slight differences for $z^* \leq 0.005$.

The present study reveals that for a given Peclet number there is a single fixed point regardless of Br in the thermally developing region, as seen in Fig.2.6, if the upstream region for $z^* \leq 0$ is included in the analysis. As the power-law index decreases, the position of the fixed point shifts closer to $z^* = 0$, i.e., to the wall temperature jump location. The occurrence of fixed points can be also seen in Nield et al., [42] who considered both viscous dissipation and fluid axial heat conduction effects in a parallel plate channel with a step change in wall temperature.

Figure 2.7 displays the conventional Nusselt number at the walls of the parallel-plates duct. The results are compared with the available data by the previous researchers [38], [62] and [74]. The numerical values of Nu in the fully developed region corresponding to the solid circles shown in Fig.2.7, are the results calculated from the following equation by Dang [38] for non-zero Br as

$$Nu_{\text{fd}} = \frac{2(4n+1)(5n+2)}{n(3n+1)} \tag{2.85}$$

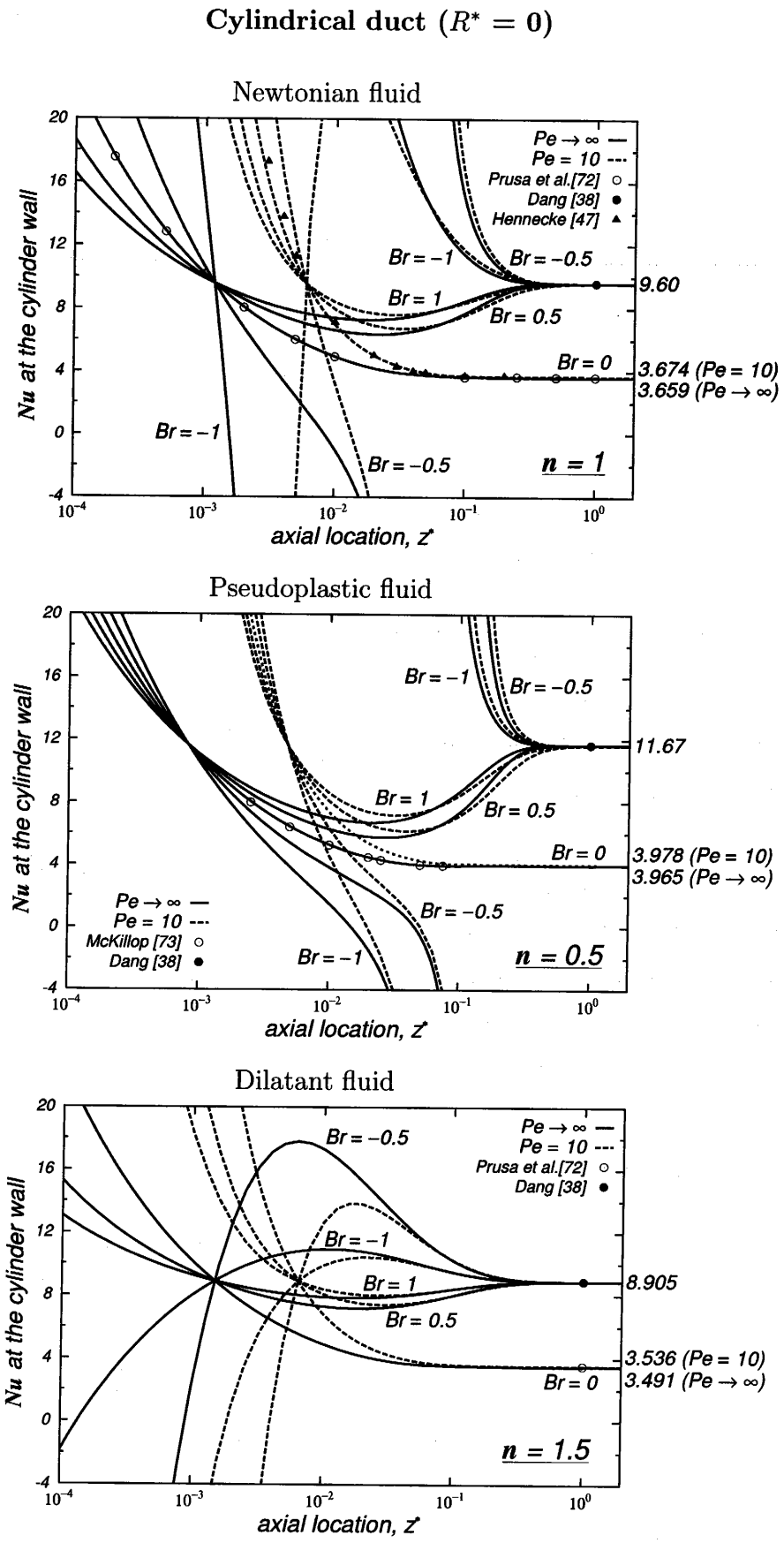

Fig. 2.6: Effects of Brinkman number and Peclet number on Nusselt number for Newtonian ($n = 1$), pseudoplastic ($n = 0.5$) and dilatant ($n = 1.5$) fluids, Cylindrical duct ($R^* = 0$)

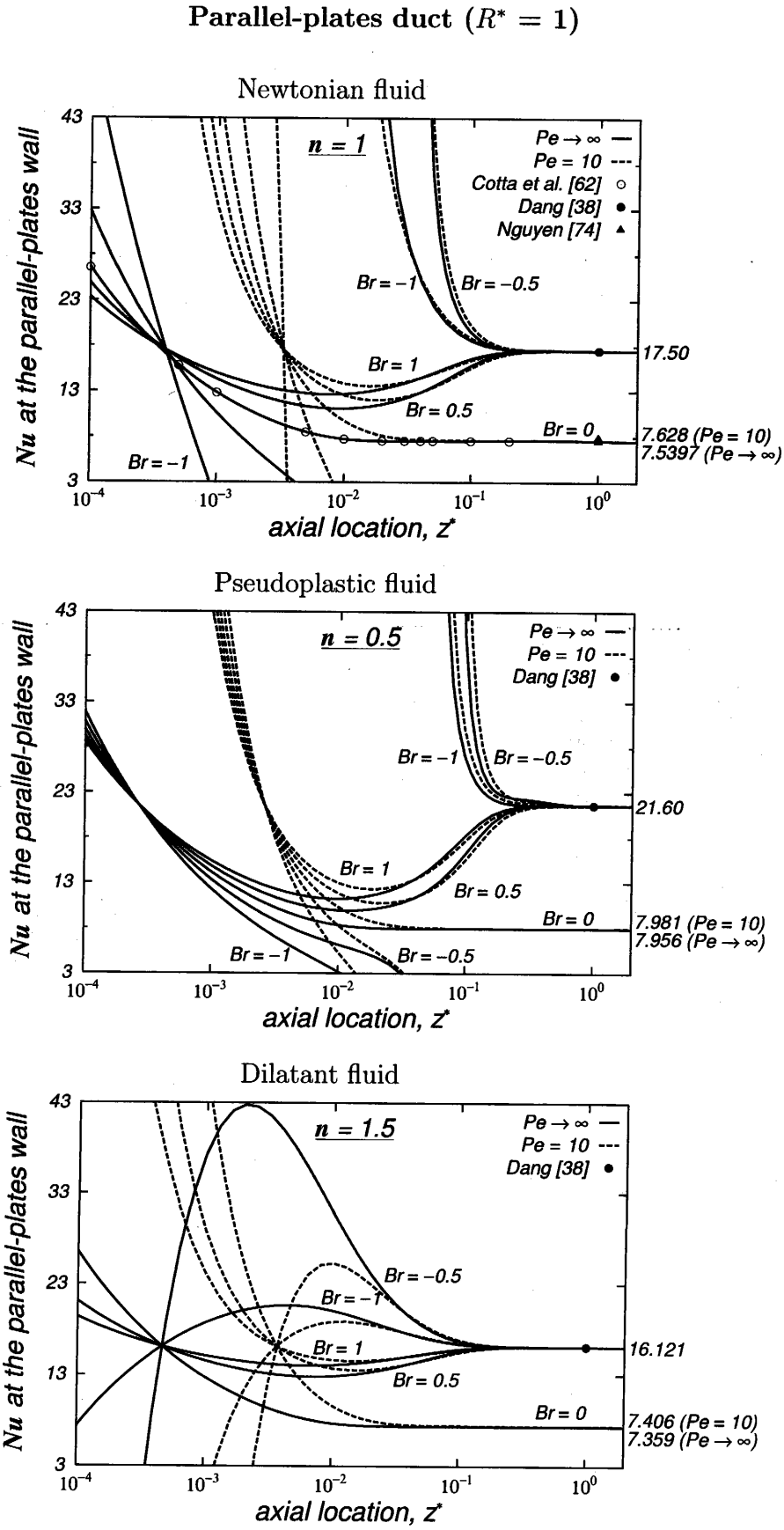

Fig. 2.7: Effects of Brinkman number and Peclet number on Nusselt number for Newtonian ($n = 1$), pseudoplastic ($n = 0.5$) and dilatant ($n = 1.5$) fluids, Parallel-plates duct ($R^* = 1$)

2.5.2 Analytical solution for $R^* = 0$

In this section, some results given in Section 2.5.1 are used to validate the calculation methodology (described in Section 2.4) applied in this work. At this point a comparison between the solutions obtained numerically and analytically is of interest. In this section, an analytical solution for the local Nusselt number will be obtained for a limiting case. The case considered here is a situation of negligible fluid axial heat conduction ($Pe \rightarrow \infty$) for a Newtonian fluid ($n = 1$) flowing in a cylindrical duct ($R^* = 0$). An additional purpose of this section is to derive the coordinates corresponding to the fixed point at the plot of Nusselt curves for the Newtonian fluid ($n = 1$) in a cylindrical duct by considering the viscous dissipation effect alone or by neglecting the fluid axial heat conduction ($Pe \rightarrow \infty$).

It is possible to obtain the expression for the Nusselt number by applying the solutions in infinite series by Brown and Newman [2] (pp. 101-102). Their solutions were for a Poiseuille flow of a Newtonian fluid in a cylindrical duct. Following Brown and Newman [2], the energy equation with the viscous dissipation term for a Poiseuille flow of a Newtonian fluid flowing in a cylindrical duct can be written as

$$(1 - r^{*2})\frac{\partial \theta}{z^*} = \frac{1}{r^*}\frac{1}{\partial r^*}\left(r^*\frac{\partial \theta}{\partial r^*}\right) + 16\ Br\ r^{*2} \tag{2.86}$$

$$\theta(0, r^*) = 1 + Br(1 - r^{*4}), \quad \theta(z^*, 1) = \theta_w = 0 \quad \text{and} \quad \partial\theta(z^*, 0)/\partial r^* = 0 \tag{2.87}$$

It should be noted that in this section the definitions of the dimensionless parameters including the dimensionless velocity and the dimensionless temperature follow as Brown [2]. $r^* = 0.5$ in the present work is equivalent to $r^* = 1$ in Brown's definition. Also the bulk temperature in Ref.[2] is $\theta_b = 4\int_0^1 \theta\ u^*\ r^*\ dr^*$.

The temperature distribution can be obtained in the following form:

$$\theta(z^*, r^*) = \Phi(z^*, r^*) + \theta_{fd}(r^*) \tag{2.88}$$

The function $\Phi(z^*, r^*)$ is to be solved in the form of

$$\Phi(z^*, r^*) = \sum_{n=1}^{\infty} C_n R_n(r^*) exp(-2\lambda_n^2 z^*) \tag{2.89}$$

θ_{fd} is the fully developed temperature profile and a function of r^* alone. For Newtonian fluids it is

$$\theta_{fd}(r^*) = Br(1 - r^{*4}) \tag{2.90}$$

The resulting equation is then given as

$$(1-r^{*2})\frac{\partial\Phi}{\partial z^*}=\frac{1}{r^*}\frac{\partial}{\partial r^*}\left(r^*\frac{\partial\Phi}{\partial r^*}\right) \tag{2.91}$$

$$\Phi(0,r^*)=1,\quad \Phi(z^*,1)=0 \tag{2.92}$$
$$\text{and}\quad \partial\Phi(z^*,0)/\partial r^*=0$$

in which the function $\Phi(z^*,r^*)$ and its inlet and boundary conditions are identical to those in Ref.[2]. The first 121 terms of the series of C_n, $R_n(r^*)$ and λ_n have been applied. Up to the first 11 terms were taken from Brown [2] and the rest of the terms were determined following Newman [2] to obtain the function $\Phi(z^*,r^*)$. By applying the obtained temperature distribution, $\theta(z^*,r^*)$, the local Nusselt number is found as

$$Nu=\frac{2}{\theta_w-\theta_b}\left(\frac{\partial\theta}{\partial r^*}\right)_{r^*=1}=\frac{8Br+4a}{5/6Br+8b} \tag{2.93}$$

where

$$a=\sum_{n=1}^{\infty}G_n exp(-2\lambda_n^2 z^*)$$
$$b=\sum_{n=1}^{\infty}(G_n/\lambda_n^2)exp(-2\lambda_n^2 z^*) \tag{2.94}$$
$$G_n=-(C_n/2)R'(1)$$

In order to obtain the values of the coordinates corresponding to the fixed point, the following calculations have been done. At the fixed point, the Nusselt number values are the same for the different Brinkman numbers or do not depend on the Brinkman number values. Therefore, for solving the coordinates of the fixed point, the derivative of Nusselt number with respect to Brinkman number is applied. The derivative $\partial Nu/\partial Br$ is zero at the axial location of the fixed point.

$$\frac{\partial Nu}{\partial Br}=\frac{8(5/6Br+8b)-5/6(8Br+4a)}{(5/6Br+8b)^2}=0$$

or

$$\frac{8Br+4a}{5/6Br+8b}=9.6 \tag{2.95}$$

In view of Eq.(2.93) and Eq.(2.95), it is seen that the local Nusselt number is independent of the Brinkman number, if the local Nusselt number is 9.6. Therefore the ordinate of the fixed point in this case is 9.6. Also Eq.(2.93) and Eq.(2.94) ensure that the local Nusselt number is 9.6 if the axial coordinate is large or

$$\lim_{z^*\to\infty}Nu=9.6 \tag{2.96}$$

On the other hand, the abscissa of the fixed point in the thermally developing region has been obtained from Eq.(2.95) by applying the Newtonian method. The abscissa of the fixed point or the axial location corresponding to the fixed point was found to be z^* =1.2e-3.

For the case of negligible fluid axial heat conduction ($Pe \rightarrow \infty$) within a Newtonian fluid ($n = 1$) in a cylindrical duct ($R^* = 0$), the numerically obtained solutions were reproduced the analytical solution with Eq.(2.93). They have been compared elsewhere [75] without distinguishable differences for the different Brinkman number values.

2.6 Results and Discussions of the Ⓣ T.B.C

The temperature field of the thermally developing flow under the Ⓣ thermal boundary condition has been obtained by solving the transformed energy equation Eq.(2.65) with Eq.(2.68). The objective herein is to display the results and to provide explanations for the solutions.

The results are presented in the form of graphs and compared to the available data by other authors. Also the results, which are given as the temperature fields and the corresponding Nusselt numbers, are discussed. The consideration is given to the effects of the problem governing parameters determined in Section 2.3.3.

2.7 Temperature Distributions of the Ⓣ T.B.C

The discussion of results begins with the presentation of the temperature profiles in an annular duct. The temperature field in the annular duct can be plotted from the results of the numerical calculation for the forced convection heat transfer. The effects of two relevant parameters, i.e. the Brinkman number, the Peclet number on the developing temperature profiles are shown for the three different fluid flow indices, corresponding to Newtonian, pseudoplastic and dilatant fluids in Figs.2.8 - 2.10. The results are given for an annular duct of radius ratio, $R^* = 0.5$.

In the following figures, $\xi = 0$ corresponds to the core tube wall and $\xi = 1$ is the outer tube wall. z^* is the axial location and in these figures the temperature profiles are shown at the axial locations of $z^* = 5 \times 10^{-3}$; 2.5×10^{-2}; 6.3×10^{-2}; 0; and 5.4×10^{-1}. At the location of $z^* = 0$, the wall temperature jump occurs.

The radial temperature profiles in Fig.2.8(a), Fig.2.9(a) and Fig.2.10(a) are ob-

tained on the basis of the assumption that the viscous dissipation and the fluid axial heat conduction are negligible or for the case of $Br = 0$ and $Pe \to \infty$. It is seen, for $Br = 0$ and $Pe \to \infty$, at $z^* = 0$ the dimensionless temperature of the fluid is zero.

The temperature profiles in Fig.2.8(b), Fig.2.9(b) and Fig.2.10(b) are obtained after disregarding the assumption of negligible viscous dissipation while the fluid axial heat conduction is negligible or for the case of $Br = 0.1$ and $Pe \to \infty$. The temperature profiles in Fig.2.8(c), Fig.2.9(c) and Fig.2.10(c) are to show the fluid axial heat conduction effect or for the case of $Br = 0$ and $Pe = 10$. The temperature profiles in Fig.2.8(d), Fig.2.9(d) and Fig.2.10(d) are for $Br = 0.1$ and $Pe = 10$.

2.7.1 Effect of Br on the temperature distributions

In the respect of the effect of Br on the dimensionless temperature, the left hand side plots (for $Br = 0$) in Figs.2.8 - 2.10 can be compared with the right hand side ones (for $Br = 0.1$). As seen in Figs.2.8(b), 2.9(b) and 2.10(b), the temperature at $z^* = 0$ is definitely deviated from 0. For the (T) thermal boundary condition, the temperature of both tube walls was set at the same level as the entering fluid temperature for $z^* \leq 0$. This increase in the unheated wall region shows that the fluid temperature increases before the fluid reaches the heated wall region because of the heat generated by the viscous dissipation and the heat generation due to viscous dissipation in the flowing fluid acts like a heat source.

2.7.2 Effect of Pe on the temperature distributions

In the respect of the effect of Pe on the dimensionless temperature, the left upper plots (for $Pe \to \infty$) in Figs.2.8 - 2.10 can be compared with the lower ones (for $Pe = 10$). Figures 2.8(c), 2.9(c) and 2.10(c) show that the fluid temperature is increased in the unheated wall region. Since both the walls' temperature was set at the same level as the entering fluid temperature in the unheated wall region, this increase is due to the heat conducted from downstream into the region of $z \leq 0$. In Figs.2.8(a), 2.9(a) and 2.10(a), which show the case of $Pe \to \infty$, no temperature increase due to the fluid axial heat conduction is observed in the unheated wall region.

2.7.3 Effect of n on the temperature distributions

In the sequence of Figs.2.8 - 2.10, the developing temperature profiles are shown for three different fluid flow indices, corresponding to Newtonian, pseudoplastic and

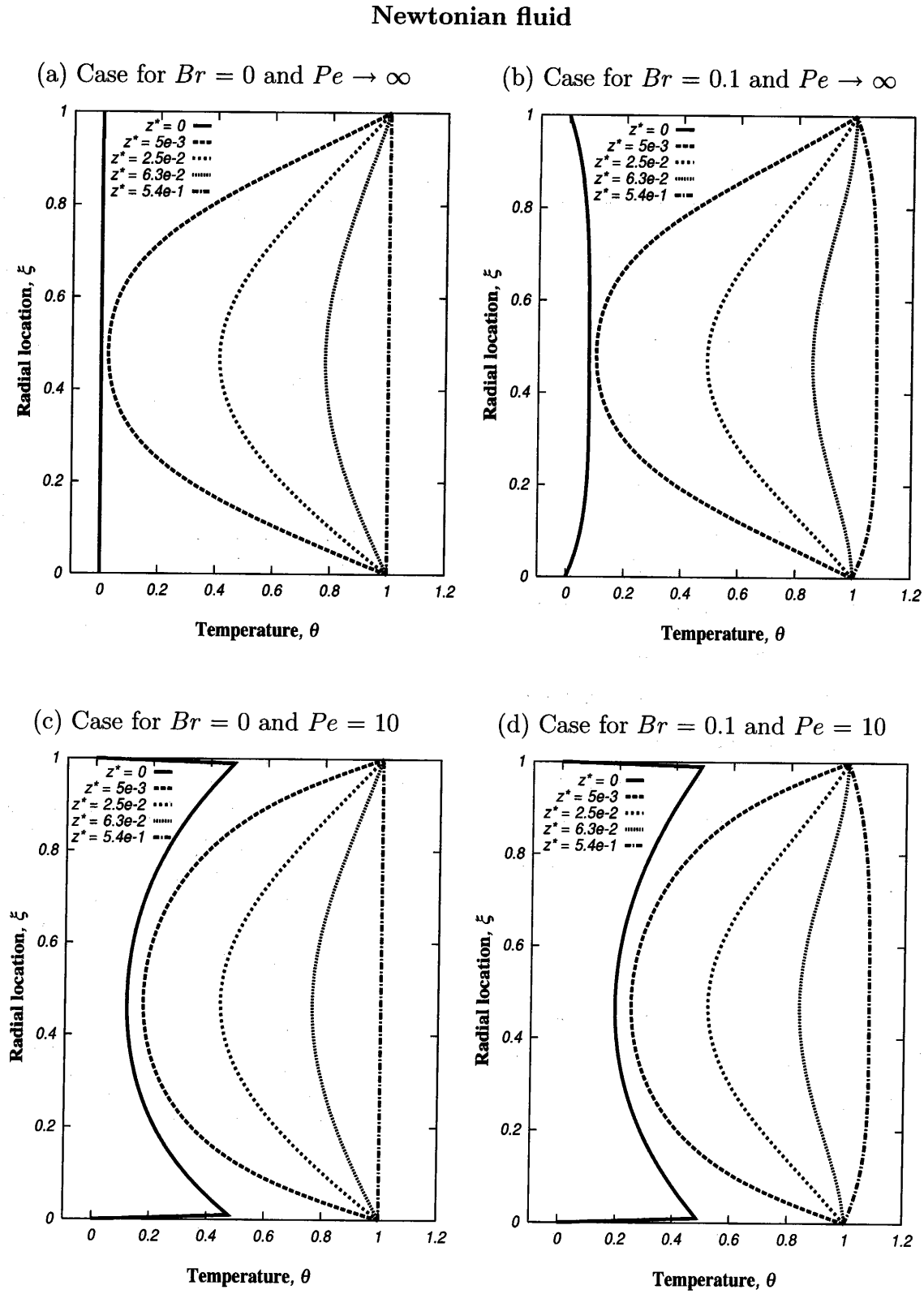

Fig. 2.8: Developing temperature profiles of a Newtonian fluid ($n = 1$) in an annular duct of $R^* = 0.5$

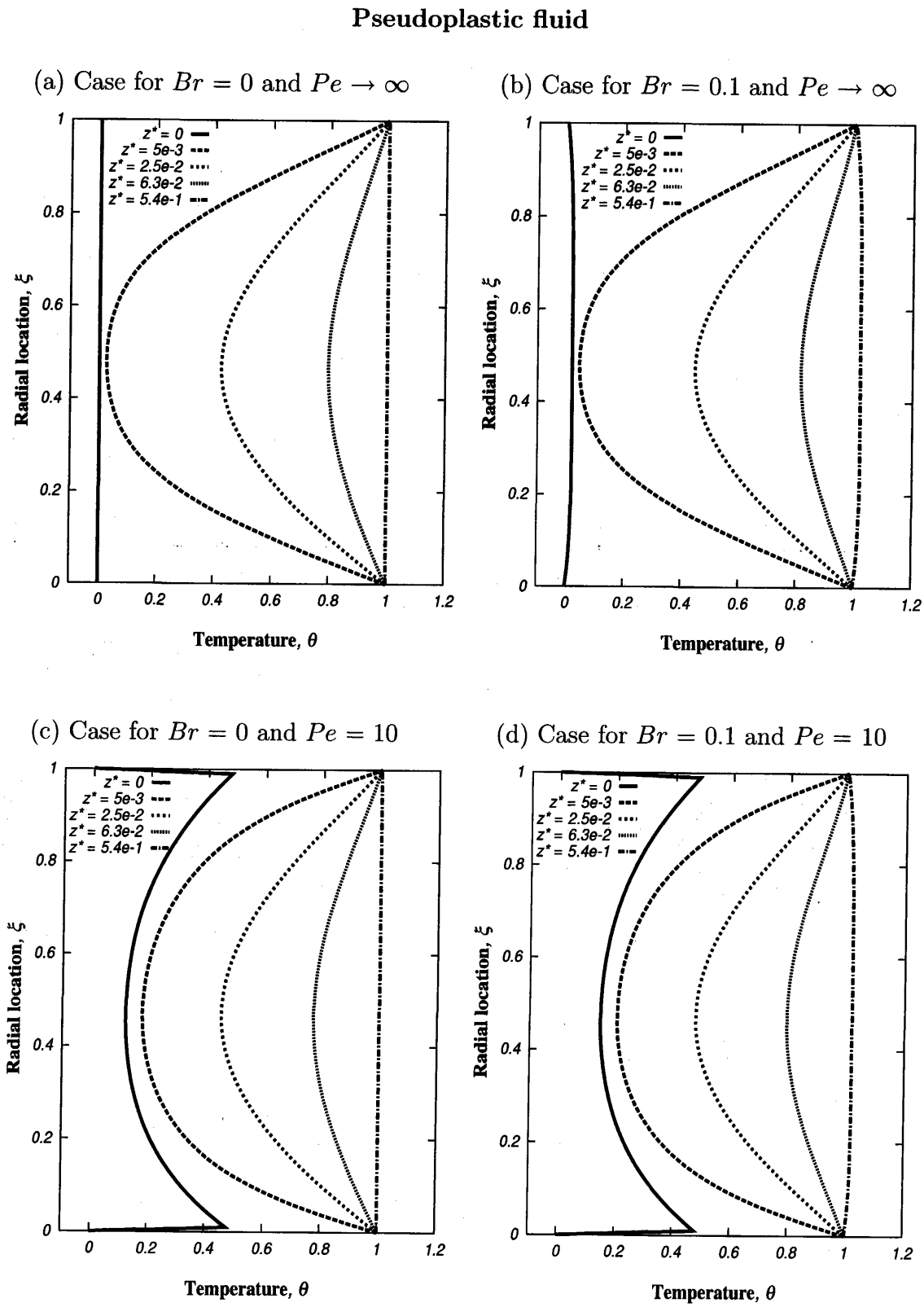

Fig. 2.9: Developing temperature profiles of a pseudoplastic fluid ($n = 0.5$) in an annular duct of $R^* = 0.5$

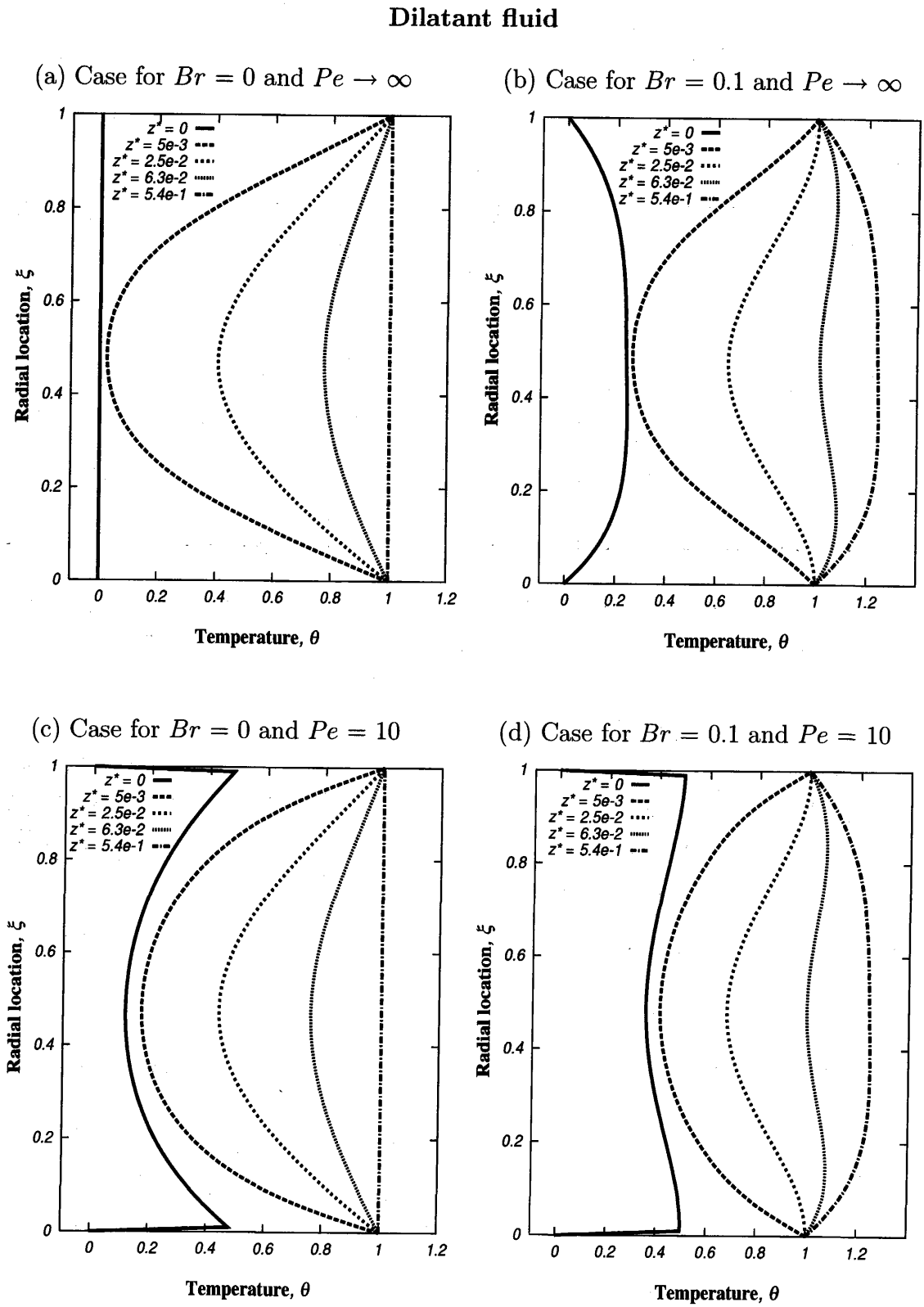

Fig. 2.10: Developing temperature profiles of a dilatant fluid ($n = 1.5$) in an annular duct of $R^* = 0.5$

dilatant fluids and the effect of flow index, n, can be seen.

The temperature distributions show quite similar behaviors for different fluids. The response of the Newtonian fluid to viscous heating is more pronounced than that of the pseudoplastic fluid but less remarkable than the dilatant fluid.

The effect of flow index, n, on heat transfer with fluid axial heat conduction is seen insignificant unlike the viscous dissipation included in heat transfer.

2.8 Nusselt Numbers of the Ⓣ T.B.C

In Figs. 2.11 - 2.13, the heat transfer results are illustrated in terms of a conventional Nusselt number for the three different radius ratios ($R^* = 0, 2, 0.5, 0.8$). In these figures the Nusselt number at the inner core, Nu_i defined by Eq.(2.42), and that at the outer cylinder, Nu_o defined by Eq.(2.43), are shown as a function of the axial coordinate with the Brinkman number and the Peclet number as parameters. Figure 2.11 shows the Nusselt numbers for a Newtonian fluid, whereas Fig.2.12 and Fig.2.13 are for pseudoplastic ($n = 0.5$) and dilatant ($n = 1.5$) fluids, respectively. The Nusselt numbers for all the cases tend to asymptotically approach some constants as the dimensionless axial distance, z^*, becomes significantly large because of full development of the temperature field.

It is worthwhile to compare the present results with the available data. In Fig.2.11, our results are compared with the data by Shah and London [2] and Weigand, et al. [14]. The circles are the solutions reported in Ref.[2] (p. 293). The solid circles and the solid triangles are the results reported in Ref.[14] for $Pe = 300$ and for $Pe = 10$, respectively. The agreement of our results with the available data is excellent for the fully developed region when both the viscous dissipation and fluid axial heat conduction are neglected [2]. It should be noted that the Nusselt curves of the present solution are given for $Pe \to \infty$ while the solid circles are the solution by Weigand, et al. [14] for $Pe = 300$.

In Sections 2.8.1 - 2.8.5, the discussions of the results on Figs.2.11 - 2.13 are given.

2.8.1 Effect of Br on the Nusselt numbers

In this study, according to the Brinkman number definition, for the negative Brinkman numbers the fluid is considered as being cooled from the wall and the positive Brinkman numbers show that the fluid is being heated. It is well known

Newtonian fluid

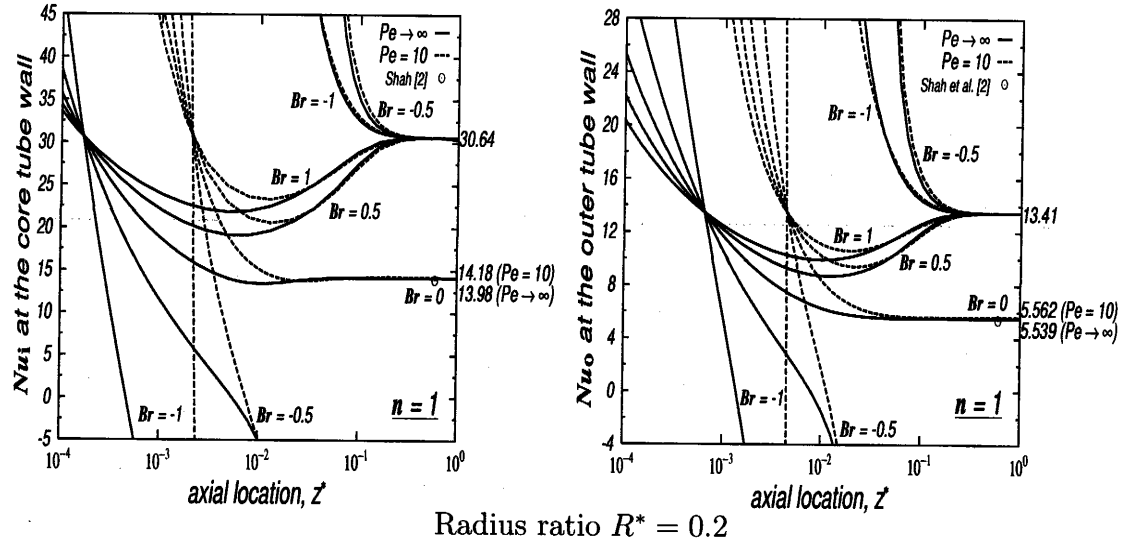

Radius ratio $R^* = 0.2$

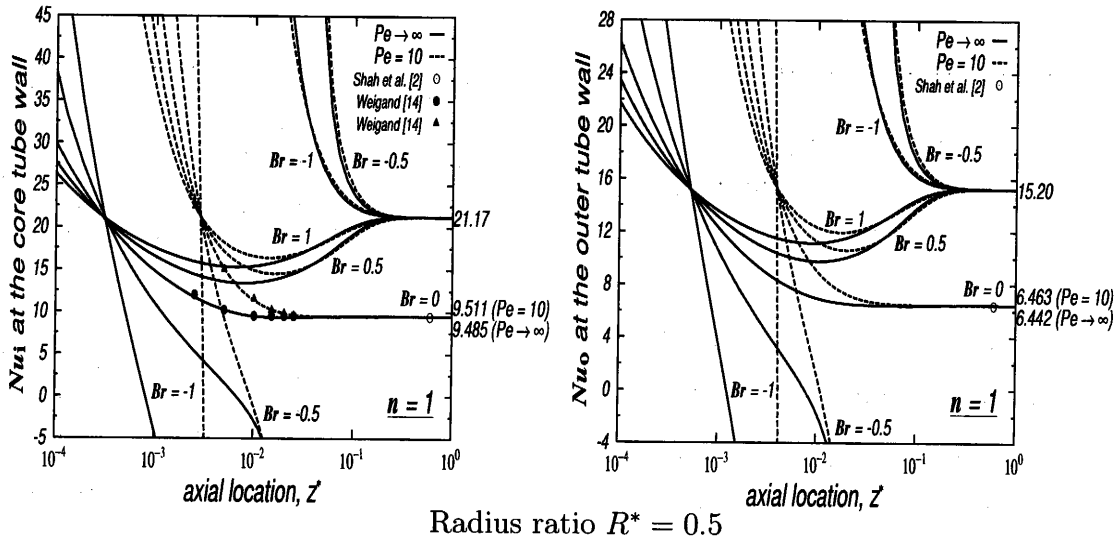

Radius ratio $R^* = 0.5$

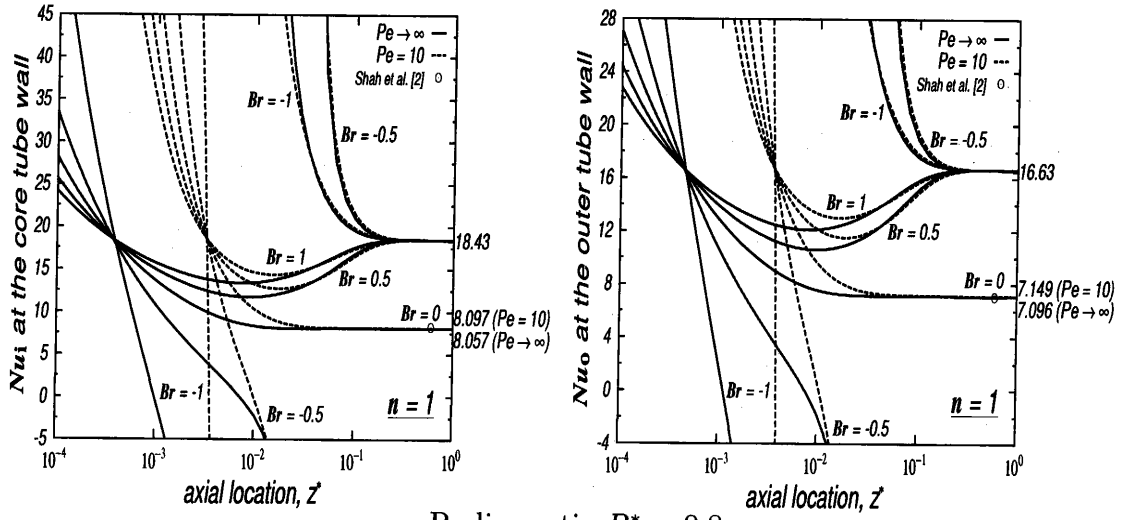

Radius ratio $R^* = 0.8$

Fig. 2.11: Local Nusselt number for a Newtonian fluid ($n = 1$) (Nu_i at the inner core and Nu_o at the outer cylinder)

Pseudoplastic fluid

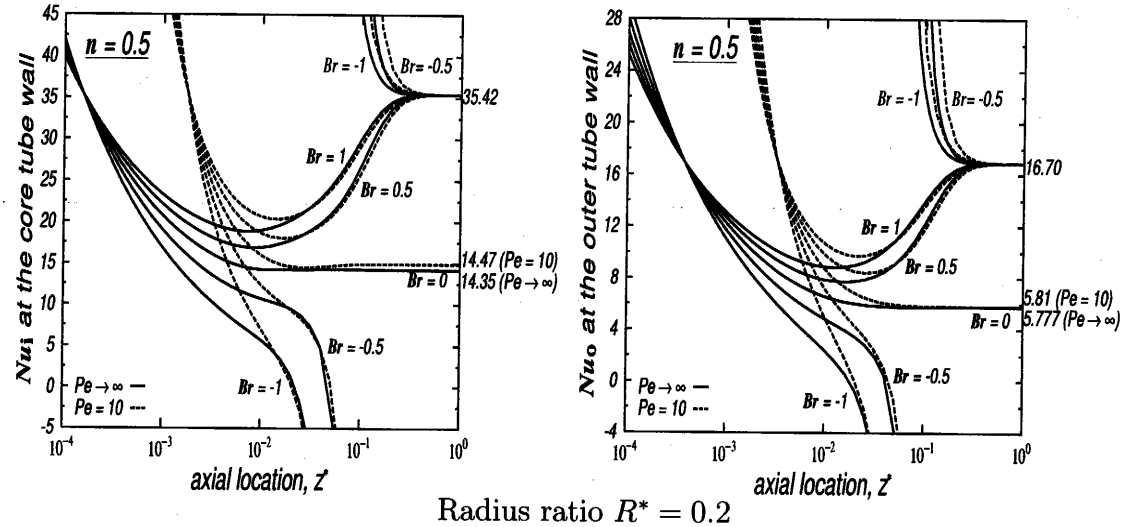

Radius ratio $R^* = 0.2$

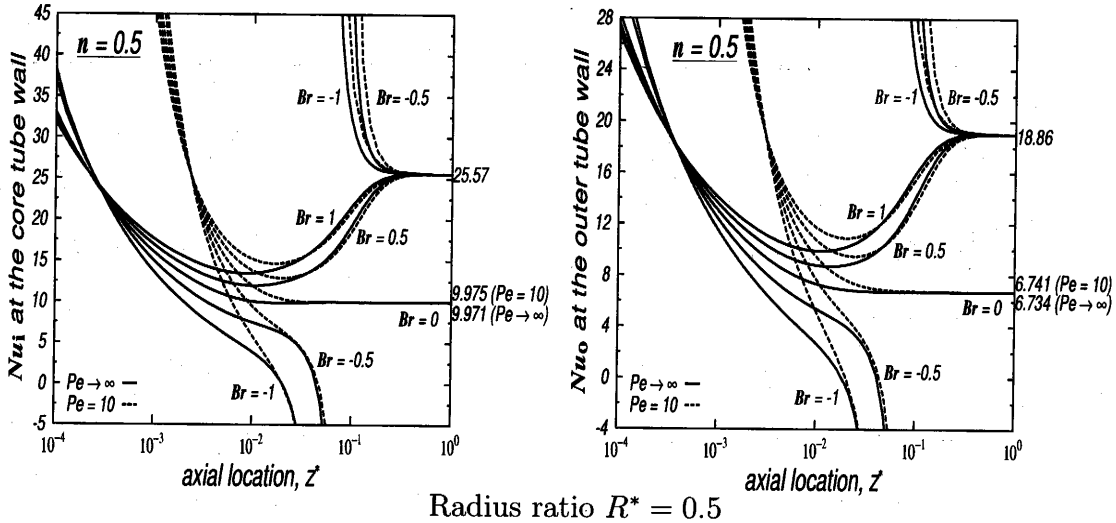

Radius ratio $R^* = 0.5$

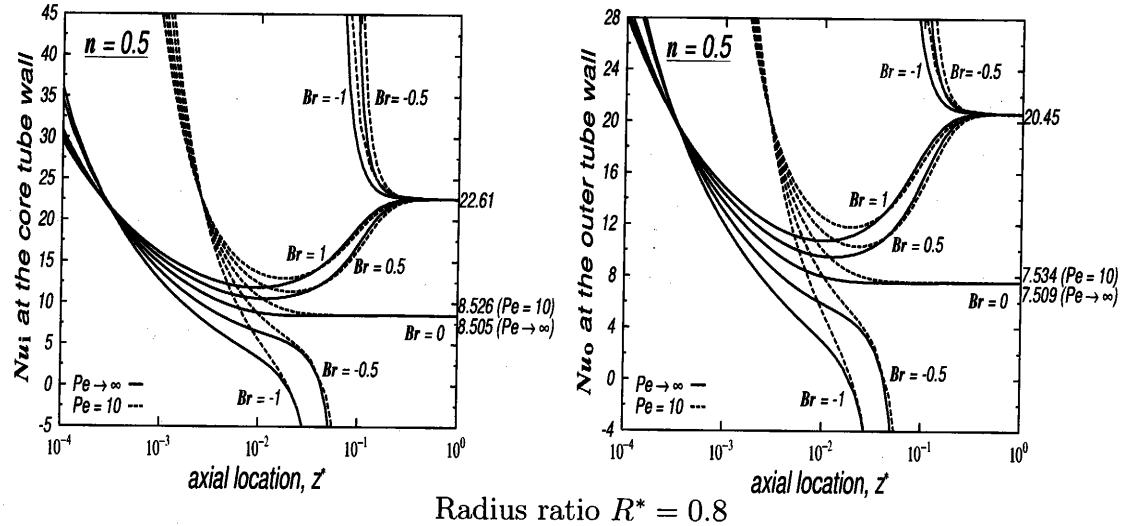

Radius ratio $R^* = 0.8$

Fig. 2.12: Local Nusselt number for a pseudoplastic fluid ($n = 0.5$) (Nu_i at the inner core and Nu_o at the outer cylinder)

Dilatant fluid

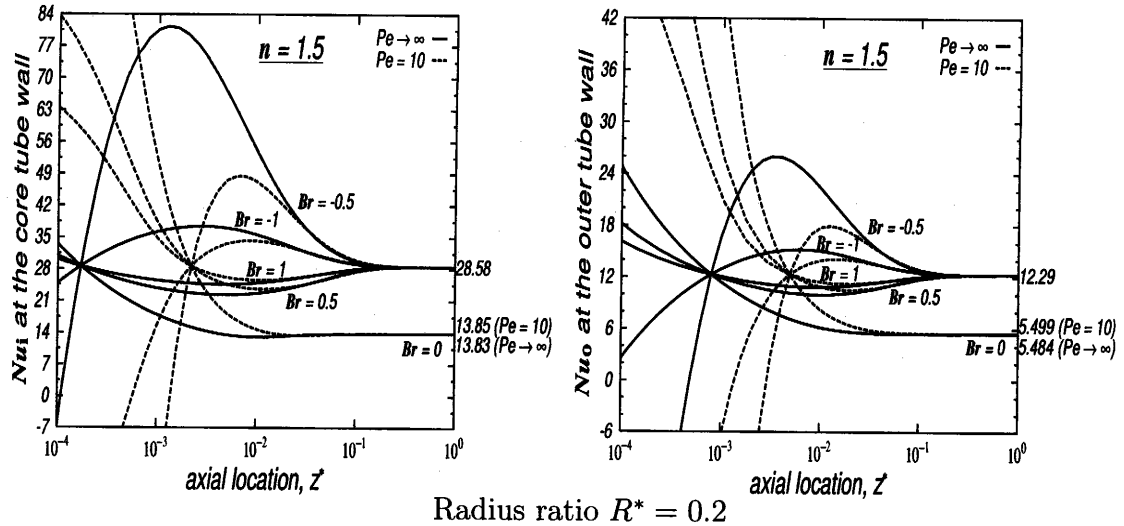

Radius ratio $R^* = 0.2$

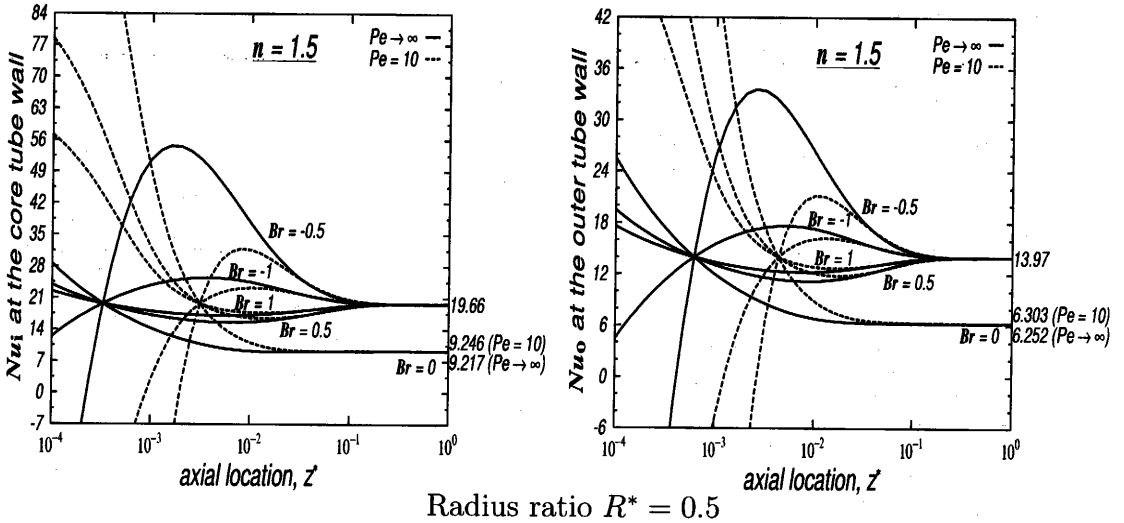

Radius ratio $R^* = 0.5$

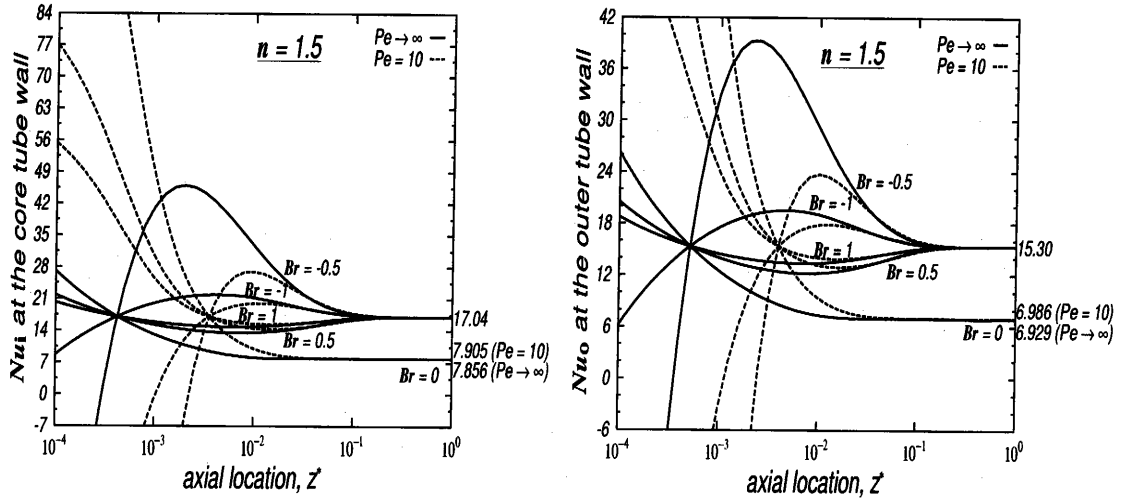

Radius ratio $R^* = 0.8$

Fig. 2.13: Local Nusselt number for a dilatant fluid ($n = 1.5$) (Nu_i at the inner core and Nu_o at the outer cylinder)

that for the Ⓣ thermal boundary condition, in the fully developed region, all non-zero Br cases result an equal value of the asymptotic Nusselt number [63].

Another relevant feature shown in Figs. 2.11 - 2.13 is that the plots show that the thermal entrance length increases due to the viscous dissipation and the flow first reaches the fully developed condition as if there is no viscous heating.

2.8.2 Effect of Pe on the Nusselt numbers

In Figs.2.11 - 2.13, the solid lines represent the case of negligible fluid axial heat conduction ($Pe \to \infty$) and the dotted lines are for $Pe = 10$. It can be seen that the Nusselt number increases with decreasing Peclet number for a given value of z^* in the thermal entrance region. For a given Peclet number, there is a fixed point where the Nusselt number values are equal for all Br in the thermally developing region.

Another relevant feature shown in the figures is that the plots show that the thermal entrance length increases due to the fluid axial heat conduction.

2.8.3 Effect of n on the Nusselt numbers

The heat transfer results show quite similar behaviors for different fluids in Figs. 2.11 - 2.13. For non-Newtonian fluids, the Nusselt number increases with decreasing a Peclet number for a given value of z^* in the thermal entrance region just as it does for the Newtonian fluid.

With increasing n, the value of z^* corresponding to the fixed point increases for both Nu_{i} and Nu_{o}.

When the viscous dissipation is included in the study, the Nusselt numbers for heat transfer to the Newtonian fluid are higher than those to the dilatant fluid but less than those to the pseudoplastic fluid.

The response of the Newtonian fluid to viscous heating is more pronounced than that of the pseudoplastic fluid but less remarkable than the dilatant fluid.

The effect of flow index, n, on heat transfer with fluid axial heat conduction is seen insignificant unlike the viscous dissipation included in heat transfer.

2.8.4 Fixed points

An appearance of the fixed points in the Nusselt curves are seen in Figs. 2.11 - 2.13. The location of the fixed point is found to depend on the flow index, n, and the radius ratio, R^*. Such an appearance of fixed points was also shown by Nield,

et al. [42]. In their results for the axial development of Nu, it is seen that there is a single fixed point independent of Br in the thermally developing region and the value of the Nusselt number at this fixed point is equal to that at the fully developed region in the case of non-zero Br.

The present solutions for the (T) thermal boundary condition demonstrate that the occurrence of the fixed point is entirely a consequence of the upstream preheated region ($z \leq 0$) where the fluid is heated due to the viscous dissipation.

A more detailed discussion for the fixed points and an analytical solution describing the location of the fixed point for a cylindrical duct ($R^* = 0$) are given in Section 2.5.2.

2.8.5 Effect of R^* on the Nusselt numbers

The position of the fixed point shifts closer to $z^* = 0$ for Nu_i as R^* decreases, whereas for Nu_o as R^* increases.

In order to show the radius ratio effects, the heat transfer results are given in Fig.2.14 for the cases of $Pe \to \infty$ and $Br = 0$; $Pe = 10$ and $Br = 1$. The results indicate that the Nusselt number at the inner core wall is greater for smaller radius ratios in the fully developed region. The Nusselt number at the outer cylinder wall is greater for larger radius ratios.

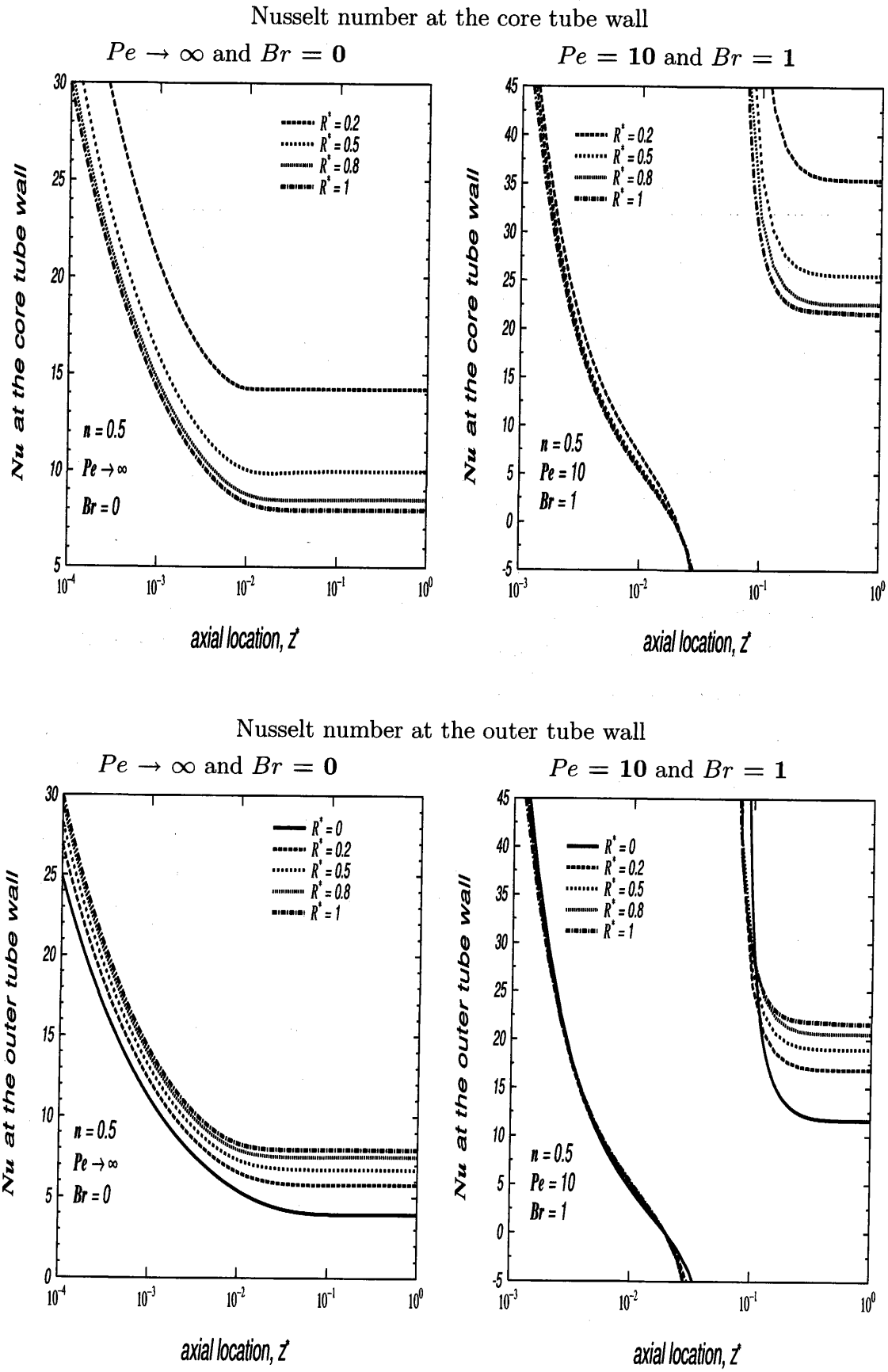

Fig. 2.14: Nusselt numbers for $R^* = 0;\ 0.2;\ 0.5;\ 0.8;\ 1$

2.9 Results and Discussions of the 1st Kind of T.B.C

The temperature field of the thermally developing flow under the 1st kind of thermal boundary condition has been obtained by solving the transformed energy equation Eq.(2.65) with Eq.(2.69). The objective herein is to display the results and to provide explanations for the solutions.

The results are presented in the form of graphs and compared to the available data by other authors. Also the results, which are given as the temperature fields and the corresponding Nusselt numbers, are discussed. The consideration is given to the effects of the problem governing parameters determined in Section 2.3.3.

2.10 Temperature Distributions of the 1st Kind of T.B.C

The temperature profile within the annular duct is discussed first. Figures 2.15 - 2.17 illustrate the developing temperature profiles of Newtonian, pseudoplastic and dilatant fluids flowing in an annular duct of radius ratio, $R^* = 0.5$. The abscissa $\xi = 0$ is the core tube wall and $\xi = 1$ is the outer tube wall. In these figures, the temperature profiles are shown at the axial locations of $z^* = 0$; 2.42×10^{-2}; and 1. At $z^* = 0$, the dimensionless temperature value at the core tube wall jumps from 0 to 1.

The figures in each graph are the temperature profiles under the same conditions except for a change in the fluid axial heat conduction term and the viscous dissipation term. The figures on the left are the temperature profiles under the same condition with the exception of the fluid axial heat conduction. If the figures on the left are compared with the figures on the right, the viscous dissipation effect on the temperature distribution can be observed. The upper figures correspond to the negligible fluid axial heat conduction case or $Pe \rightarrow \infty$. The lower ones show the temperature distributions when $Pe = 10$. If the upper figures are compared with the lower ones the fluid axial heat conduction effect on the temperature distribution can be observed. As the fluid flows, its temperature rises due to the heat input from the wall, from the fluid axial heat conduction and the viscous dissipation. These results display the expected temperature increase. From these figures it can be ob-

served that the fluid temperature increases in the region for $z^* \leq 0$ or before the fluid reaches the heated wall region when $Pe = 10$ and $Br = 0.1$. This indicates that the fluid temperature increase is due to the viscous dissipation and to the fluid axial heat conduction.

2.10.1 Effect of Br on the temperature distributions

As seen in Figs.2.15(b), 2.16(b) and 2.17(b), the dimensionless temperature at $z^* = 0$ is definitely deviated from zero for $Br = 0.1$ and $Pe \to \infty$. This shows that the fluid temperature increases before the fluid reaches the heated wall region because of the heat generated by the viscous dissipation.

2.10.2 Effect of Pe on the temperature distributions

Figures 2.15(c), 2.16(c) and 2.17(c) show that the fluid temperature is increased for $Pe = 10$ in the unheated wall region. Since both the walls' temperature was set at the same level as the entering fluid temperature in the unheated wall region, this increase is due to the heat conducted from downstream into the region of $z \leq 0$.

2.10.3 Effect of n on the temperature distributions

The temperature distributions show quite similar behaviors for different fluids. The response of the Newtonian fluid to viscous heating is more pronounced than that of the pseudoplastic fluid but less remarkable than the dilatant fluid.

The effect of flow index, n, on heat transfer with fluid axial heat conduction is seen insignificant unlike the viscous dissipation included in heat transfer.

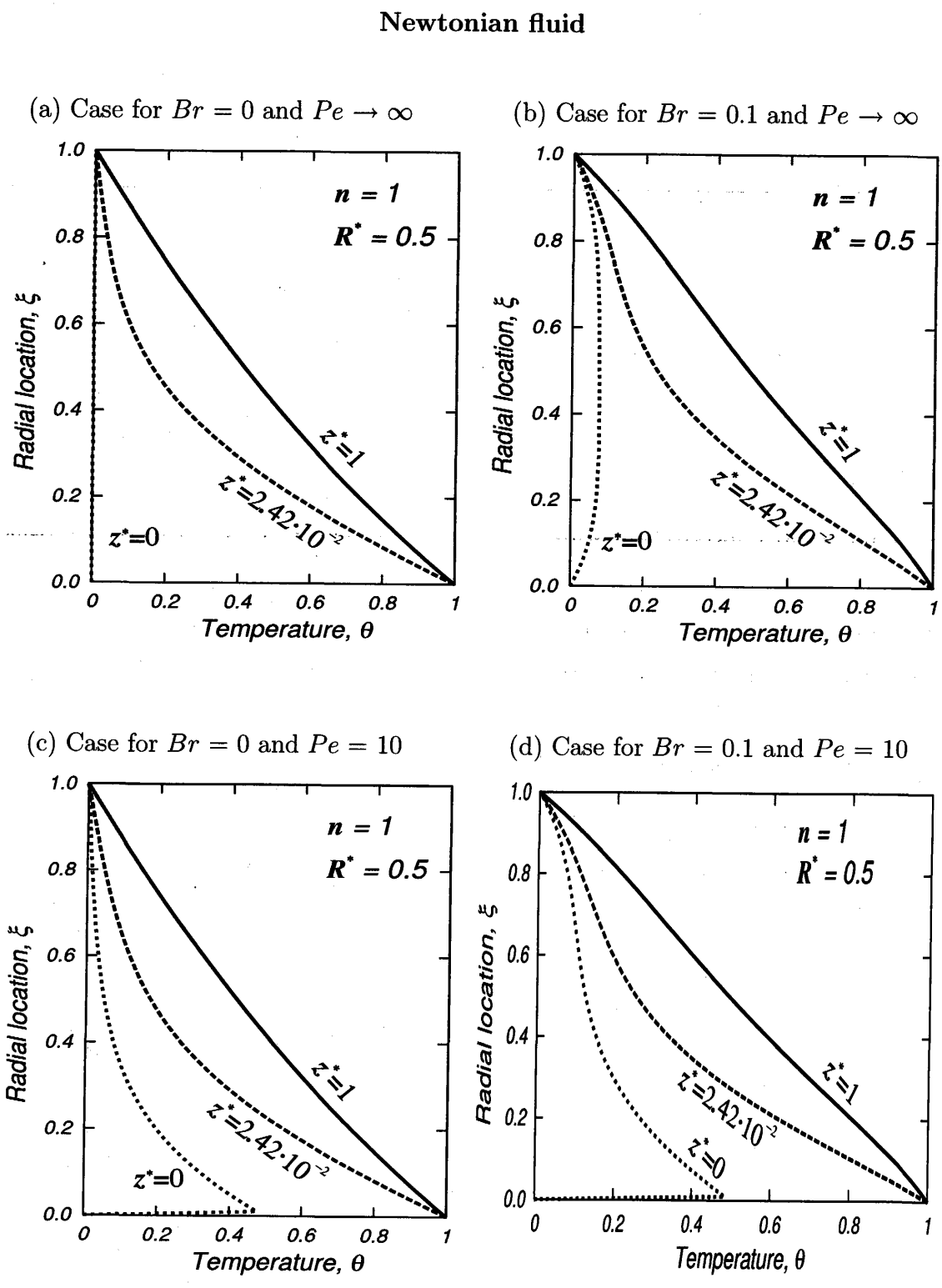

Fig. 2.15: Developing temperature profiles of a Newtonian fluid.
The plots refer to different degrees of viscous dissipation and fluid axial heat conduction

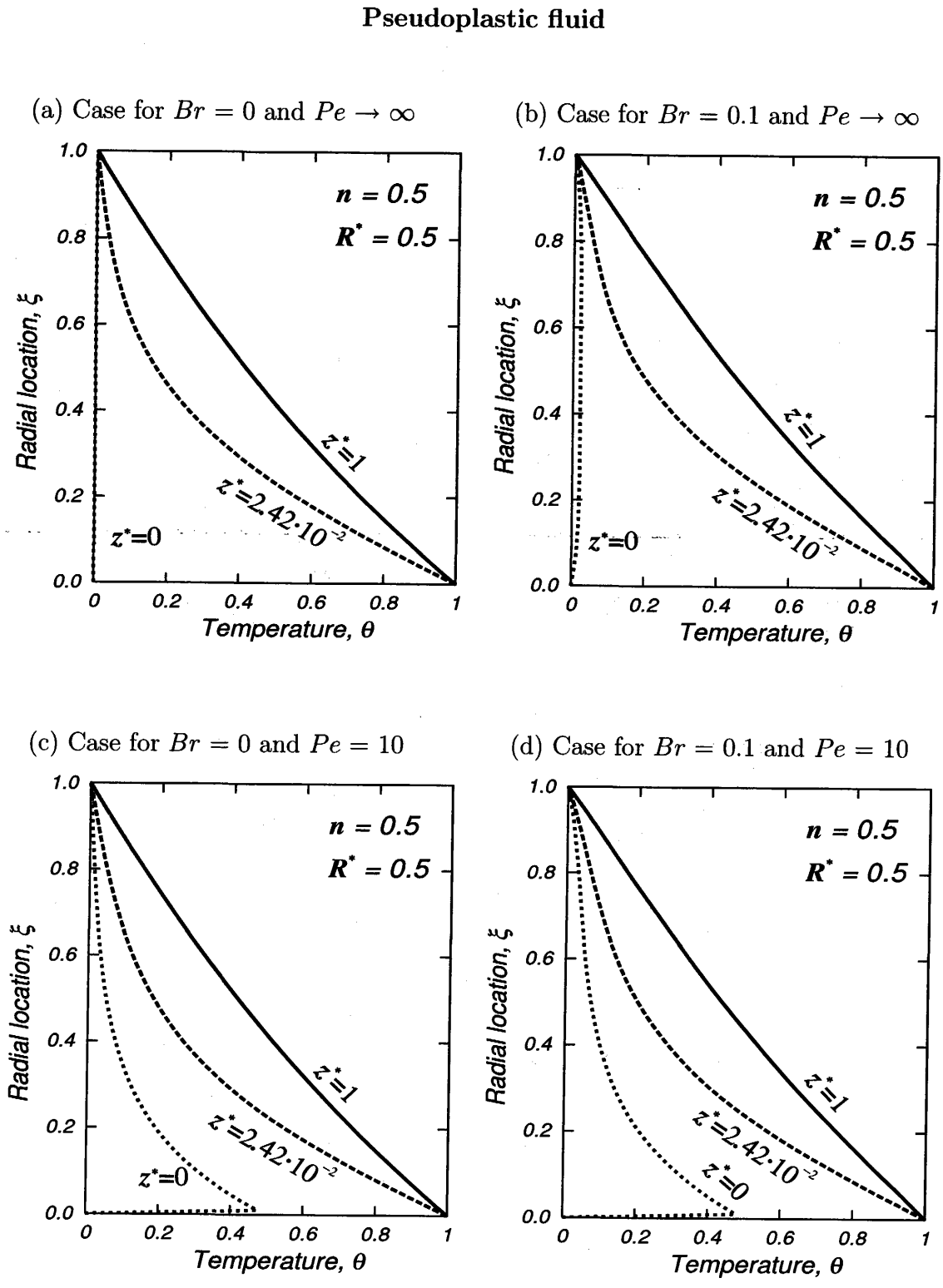

Fig. 2.16: Developing temperature profiles of a pseudoplastic fluid, $n = 0.5$. The plots refer to different degrees of viscous dissipation and fluid axial heat conduction

Dilatant fluid

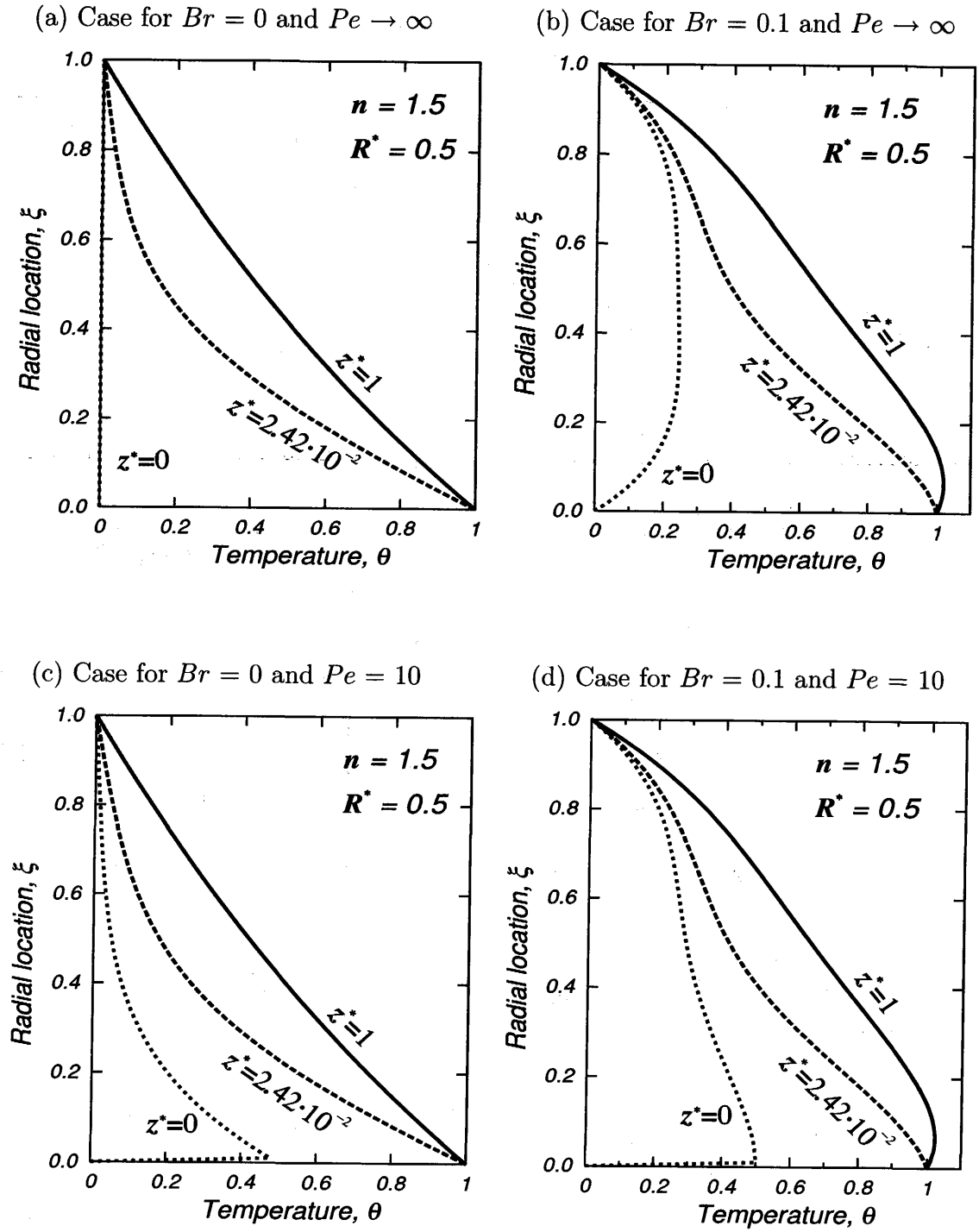

Fig. 2.17: Developing temperature profiles of a dilatant fluid, $n = 1.5$.
The plots refer to different degrees of viscous dissipation and fluid axial heat conduction

2.11 Nusselt Numbers of the 1st Kind of T.B.C

In Figs. 2.18 - 2.20, the heat transfer results are illustrated in terms of a conventional Nusselt number for the three different radius ratios ($R^* = 0.2, 0.5, 0.8$). In these figures the Nusselt number at the inner core, Nu_i defined by Eq.(2.44), and that at the outer cylinder, Nu_o defined by Eq.(2.45), are shown as a function of the axial coordinate with the Brinkman number and the Peclet number as parameters. Figure 2.18 shows the Nusselt numbers for a Newtonian fluid, whereas Fig.2.19 and Fig.2.20 are for pseudoplastic ($n = 0.5$) and dilatant ($n = 1.5$) fluids, respectively.

The case with negligible viscous dissipation and fluid axial heat conduction is compared with the available results in Ref.[2] (p. 304) and Ref.[10] (p. 1702).

In Sections 2.11.1 - 2.11.4, the discussions of the results in Figs.2.18 - 2.20 are given.

2.11.1 Effect of Br on the Nusselt numbers

In Figs.2.18 - 2.20 illustrating the Nusselt numbers at the cylinder walls, the Brinkman number value varies as 0; 0.05 and 0.1.

Including the viscous dissipation causes an increase in Nusselt number at the outer cylinder wall Nu_o, and causes a decrease in Nusselt number at the core cylinder wall Nu_i.

The Nusselt curves, Nu_i, for the core tube are almost identical in the thermally developing region for the different Brinkman numbers.

2.11.2 Effect of Pe on the Nusselt numbers

The effect of fluid axial heat conduction is illustrated in terms of the Peclet number, Pe. In Figs.2.18 - 2.20, the solid lines represent the case of negligible fluid axial heat conduction ($Pe \to \infty$) and the dotted lines are for $Pe = 10$.

It is seen that the Nusselt numbers, Nu_i and Nu_o, at the tube walls increase with a decrease in Peclet number in the thermal entrance region. This implies that the effect of fluid axial heat conduction on heat transfer rate is strong in the thermal entrance region.

The Nusselt number, Nu_i, at the location where the wall heating commences is of course extremely large for $Pe \to \infty$ and rapidly decreases to a limiting value showing the temperature profile is fully developed.

Newtonian fluid

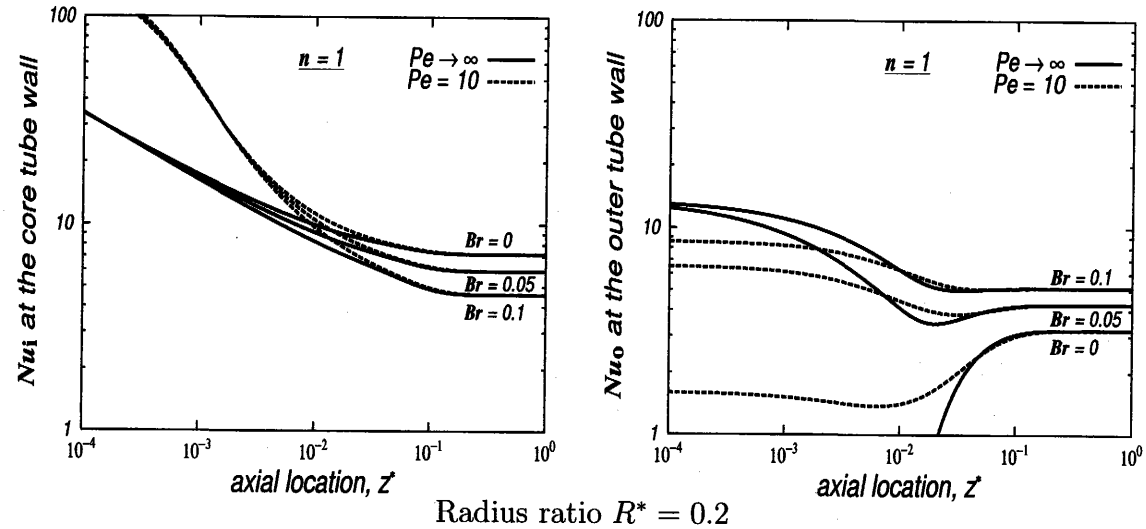

Radius ratio $R^* = 0.2$

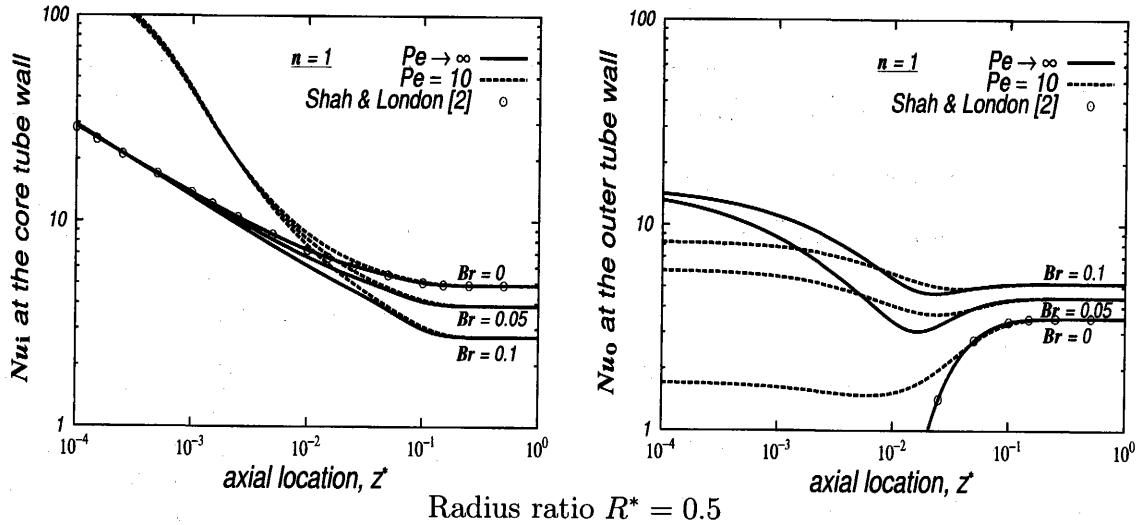

Radius ratio $R^* = 0.5$

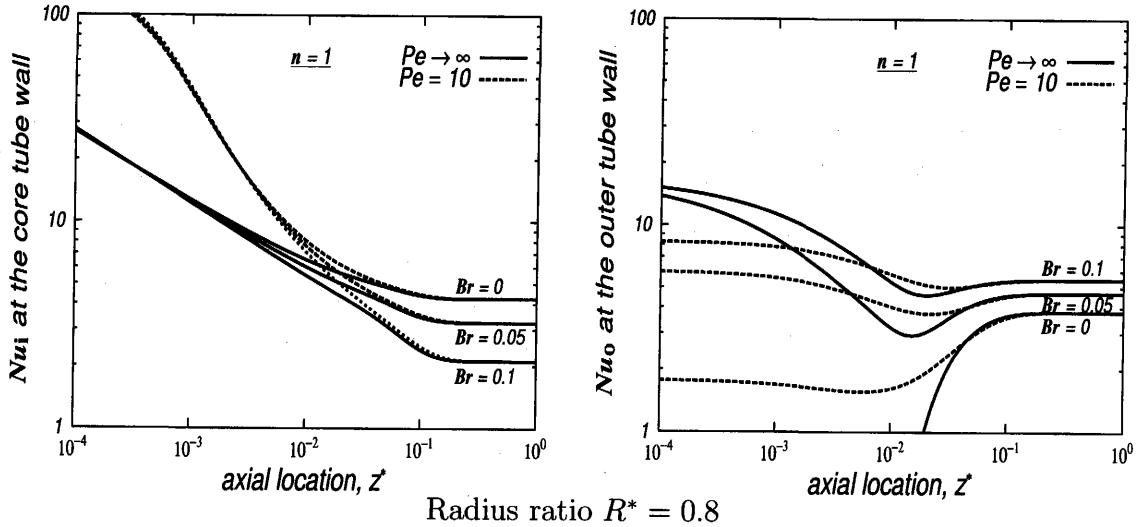

Radius ratio $R^* = 0.8$

Fig. 2.18: Local Nusselt number for a Newtonian fluid ($n = 1$) (Nu_i at the inner core and Nu_o at the outer cylinder)

Pseudoplastic fluid

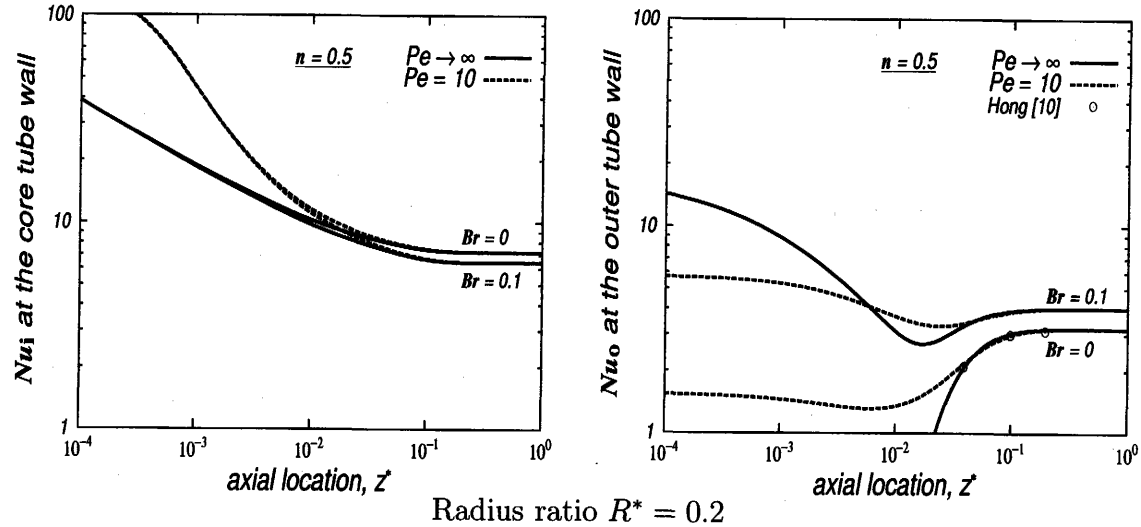

Radius ratio $R^* = 0.2$

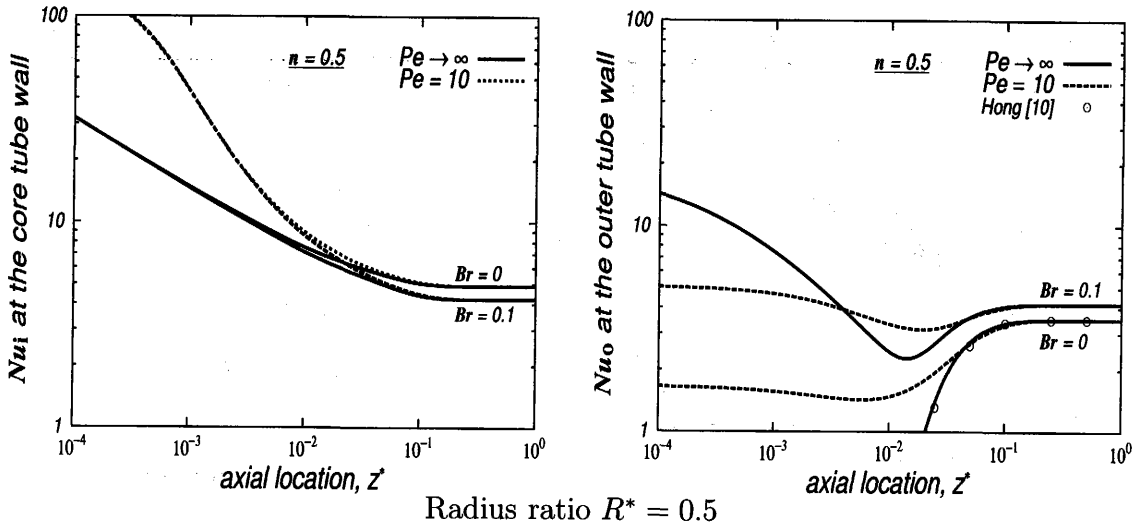

Radius ratio $R^* = 0.5$

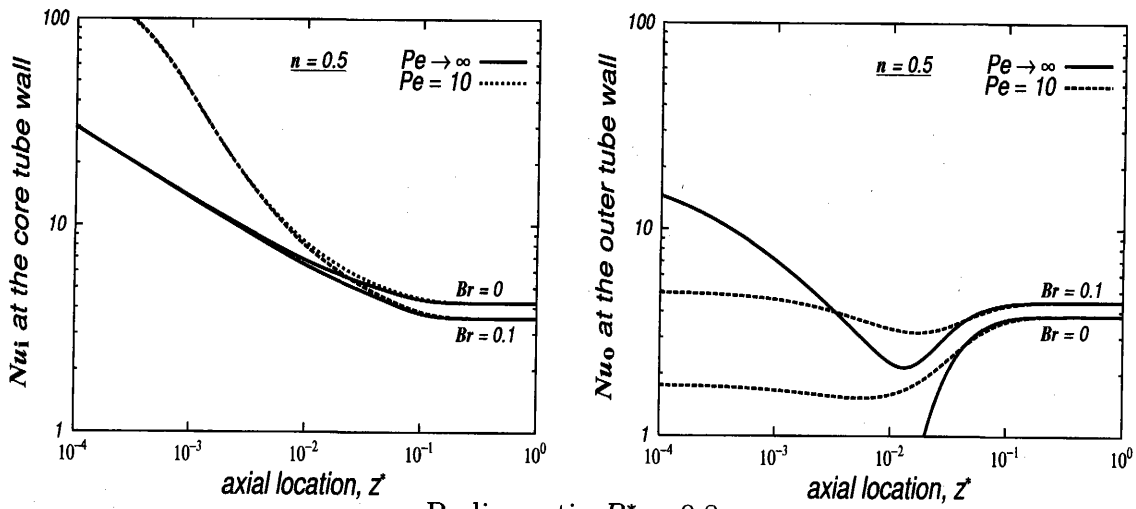

Radius ratio $R^* = 0.8$

Fig. 2.19: Local Nusselt number for a pseudoplastic fluid ($n = 0.5$) (Nu_i at the inner core and Nu_o at the outer cylinder)

Dilatant fluid

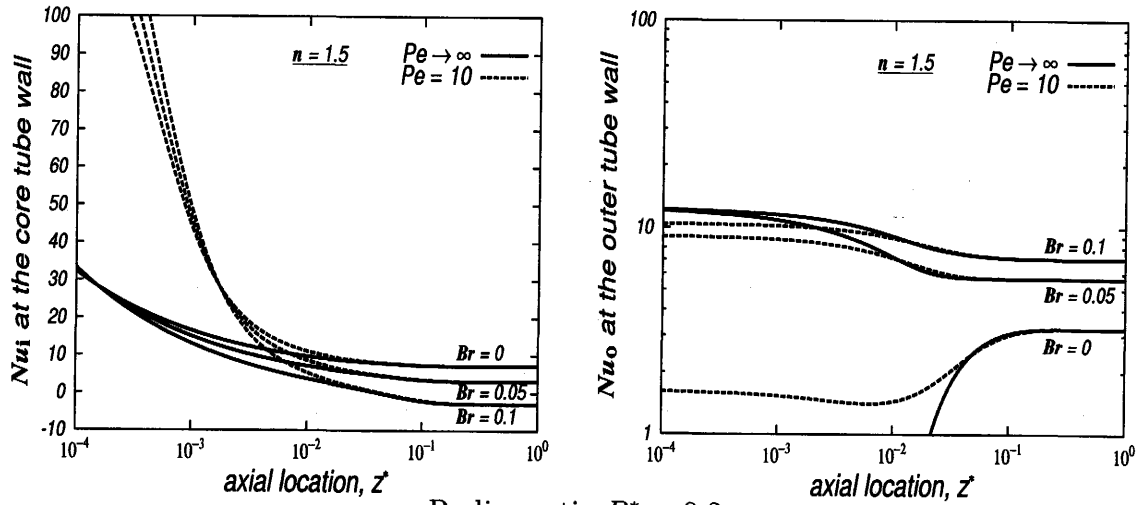

Radius ratio $R^* = 0.2$

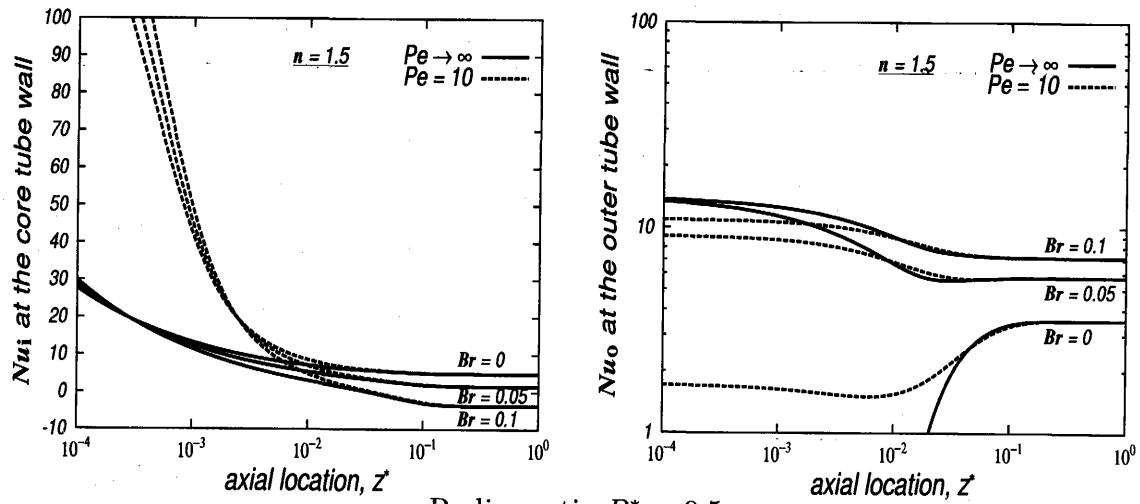

Radius ratio $R^* = 0.5$

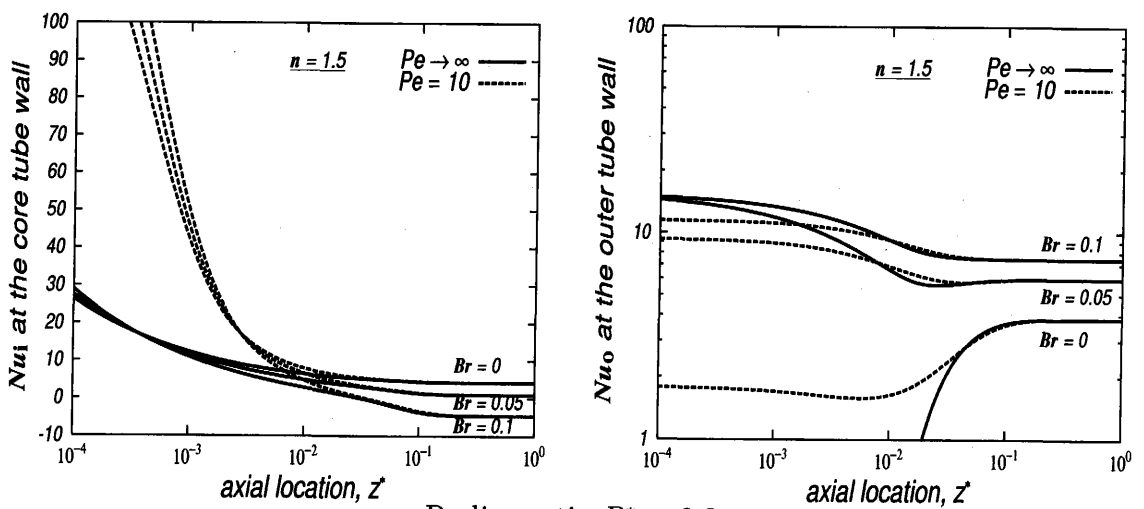

Radius ratio $R^* = 0.8$

Fig. 2.20: Local Nusselt number for a dilatant fluid ($n = 1.5$) (Nu_i at the inner core and Nu_o at the outer cylinder)

The Nusselt number, Nu_i, at the core tube wall increases with a decrease in Peclet number in the thermal entrance region. This implies that the effect of fluid axial heat conduction on heat transfer rate is strong in the thermal entrance region. This effect is diminished as Peclet number is increased.

The inclusion of the fluid axial heat conduction in the study causes a higher Nusselt number, Nu_o, at the outer cylinder wall (whose temperature is maintained at a constant value equal to the entering fluid temperature). This behavior is attributed to that the fluid temperature increase due to the fluid axial heat conduction (for $z^* \leq 0$) before the fluid flow reaches the heated wall.

2.11.3 Effect of n on the Nusselt numbers

The heat transfer results show quite similar behaviors for different fluids. For the non-Newtonian fluids, the Nusselt number increases with decreasing a Peclet number for a given value of z^* in the thermal entrance region just as it does for the Newtonian fluid.

When the viscous dissipation is included in the study, the Nusselt numbers, Nu_i, for heat transfer to the Newtonian fluid are higher than those to the dilatant fluid but less than those to the pseudoplastic fluid.

The response of the Newtonian fluid to viscous heating is more pronounced than that of the pseudoplastic fluid but less remarkable than the dilatant fluid.

The flow index, n, effect on heat transfer with fluid axial heat conduction is seen insignificant unlike the viscous dissipation included in heat transfer.

2.11.4 Effect of R^* on the Nusselt numbers

The results in Figs. 2.18 - 2.20, indicate that the Nusselt number, Nu_i, at the inner core wall is greater for smaller radius ratios in the fully developed region. The Nusselt number, Nu_o, at the outer cylinder wall is greater for larger radius ratios.

The radius ratio $R^* = 0.2$ is superior to $R^* = 0.5$ and $R^* = 0.8$ from the view point of heat transfer at the core under the same conditions. More discussion about the effect of R^* on Nu can be found in Section 3.6.4.

2.12 Results and Discussions of the 2nd Kind of T.B.C

The temperature field of the thermally developing flow under the 2nd kind of thermal boundary condition has been obtained by solving the transformed energy equation Eq.(2.65) with Eq.(2.70). The objective herein is to display the results and to provide explanations for the solutions.

The results are presented in the form of graphs and compared to the available data by other authors. Also the results, which are given as the temperature fields and the corresponding Nusselt numbers, are discussed. The consideration is given to the effects of the problem governing parameters determined in Section 2.3.3.

2.13 Temperature Distributions of the 2nd Kind of T.B.C

Figures 2.21 - 2.23 illustrate the developing temperature profiles of Newtonian, pseudoplastic and dilatant fluids flowing in an annular duct of radius ratio, $R^* = 0.5$. In these figures the temperature profiles are shown at the axial locations of $z^* = 0$; 0.1; 0.42 and 1. At $z^* = 0$, the wall heat flux at the core tube jumps. In these figures, the abscissa $\xi = 0$ is the core tube wall and $\xi = 1$ is the outer tube wall.

2.13.1 Effect of Br on the temperature distributions

In Figs.2.21 - 2.23, the dimensionless temperature at $z^* = 0$ is definitely deviated from zero for $Br = 0.1$. This shows that the fluid temperature increases before the fluid reaches the heated wall region because of the heat generated by the viscous dissipation.

2.13.2 Effect of Pe on the temperature distributions

Figures 2.21 - 2.23 show that the fluid temperature is increased slightly for $Pe = 10$ in the unheated wall region. Since both the walls' are insulated in the unheated wall region (for $z^* \leq 0$), this increase of temperature is due to the heat conducted from downstream of $z^* > 0$.

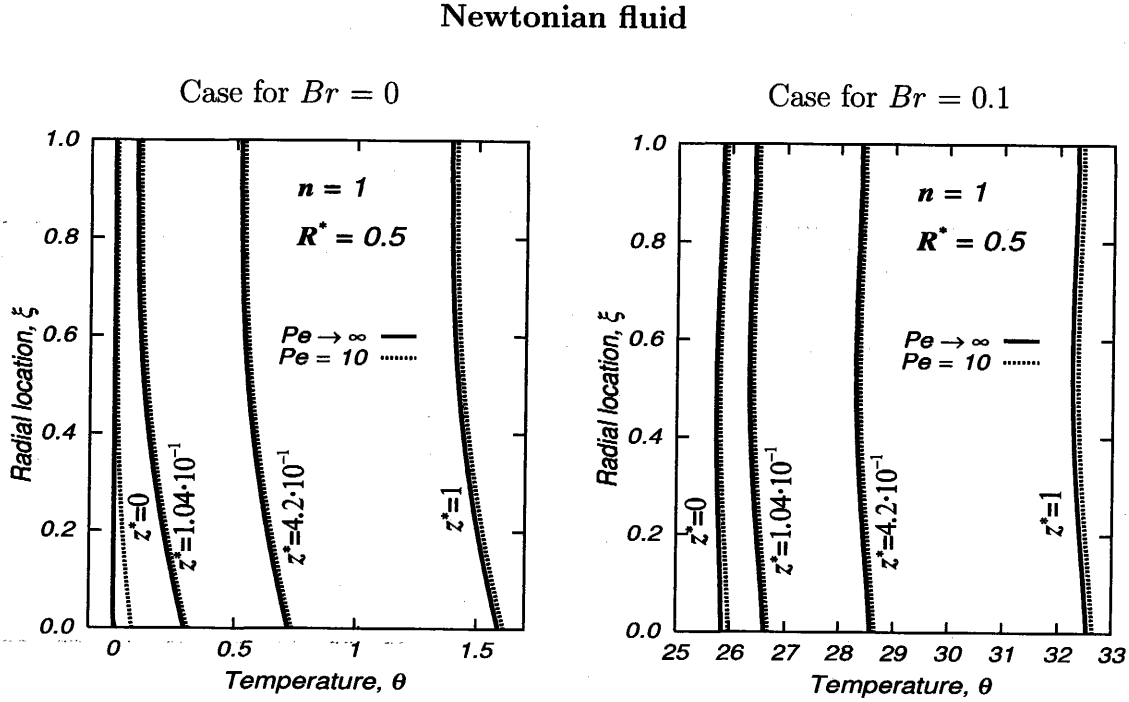

Fig. 2.21: Developing temperature profiles of a Newtonian fluid.

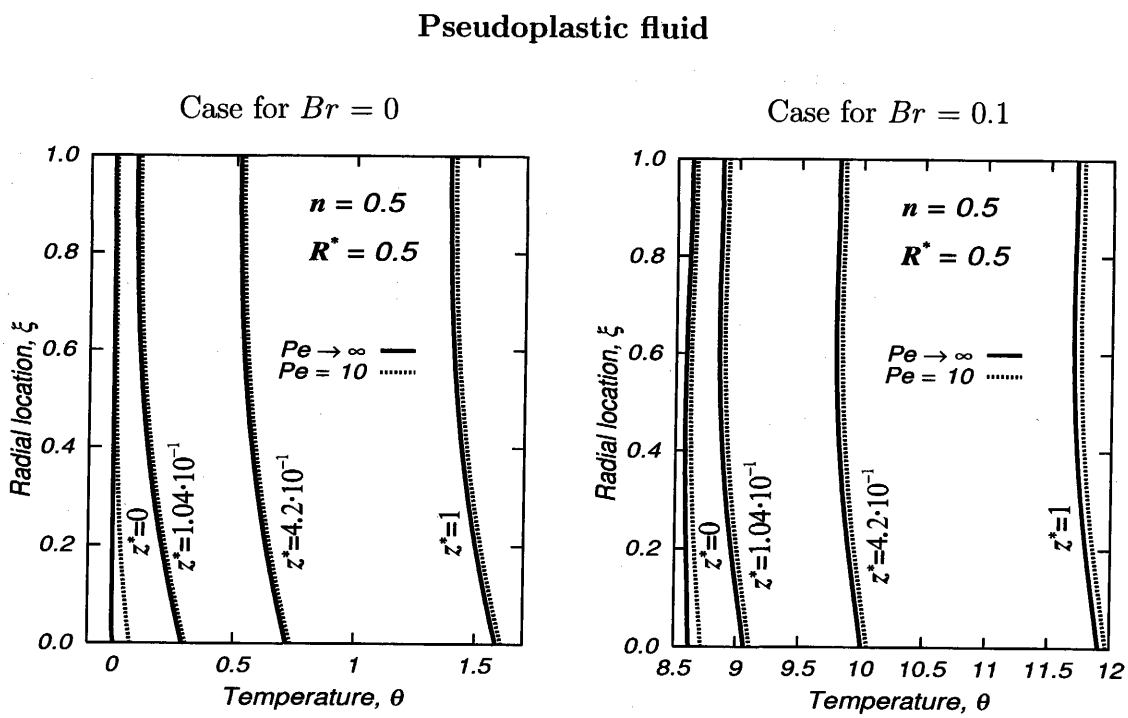

Fig. 2.22: Developing temperature profiles of a pseudoplastic fluid.

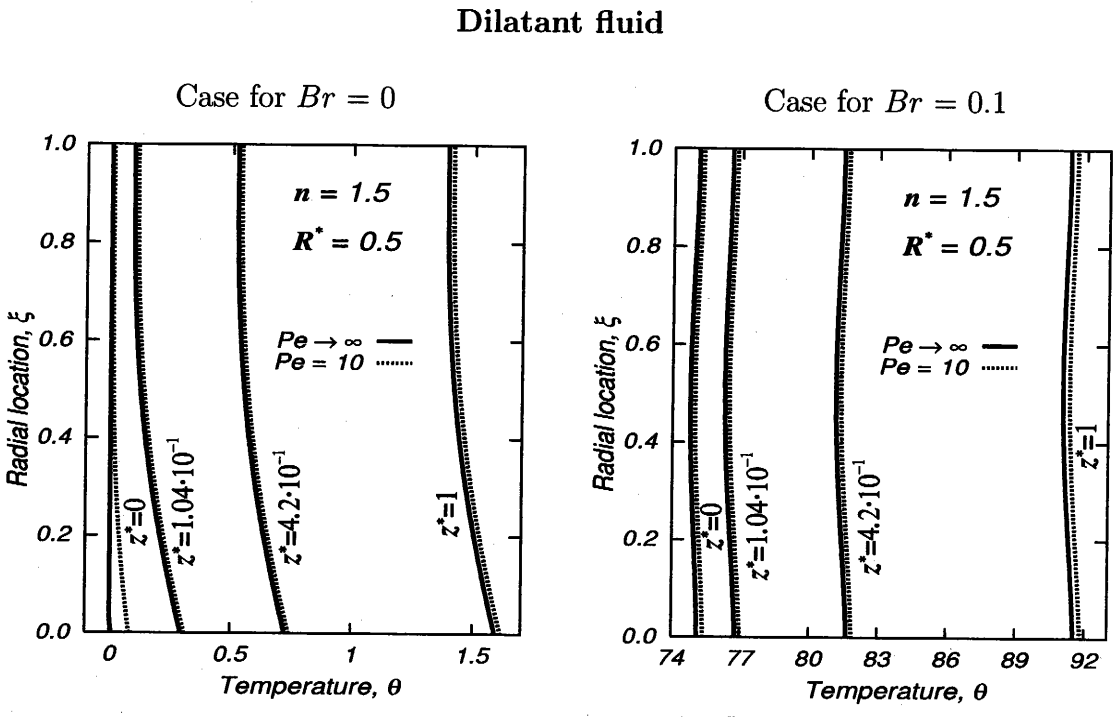

Fig. 2.23: Developing temperature profiles of a dilatant fluid.

2.13.3 Effect of n on the temperature distributions

An inspection of Figs.2.21 - 2.23 shows that the temperature distributions show quite similar behaviors for different fluids. The response of the Newtonian fluid to viscous heating is more pronounced than that of the pseudoplastic fluid but less remarkable than the dilatant fluid.

The effect of flow index, n, on heat transfer with fluid axial heat conduction is seen insignificant unlike the viscous dissipation included in heat transfer.

2.14 Nusselt Numbers of the 2nd Kind of T.B.C

In Figs. 2.24 - 2.25, the heat transfer results are illustrated in terms of a conventional Nusselt number for the three different radius ratios ($R^* = 0, 2,\ 0.5,\ 0.8$). The variations of Nusselt number are shown with the different values of Pe and Br.

2.14.1 Effect of Br on the Nusselt numbers

As seen in Figs. 2.24 - 2.25, Brinkman number has a strong effect on the Nusselt number both in the thermally developing region and in the thermally fully developed region unlike for the case of the 1st kind of thermal boundary condition.

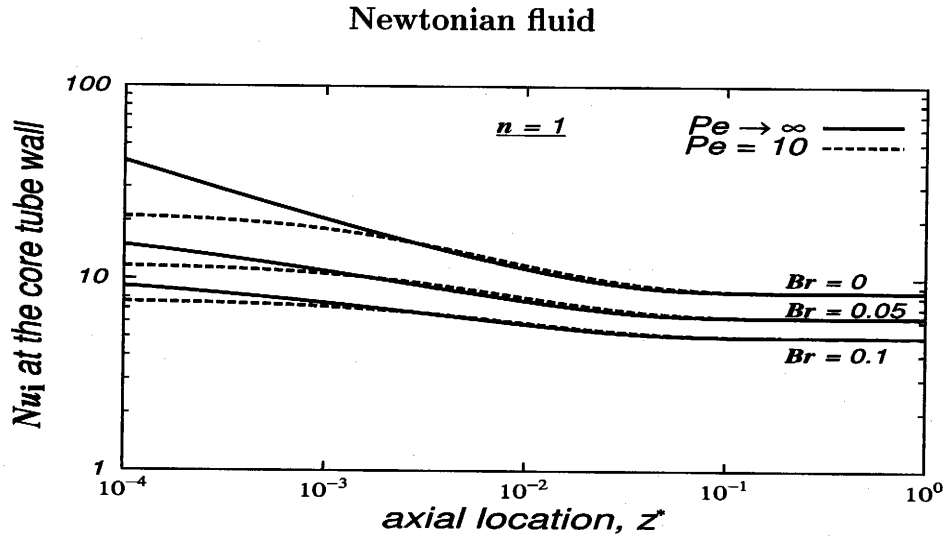

Radius ratio $R^* = 0.2$

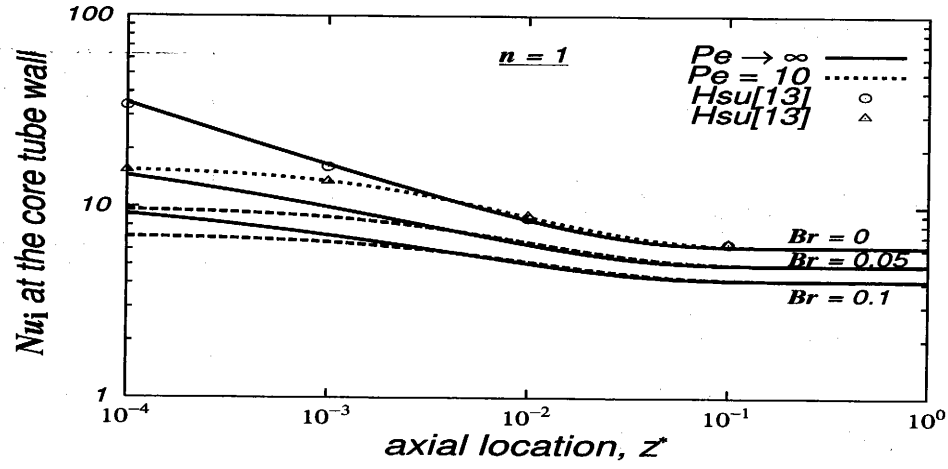

Radius ratio $R^* = 0.5$

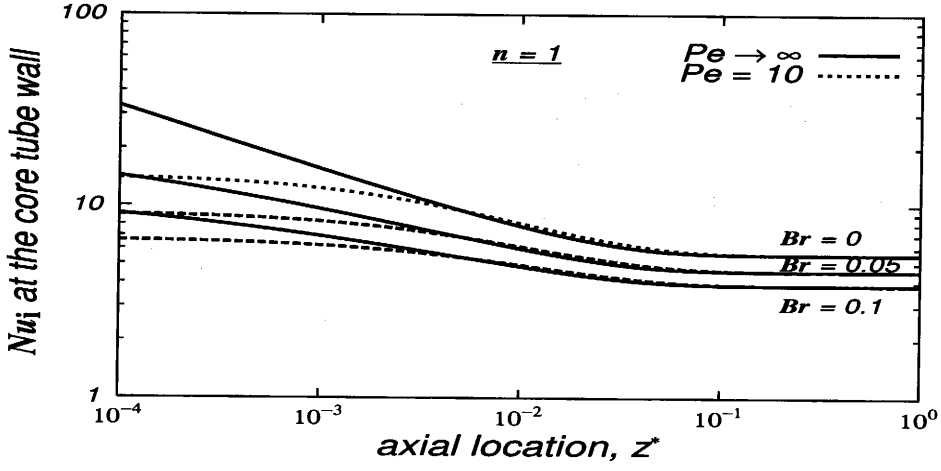

Radius ratio $R^* = 0.8$

Fig. 2.24: Local Nusselt number for a Newtonian fluid ($n = 1$) (Nu_i at the inner core)

Pseudoplastic and dilatant fluids

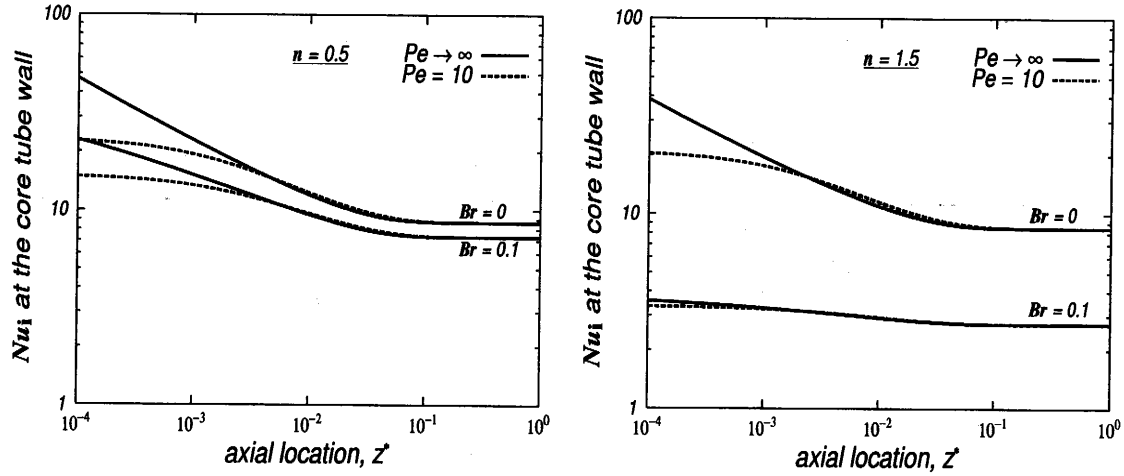

Radius ratio $R^* = 0.2$

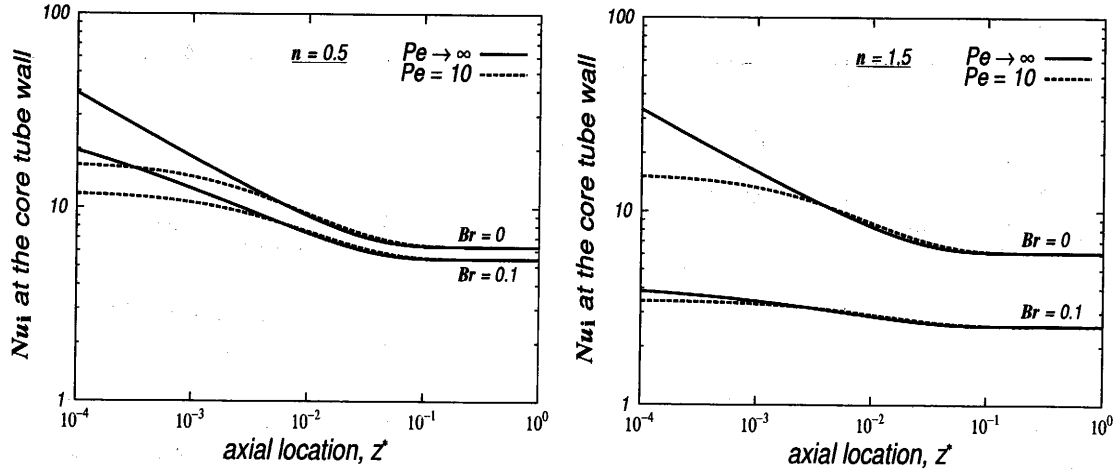

Radius ratio $R^* = 0.5$

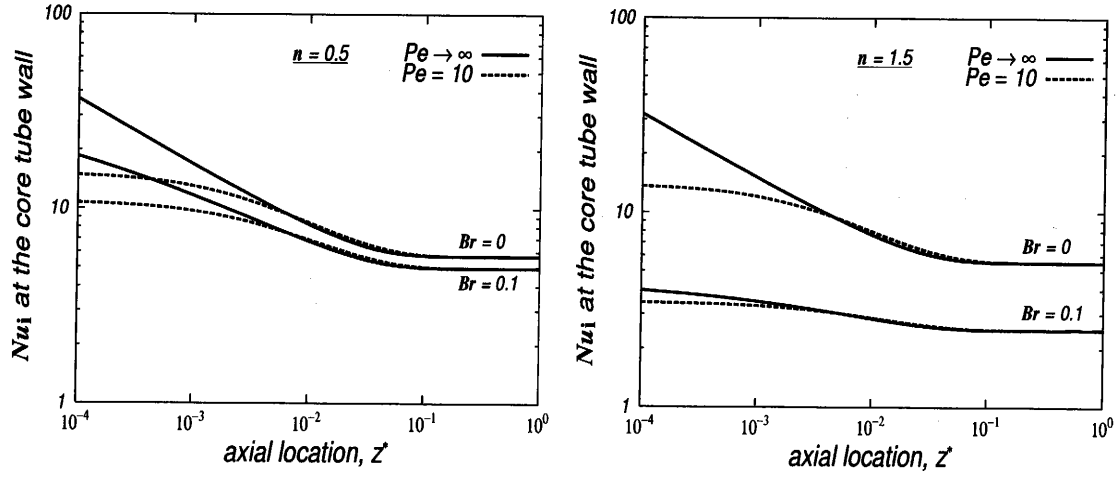

Radius ratio $R^* = 0.8$

Fig. 2.25: Local Nusselt numbers for a pseudoplastic fluid ($n = 0.5$) and for a dilatant fluid ($n = 1.5$)(Nu_i at the inner core)

The Nusselt number at the core decreases with an increase in Brinkman number in the fully developed region and in the thermally developing region.

2.14.2 Effect of Pe on the Nusselt numbers

The solid lines represent the case of negligible fluid axial heat conduction ($Pe \rightarrow \infty$) and the dotted lines are for $Pe = 10$ in Figs.2.24 - 2.25.

Unlike the cases for the (T) and 1st kind of thermal boundary conditions, Nu_i values at the heated core in the thermal entrance region tend to decrease near $z^* = 0$ with a decrease in Pe.

There is no effect of Pe on the Nusselt number in the fully developed region.

2.14.3 Effect of n on the Nusselt numbers

The heat transfer results show quite similar behaviors for different fluids. For the non-Newtonian fluids, the Nusselt number increases with decreasing a Peclet number for a given value of z^* in the thermal entrance region just as it does for the Newtonian fluid.

When the viscous dissipation is included in the study, the Nusselt numbers for heat transfer to the Newtonian fluid are higher than those to the dilatant fluid but less than those to the pseudoplastic fluid.

The response of the Newtonian fluid to viscous heating is more pronounced than that of the pseudoplastic fluid but less remarkable than the dilatant fluid.

The flow index, n, effect on heat transfer with fluid axial heat conduction is seen insignificant unlike the viscous dissipation included in heat transfer.

2.14.4 Effect of R^* on the Nusselt numbers

The results indicate that the Nusselt number at the inner core wall is greater for smaller radius ratios in the fully developed region.

The radius ratio $R^* = 0.2$ is superior to $R^* = 0.5$ and $R^* = 0.8$ from the view point of heat transfer at the core under the same conditions.

More discussion about the effect of R^* on Nu can be found in Section 3.9.4.

2.15 Concluding Remarks

The heat transfer problem for laminar flow of Newtonian and non-Newtonian fluids flowing in annular ducts has been treated by including both the viscous dissipation and the fluid axial heat conduction. The ducts are considered to be under a step jump in the wall temperature or in the wall heat flux. The obtained numerical solutions were compared with the data by the previous researchers that are available for the limiting cases. For all cases compared, excellent agreement was obtained. It indicates that the descriptions of the flow field and the temperature field are accurate.

A temperature increase was observed in the unheated wall region for $Pe = 10$ and $Br \neq 0$. This observation for Peclet number effect on heat transfer result confirms the role of Peclet number in the fluid axial heat conduction term in the energy equation. Also for Brinkman number, this confirms the role of Brinkman number in the viscous dissipation term in the energy equation.

As a main contribution of this investigation, the Nusselt numbers for a wide range of parameters have been calculated. The numerical results are given graphically in terms of the conventional Nusselt number for Newtonian and power-law non-Newtonian fluids showing the effects of the Brinkman number and the Peclet number. An appearance of a fixed point in the plots of the axial development of the Nusselt numbers was observed as a consequence of including the preheating of incoming fluid due to viscous dissipation and fluid axial heat conduction for the thermal boundary condition of (T) kind. Analytical solutions by the previous researchers [2] have been applied in order to check the values of the coordinates of the fixed point in the Nusselt curves. Comparison of the present results with the data of the analytical study in the literature of Newtonian fluids support the numerical solutions of this study as having sufficient accuracy.

The results showed that the radius ratio effect on the Nusselt number in the fully developed region is as follows: at the core tube wall, the Nusselt number increases for smaller radius ratios but at the outer wall wall, the Nusselt number is greater for larger radius ratios.

Chapter 3

Annular Duct with an Axially Moving Core

In this chapter Objective 2 of the present research has been achieved. This chapter is organized as follows. In Section 3.1, the problem formulation including a brief description of the application is given and, the assumptions and conditions are described. In Sections 3.2.1 - 3.2.2, the basic equations and the solutions for the velocity field are presented for Newtonian and non-Newtonian fluids, respectively. In Sections 3.3.1 - 3.3.5, the energy equation and the method of solution are given. The results for various values of the relevant parameters are presented and discussed in Sections 3.4 - 3.6.4 for the 1st kind of thermal boundary condition and in Sections 3.7 - 3.9.4 for the 2nd kind of thermal boundary condition. The results are summarized in Section 3.10.

3.1 Problem Formulation

The problem considered in this chapter is a counterpart of the problem treated in Chapter 2. The study in this chapter differs from those of Chapter 2 in that with axially moving core. Problems involving fluid flow and heat transfer in an annular duct with an axially moving core can be found in many manufacturing processes such as extrusion, drawing, polymer coatings of wires or tubes for corrosion protection and hot rolling, etc [76]. In these manufacturing processes a very commonly encountered circumstance is that a moving core continuously exchanges heat with the surrounding environment. In most of the listed manufacturing processes when the moving boundary emerges from the die or the rollers, it is at a temperature

higher than that of the surroundings and in many practical circumstances, the extruded material passes through a cooling bath or trough. As a concrete example, in coating processes, the wire is coated with a plastic sheath from an extruder and then the coated wire passes through a cooling system. Also the coating is an essential part of optical fiber which affects its long term reliability. Various materials such as polymers, metals and carbon are applied to silica optical fiber [77].

For such cases, the fluid involved may be Newtonian or non-Newtonian and the flow situations encountered can be either laminar or turbulent. In many applications such as in the cooling of optical fibers, laminarly flowing cooling agent is preferred to avoid excessive flow over the fiber that may abrade the fiber surface, and localized dynamic pressure may also enhance the surface degradation by abrasion or fatigue [78].

In this chapter, the fluid between the tubes flows to or against the direction of the core movement. The physical situation under consideration in this chapter is shown is in Fig.3.1. The flow is a Couette flow with a superimposed axial pressure driven flow or in other words a Poiseuille-Couette flow. The outer tube is stationary and the core tube is axially moving at a constant velocity, U. In this study, the velocity U is proposed to serve as a controlling index that properly indicates the relative importance of the velocity of the core. The sign of "+" before U reflects the case when the core direction coincides with the flow direction and "-" is vice versa.

All the assumptions given in Sections 2.1.1 are applied in this chapter except Assumption 2 that is for non-Newtonian fluids. The modified power-law model [20] is applied to describe the flow as this model insures an accurate velocity field even in the lower shear rates including zero shear rate. Since the moving core deforms the velocity profile of the flow, it is important to study the heat transfer by applying an accurate velocity field.

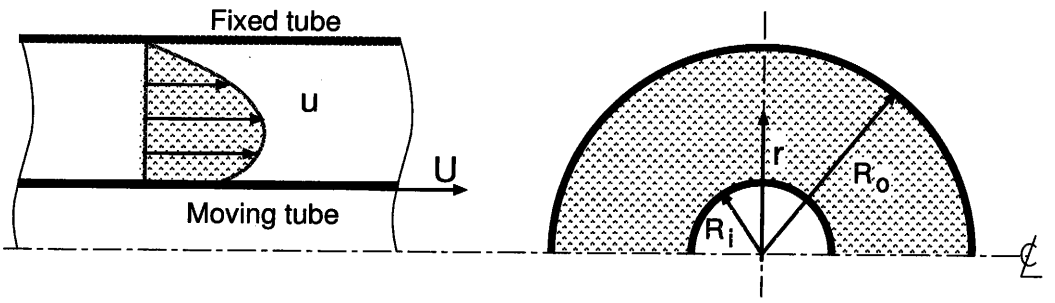

Fig. 3.1: Schematic of a Poiseuille-Couette flow in an annular duct

In this chapter, the laminar heat transfer is studied when the cylinders are held at different temperatures or heat fluxes in the heated wall region. Thus the 1st and 2nd kind of thermal boundary conditions described in Section 2.1.2 are applied while the Ⓣ thermal boundary condition is not considered.

3.2 Laminar Flow

In this section, an accurate velocity field in an annular duct consisting of an axially moving core and a stationary outer tube is given. As discussed in Section 2.1.1, the velocity field information is necessary for performing the heat transfer study.

As mentioned previously the assumptions listed in Sections 2.1.1 will be applied. However, the assumption regarding the non-Newtonian fluid is different (Assumption 2). In order to accurately clarify the effects of the moving core velocity on heat transfer, the modified power-law model [20] is used to describe the fluid. For a Newtonian fluid flowing in an annular duct with an axially moving core, an analytical solution was available and this will be given first.

3.2.1 Newtonian fluid flow

An analytical solution for a Newtonian fluid flowing in an annular duct with an axially moving core is available in Ref. [79]. With some manipulations the velocity is given as

$$u = \frac{R_o^2}{4\mu}\left(-\frac{dP}{dz}\right)\left\{1-\left(\frac{r}{R_o}\right)^2 + B\ln\left(\frac{r}{R_o}\right)\right\} + \frac{U}{\ln R^*}\ln\left(\frac{r}{R_o}\right) \tag{3.1}$$

Here constant, B, and radius ratio, R^*, are given respectively by Eq.(2.9) and Eq.(2.12) on page 17.

The average velocity, u_m, is

$$u_m \equiv \frac{2}{R_o^2 - R_i^2}\int_{R_i}^{R_o} u\, r dr = \frac{R_o^2}{4\mu}\left(-\frac{dP}{dz}\right)\frac{M}{2} + HU \tag{3.2}$$

where M is given in Eq.(2.10) and H is a constant defined as

$$H \equiv \frac{R^{*2} - (B/2)}{R^{*2} - 1}. \tag{3.3}$$

Then the resulting dimensionless velocity, u^*, and its gradient, du^*/dr^*, are:

$$u^* = \frac{2}{M}(1 - HU^*)\left\{1 - (Nr^*)^2 + B^*\ln(Nr^*)\right\} \tag{3.4}$$

$$\frac{du^*}{dr^*} = \frac{2}{M}(1 - HU^*)\left[-2N^2r^* + \frac{B^*}{r^*}\right] \tag{3.5}$$

Constant N is defined by Eq.(2.11) and B^* is

$$B^* \equiv B\frac{1 - (U^*/2)}{1 - HU^*} \tag{3.6}$$

The dimensionless relative velocity of the core, U^*, is defined as

$$U^* = \frac{U}{u_{\mathrm{m}}} \tag{3.7}$$

In Fig 3.2, the results showing the velocity field of a Newtonian fluid flowing in annular duct are presented. Here the predictions of the dimensionless velocity profiles and the square of the velocity gradient are shown. In these figures, the velocity and the square of the velocity gradient are given in pairs for the given values of radius ratio, R^*. The radius ratio, R^*, has the values of 0.2; 0.5 and 0.8. Figure 3.2 presents the profiles of the dimensionless velocity and its gradient square as functions of ξ, which is the dimensionless radial coordinate. ξ equal 0 corresponds to the core tube wall, while $\xi = 1$ is the outer tube wall. The effect of the axially moving core, U^*, on the velocity distribution, u^*, of the Newtonian fluid flow within the annular duct is seen clear from these figures. The relative velocity is the parameter on the curves. The relative velocity varies in these figures in the range of -1 $\leq U^* \leq$ 3.

The curves in the figures compare how the moving core deforms the fluid velocity field. For $U^* < 0$, the velocity profile is parabolic having a larger maximum value with increasing values of R^*. The square of velocity gradients are useful for clarification of the viscous dissipation effects as will be seen in Eq.(3.28). It is observed that the square of velocity gradient has higher values for U^* = -1 than for $U^* \geq 0$ near the tube walls ($\xi = 0$ and $\xi = 1$). With increasing U^*, the square of velocity gradient at the outer tube wall is decreased, however at the core tube its behavior is complicated. With increasing R^*, the magnitude of dependence of the square of velocity gradient on U^* is decreased near the core tube and increased near the outer tube.

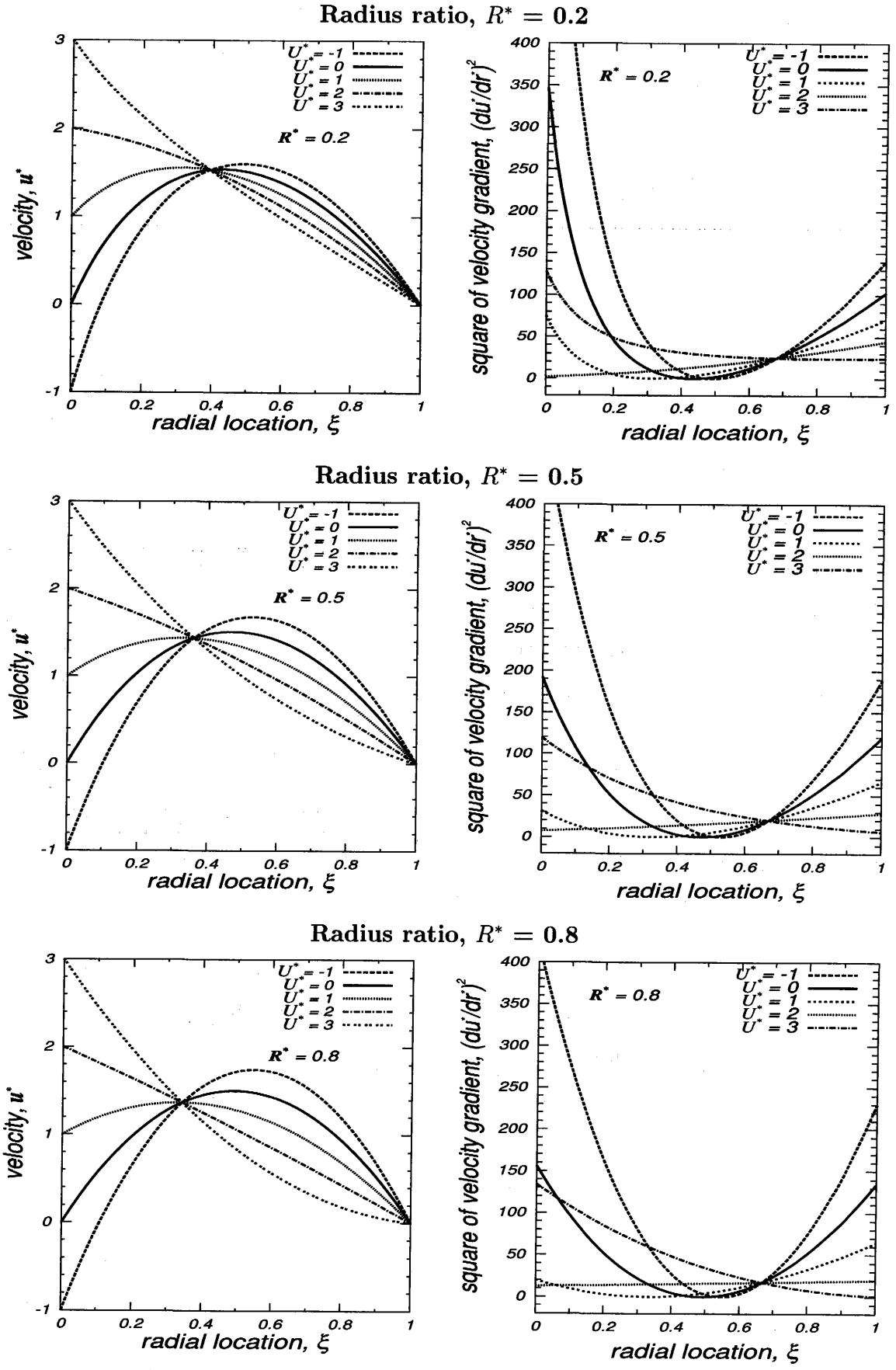

Fig. 3.2: Velocity profile and square of velocity gradient for $R^* = 0.2$; 0.5 and 0.8

3.2.2 Non-Newtonian fluid flow

In this section, a numerical analysis is made for a non-Newtonian fluid flow with pressure gradient. The fluid flows in an annular duct consisting of an axially moving core and a stationary outer tube. With the assumptions described in Section 2.1.1 and Section 3.2 regarding the non-Newtonian fluid flow, the governing momentum equation is

$$\frac{1}{r}\frac{d}{dr}(r\tau) = -\frac{dP}{dz}. \tag{3.8}$$

The boundary conditions are:

$$\begin{cases} u = U \quad \text{at} \quad r = R_{\mathrm{i}} \\ u = 0 \quad \text{at} \quad r = R_{\mathrm{o}}. \end{cases} \tag{3.9}$$

Shear stress, τ, is given by the modified power-law model [20].

$$\tau = -\eta_a \frac{du}{dr} \tag{3.10}$$

where η_a is the apparent viscosity defined by

$$\eta_a = \eta_0 \Big/ \left(1 + \frac{\eta_0}{m}\left|\frac{du}{dr}\right|^{1-n}\right) \qquad \text{for} \quad n < 1 \tag{3.11}$$

$$\eta_a = \eta_0 \left(1 + \frac{m}{\eta_0}\left|\frac{du}{dr}\right|^{n-1}\right) \qquad \text{for} \quad n > 1 \tag{3.12}$$

The momentum equation and its boundary conditions are reduced to

$$\frac{1}{r^*}\frac{d}{dr^*}\left(r^*\eta_a^*\frac{du^*}{dr^*}\right) = -2\, f Re_{\mathrm{M}} \tag{3.13}$$

$$\begin{cases} u^* = U^* \quad \text{at} \quad r^* = \dfrac{R^*}{2(1-R^*)} \\ u^* = 0 \quad \text{at} \quad r^* = \dfrac{1}{2(1-R^*)}. \end{cases} \tag{3.14}$$

Where f is the friction factor defined by Eq.(2.17) and Re_{M} is the modified Reynolds number defined as

$$Re_{\mathrm{M}} = \frac{\rho u_{\mathrm{m}} D_{\mathrm{h}}}{\eta}. \tag{3.15}$$

The dimensionless apparent viscosity η_a^* is defined as

$$\eta_a^* = \frac{\eta_a}{\eta} = \frac{1+\beta}{1+\beta\left|\dfrac{du^*}{dr^*}\right|^{1-n}} \qquad \text{for} \quad n < 1 \tag{3.16}$$

$$\eta_a^* = \frac{\eta_a}{\eta} = \frac{\beta + \left|\frac{du^*}{dr^*}\right|^{n-1}}{\beta + 1} \qquad \text{for } n > 1 \tag{3.17}$$

where

$$\eta = \eta_0 / (1+\beta) \qquad \text{for } n < 1 \tag{3.18}$$

$$\eta = \eta_0 \left(1 + \frac{1}{\beta}\right) \qquad \text{for } n > 1 \tag{3.19}$$

$$\beta = \frac{\eta_0}{m} \left(\frac{u_m}{D_h}\right)^{1-n} \tag{3.20}$$

The modified power-law model and the parameter β have been extensively discussed in Ref.[29].

For determining the velocity field, the expression for the average velocity defined by Eq.(2.5) is used. Equation 2.5 can be written in the dimensionless form as:

$$\frac{8(1-R^*)}{(1+R^*)} \int_{\frac{R^*}{2(1-R^*)}}^{\frac{1}{2(1-R^*)}} u^* r^* dr^* = 1 \tag{3.21}$$

The dimensionless velocity, u^*, is numerically determined from Eqs.(3.13) - (3.14) and Eq.(3.21). First, we assume the value of fRe_M for a given set of parameters: n, β and U^* to solve Eq.(3.13) with Eq.(3.14). Then, Eq.(3.21) is checked by substituting the obtained velocity distribution, u^*, into it. Unless Eq.(3.21) is satisfied within the accuracy of 10^{-5}, a new value of fRe_M is assumed. This process is repeated until the correct value of fRe_M is obtained.

Computations of the velocity field have been made for a range of values of radius ratio, R^*, and in general their behaviors were quite similar. Therefore only predictions for $R^* = 0.5$ are discussed in this section. The predictions of friction factor in terms of fRe_M are graphically presented in Fig.3.3 taking the flow index n as a parameter. In these figures, the relative velocity of the moving core, U^*, is -1, 0 and 1. From Fig.3.3, the effect of parameter β on friction factor is seen. The values of fRe_M at the extremes of $\beta \to 0$ and $\beta \to \infty$ approach, respectively, to the values for a Newtonian fluid and for power law fluids. It is seen in Fig.3.3 that the values of fRe_M become greater with a decrease in U^*.

For the power-law fluids flowing in an annular duct with an axially moving core, an analytical solution is available in Ref.[80]. The power-law asymptotic values of fRe_M are tabulated in Appendix (Table 4.1) on page 134. From the data listed in

Table 4.1, it is noted that fRe_M increases with an increase in radius ratio, R^*, for U^* = -2, U^* = -1, and U^* = 0, and fRe_M decreases with an increase in R^* for U^* = 1 and U^* = 2.

Figure 3.4 contains the profiles of the dimensionless velocity, u^*, as a function of the dimensionless radial coordinate, ξ. The dimensionless radial coordinate ξ equal 0 corresponds to the core tube wall, while $\xi = 1$ is the outer tube wall. The relative velocity of the core, U^*, varies in the figures in the horizontal direction having values -1; 0 and 1. The fluid flow index, n, has the value of 0.5 in the upper figures and the value of 1.5 in the lower figures. The dimensionless shear rate parameter, β, is the parameter on the curves. It can be observed in the figures that the asymptotic velocity profiles of $n = 0.5$ for $\beta = 10^5$ are identical to the profiles for $n = 1.5$ for $\beta = 10^{-5}$, conforming Eqs.(3.16) - (3.17). These asymptotic profiles show Newtonian fluid flow behavior. From Fig.3.4, one can see the effects of the moving core on the velocity profile of the flow inside the annular duct.

In Fig.3.5, the predictions for square of velocity gradient of each previous case are shown. These would provide the velocity field effects on heat transfer with respect to viscous dissipation. Close to the tube walls, the square of velocity gradients are higher, specially near the stationary tubes and if the core tube moves to the opposite direction of the fluid flow.

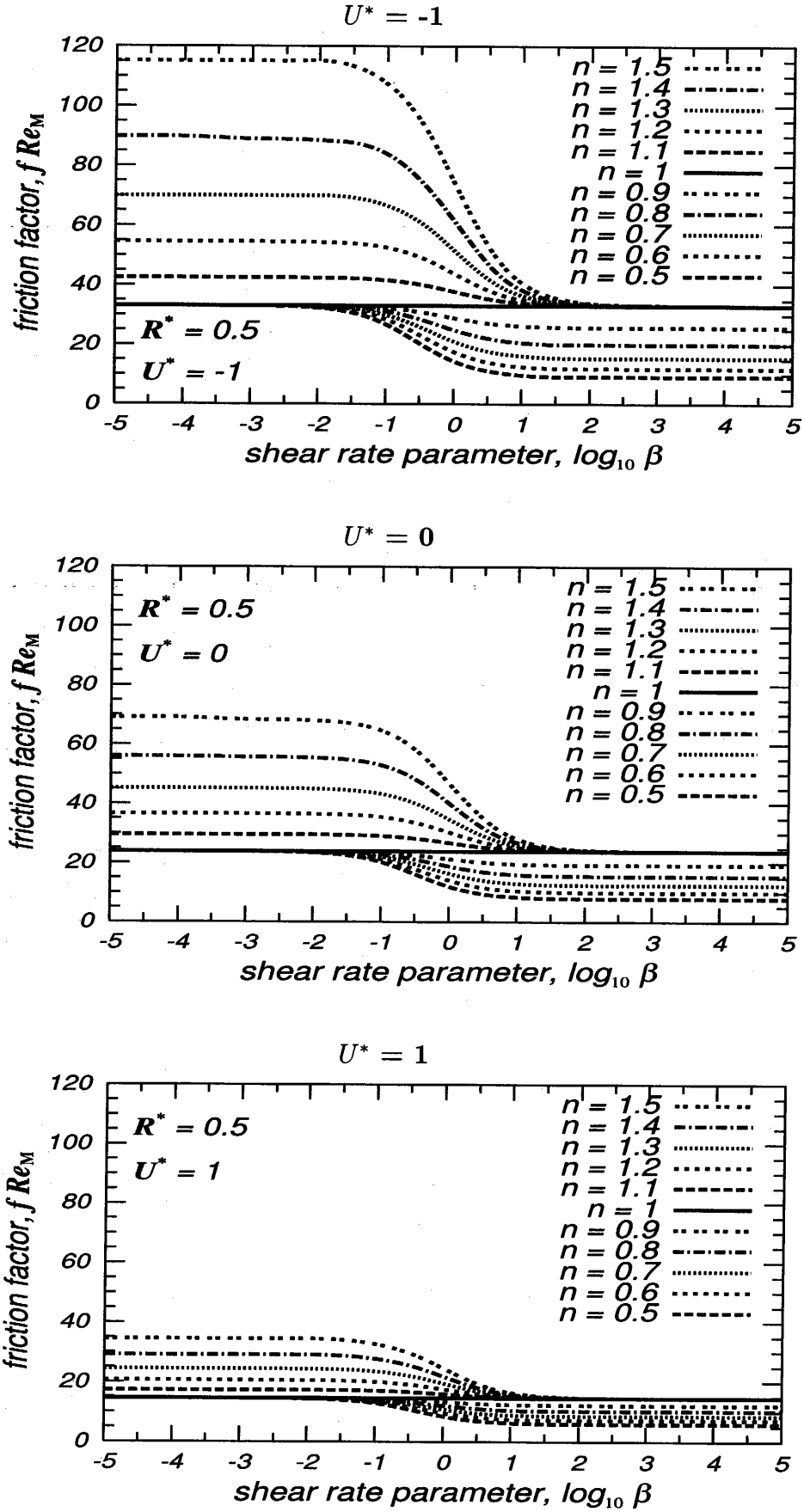

Fig. 3.3: Friction factor

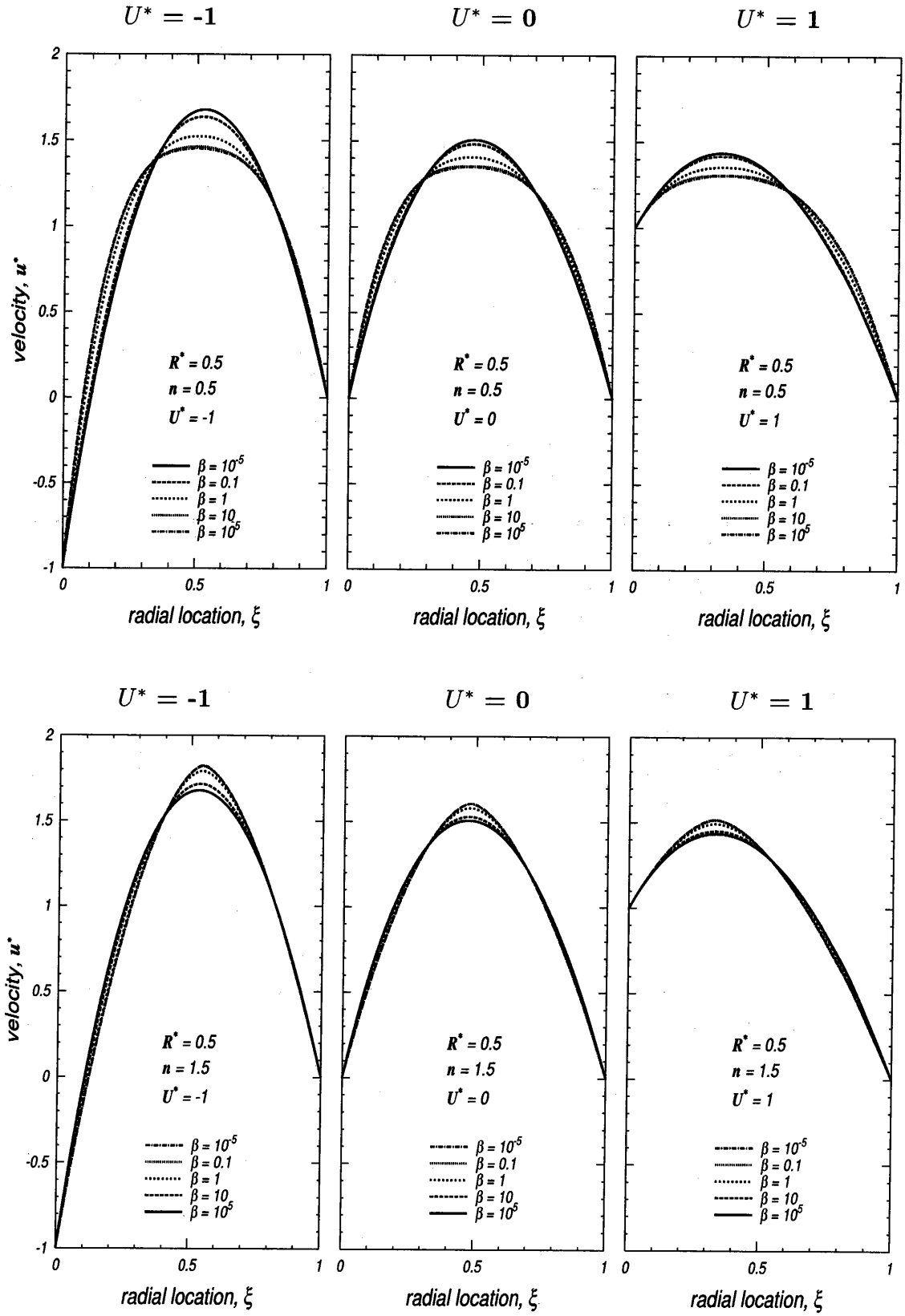

Fig. 3.4: Velocity profiles for modified power law fluids

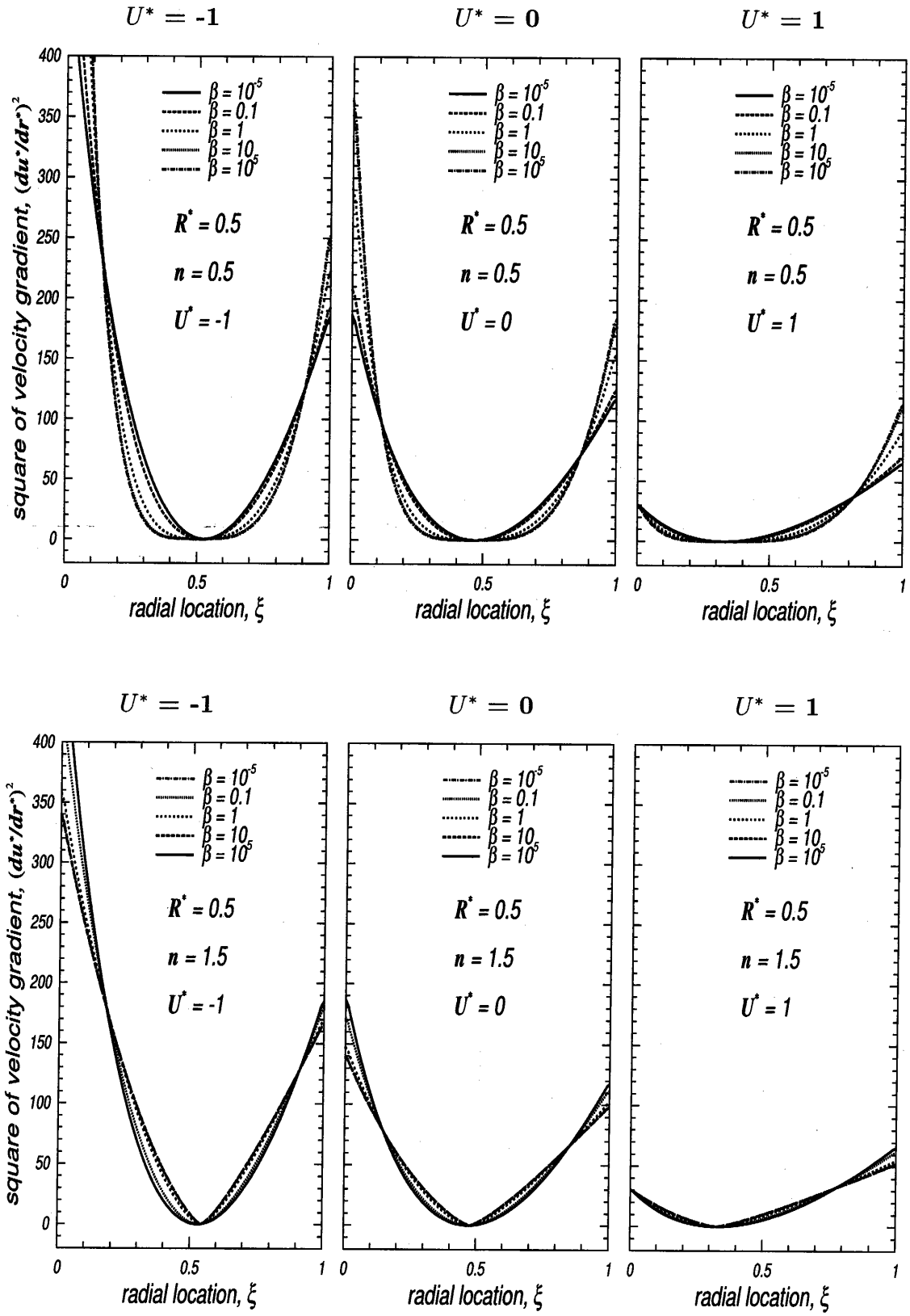

Fig. 3.5: Square of velocity gradient for modified power law fluids

3.3 Heat Transfer

3.3.1 Energy equation

Once the velocity field is solved, the temperature distribution can also be determined. The purpose in this section is to analyze the heat transfer in thermally developing flow in a concentric annular duct consisting of an axially moving core and a stationary outer tube. The effects of viscous dissipation and fluid axial heat conduction are considered along with the core velocity effect on the heat transfer. In order to analyze the heat transfer problem of a non-Newtonian fluid that follows the modified power-law model, here the steady forced convection in a thermally developing, hydrodynamically developed laminar flow is considered. The thermal boundary conditions and the coordinate system for the analysis are given in Fig.2.1 on page 14. However as it was discussed in Section 3.1, this chapter is designated for the study of heat transfer in an annular duct consisting of a core tube moving at a constant velocity in the streamwise direction and a fixed outer tube. In order to acquire more accurate information on the velocity field, the modified power-law model [20] was applied and the energy equation is

$$k\left[\frac{1}{r}\frac{\partial}{\partial r}\left(r\frac{\partial T}{\partial r}\right)+\frac{\partial^2 T}{\partial z^2}\right]+\eta_a\left(\frac{du}{dr}\right)^2=\rho c_p u\frac{\partial T}{\partial z} \tag{3.22}$$

The term containing η_a, defined by Eq.(3.11) or Eq.(3.12), is the viscous dissipation term. As it is seen, the viscous dissipation term is directly proportional to the velocity gradient raised to square power. $\partial^2 T/\partial z^2$ is the axial heat conduction term, the heat conduction from downstream. Including the fluid axial heat conduction term requires the solution in the region $-\infty \leq z \leq \infty$ as discussed in Section 2.3.1.

Along with certain additional manipulations related with the fluid flow information, the present energy equation Eq.(3.22) can be solved just like that Eq.(2.20) in Chapter 2. The energy equation is solved with the 1st and 2nd kinds of thermal boundary conditions, which defined by Eqs.(2.2) - (2.3) on page 15.

3.3.2 Non-dimensional formulation

In this section, the definitions of the dimensionless quantities will be introduced. The dimensionless temperatures are defined just as in Chapter 2 and they are given by Eqs.(2.30) - (2.31).

The calculation of the temperature field is carried out using two dimensionless numbers, namely the Peclet (Pe) and Brinkman (Br) numbers. Their definitions are different than that in Chapter 2 due to the different fluid flow information. The Peclet number, which is the ratio of the heat transport by convection and the heat transport by conduction, is

$$Pe = \frac{\rho c_{\mathrm{p}} u_{\mathrm{m}} D_{\mathrm{h}}}{k} = Re_{\mathrm{M}} \cdot Pr_{\mathrm{M}} \tag{3.23}$$

$$Pr_{\mathrm{M}} \equiv \frac{c_{\mathrm{p}} \eta}{k} \tag{3.24}$$

The modified Reynolds number, Re_{M}, is given by Eq.(3.15). The Brinkman number, which is the ratio of the heat production by viscous dissipation and the heat transport by conduction, is defined as

$$Br^{(1)} \equiv \frac{\eta u_{\mathrm{m}}^2}{k\left[T_{\mathrm{i}}^{(1)} - T_e\right]} \tag{3.25}$$

$$Br^{(2)} \equiv \frac{\eta u_{\mathrm{m}}^2}{D_{\mathrm{h}} q_{\mathrm{i}}} \tag{3.26}$$

From the analysis, it is obvious that the effect of viscous dissipation is quantitatively significant if the Brinkman number is of appreciable magnitude. The Brinkman number clearly depends on fluid properties as well as on the flow conditions and $k\left[T_{\mathrm{i}}^{(1)} - T_e\right]$ or q_{i}.

The axial coordinate is nondimensionlized as

$$z^* = \frac{z}{PeD_{\mathrm{h}}} \tag{3.27}$$

By employing the relevant definitions for the dimensionless quantities, the dimensionless energy equation and boundary conditions are given as:

$$\frac{1}{r^*}\frac{\partial}{\partial r^*}\left(r^*\frac{\partial\theta}{\partial r^*}\right) + \frac{1}{Pe^2}\frac{\partial^2\theta}{\partial z^{*2}} + Br\cdot\eta_a^*\left(\frac{du^*}{dr^*}\right)^2 = u^*\frac{\partial\theta}{\partial z^*} \tag{3.28}$$

$$\text{in} \quad \frac{R^*}{2(1-R^*)} \le r^* \le \frac{1}{2(1-R^*)} \quad \text{and} \quad -\infty \le z^* \le \infty$$

(1) The first kind T.B.C.:

$$\begin{cases} \theta = 1 \quad \text{at} \quad r^* = \dfrac{R^*}{2(1-R^*)} & 0 < z^* \\ \theta = 0 \quad \text{at} \quad r^* = \dfrac{1}{2(1-R^*)} & 0 < z^* \\ \theta = 0 \quad \text{at} \quad r^* = \dfrac{R^*}{2(1-R^*)} & z^* \leq 0 \\ \theta = 0 \quad \text{at} \quad r^* = \dfrac{1}{2(1-R^*)} & z^* \leq 0 \\ \theta = 0 \quad \text{at} \quad \dfrac{R^*}{2(1-R^*)} \leq r^* \leq \dfrac{1}{2(1-R^*)} & z^* \to -\infty \\ \theta = \theta_{\text{fd}} \quad \text{at} \quad \dfrac{R^*}{2(1-R^*)} \leq r^* \leq \dfrac{1}{2(1-R^*)} & z^* \to \infty \end{cases} \tag{3.29}$$

(2) The second kind T.B.C.:

$$\begin{cases} \dfrac{\partial\theta}{\partial r^*} = -1 \quad \text{at} \quad r^* = \dfrac{R^*}{2(1-R^*)} & 0 < z^* \\ \dfrac{\partial\theta}{\partial r^*} = 0 \quad \text{at} \quad r^* = \dfrac{1}{2(1-R^*)} & 0 < z^* \\ \dfrac{\partial\theta}{\partial r^*} = 0 \quad \text{at} \quad r^* = \dfrac{R^*}{2(1-R^*)} & z^* \leq 0 \\ \dfrac{\partial\theta}{\partial r^*} = 0 \quad \text{at} \quad r^* = \dfrac{1}{2(1-R^*)} & z^* \leq 0 \\ \theta = 0 \quad \text{at} \quad \dfrac{R^*}{2(1-R^*)} \leq r^* \leq \dfrac{1}{2(1-R^*)} & z^* \to -\infty \\ \theta = \theta_{\text{fd}} \quad \text{at} \quad \dfrac{R^*}{2(1-R^*)} \leq r^* \leq \dfrac{1}{2(1-R^*)} & z^* \to \infty \end{cases} \tag{3.30}$$

3.3.3 Governing parameters for the problem

Besides the parameters, Pe, Br, n and R^*, which are described on page 25 in Section 2.3.3, the following parameters are applied.

- The dimensionless relative velocity of the moving core, U^*, defined by Eq.(3.7), which is the ratio of the moving core velocity to the average velocity of the fluid flow. The sign of "+" before U^* reflects the case when the core direction coincides with the flow direction and "-" is vice versa.

- The rheological parameters such as the dimensionless shear rate parameter β defined by Eq.(3.20). Numerical values of a practical example can be found in Ref.[81] (p. 369).

3.3.4 Transformed dimensionless energy equation

The semi-infinite solution domain was transformed into a finite domain by utilizing the relation employed in Section 2.4.2. By introducing the transformed coordinate z_t^* defined by Eq.(2.64), the energy equation and the boundary conditions become

$$\frac{\partial^2\theta}{\partial r^{*2}} + l_2\frac{\partial^2\theta}{\partial z_t^{*2}} + \frac{1}{r^*}\frac{\partial\theta}{\partial r^*} + Br\cdot\eta_a^*\left(\frac{du^*}{dr^*}\right)^2 = l_1\frac{\partial\theta}{\partial z_t^*} \tag{3.31}$$

$$\text{in} \quad \frac{R^*}{2(1-R^*)} \le r^* \le \frac{1}{2(1-R^*)} \quad \text{and} \quad -0.5 \le z_t^* \le 0.5$$

where

$$l_1 = \frac{\cos^2(\pi z_t^*)}{\pi E}\left[u^* + \frac{1}{Pe^2}\frac{\sin(2\pi z_t^*)}{E}\right] \tag{3.32}$$

$$l_2 = \frac{1}{Pe^2}\left[\frac{\cos^2(\pi z_t^*)}{\pi E}\right]^2 \tag{3.33}$$

The boundary conditions, Eqs.(3.29) - (3.30), are unchanged except that $z^* \to -\infty$ and $z^* \to \infty$ are replaced by $z_t^* = -0.5$ and $z_t^* = 0.5$, respectively. They can be written as follows,

(1) the 1st kind of thermal boundary condition:

$$\begin{cases} \theta = 1 \ \text{ at } & r^* = \dfrac{R^*}{2(1-R^*)} & 0 < z_t^* \\ \theta = 0 \ \text{ at } & r^* = \dfrac{1}{2(1-R^*)} & 0 < z_t^* \\ \theta = 0 \ \text{ at } & r^* = \dfrac{R^*}{2(1-R^*)} & z_t^* \le 0 \\ \theta = 0 \ \text{ at } & r^* = \dfrac{1}{2(1-R^*)} & z_t^* \le 0 \\ \theta = 0 \ \text{ at } & \dfrac{R^*}{2(1-R^*)} \le r^* \le \dfrac{1}{2(1-R^*)} & z_t^* = -0.5 \\ \theta = \theta_{\text{fd}} \ \text{ at } & \dfrac{R^*}{2(1-R^*)} \le r^* \le \dfrac{1}{2(1-R^*)} & z_t^* = 0.5 \end{cases} \tag{3.34}$$

(2) the 2nd kind of thermal boundary condition:

$$\begin{cases} \dfrac{\partial\theta}{\partial r^*} = -1 \quad \text{at} \quad r^* = \dfrac{R^*}{2(1-R^*)} & 0 < z_t^* \\ \dfrac{\partial\theta}{\partial r^*} = 0 \quad \text{at} \quad r^* = \dfrac{1}{2(1-R^*)} & 0 < z_t^* \\ \dfrac{\partial\theta}{\partial r^*} = 0 \quad \text{at} \quad r^* = \dfrac{R^*}{2(1-R^*)} & z_t^* \leq 0 \\ \dfrac{\partial\theta}{\partial r^*} = 0 \quad \text{at} \quad r^* = \dfrac{1}{2(1-R^*)} & z_t^* \leq 0 \\ \theta = 0 \quad \text{at} \quad \dfrac{R^*}{2(1-R^*)} \leq r^* \leq \dfrac{1}{2(1-R^*)} & z_t^* = -0.5 \\ \theta = \theta_{\text{fd}} \quad \text{at} \quad \dfrac{R^*}{2(1-R^*)} \leq r^* \leq \dfrac{1}{2(1-R^*)} & z_t^* = 0.5 \end{cases} \tag{3.35}$$

The transformed energy equation Eq.(3.31), which is an elliptic, non-homogeneous differential equation, is solved numerically by a finite difference procedure. Further detail of the calculation method is available in Section 2.4.

3.3.5 Solutions for $z \rightarrow \infty$

As stated in Section 2.4, the temperature distribution at infinitely large axial location ($z^* \rightarrow \infty$) is necessary. For very large axial coordinate, fully developed temperature profiles are approached. At this stage the attention is restricted to the fully developed flows under the 1st kind and 2nd kind of thermal boundary conditions.

One of the characteristic features of laminar heat transfer in ducts of constant cross section is, that, as fully developed velocity and temperature profiles are approached, the Nusselt number converges to a constant value [82]. In the following two subsections, the Nusselt numbers are shown as functions of the dimensionless shear rate parameter, β, for the 1st kind and 2nd kind of thermal boundary conditions respectively.

The temperature fields in the fully developed region were calculated from Eq.(2.49) and Eq.(2.58) with some manipulations related with the fluid flow information. Obviously the velocity fields obtained in Section 3.2 have been applied into Eq.(2.49) and Eq.(2.58). Also it should be noted that, the definitions of Brinkman number and dimensionless apparent viscosity are given by Eqs.(3.25) - (3.26) and Eqs.(3.16) - (3.17). By applying the calculated results for the temperature field, the Nusselt numbers were obtained from Eqs.(2.44) - (2.46).

The 1st kind of T.B.C (solutions for $z \to \infty$)

In Figs.3.6 - 3.8, the results are illustrated for an annular duct of the radius ratio, R^* equal 0.5. Figure 3.6 shows the radial temperature profiles for pseudoplastic (n = 0.5, β = 1), Newtonian (n = 1) and dilatant (n = 1.5, β = 1) fluids. Figure 3.7 shows the Nusselt number at the core tube wall, Nu_{i} defined by Eq.(2.44), as a function of the dimensionless shear rate parameter β. Figure 3.8 is for the Nusselt number at the outer tube wall, Nu_{o}, defined by Eq.(2.45). In Figs.3.7 - 3.8, the upper plots are for $n \leq 1$ and the lower plots are for $n \geq 1$. The relative velocity of the core, U^*, varies in the figures in the horizontal direction having the values -1, 0 and 1. The parameter in these figures are the Brinkman number having the values 0; 0.1 and 0.5. With an increase in the Brinkman number, the Nusselt number at the core tube decreases while Nu_{o} increases.

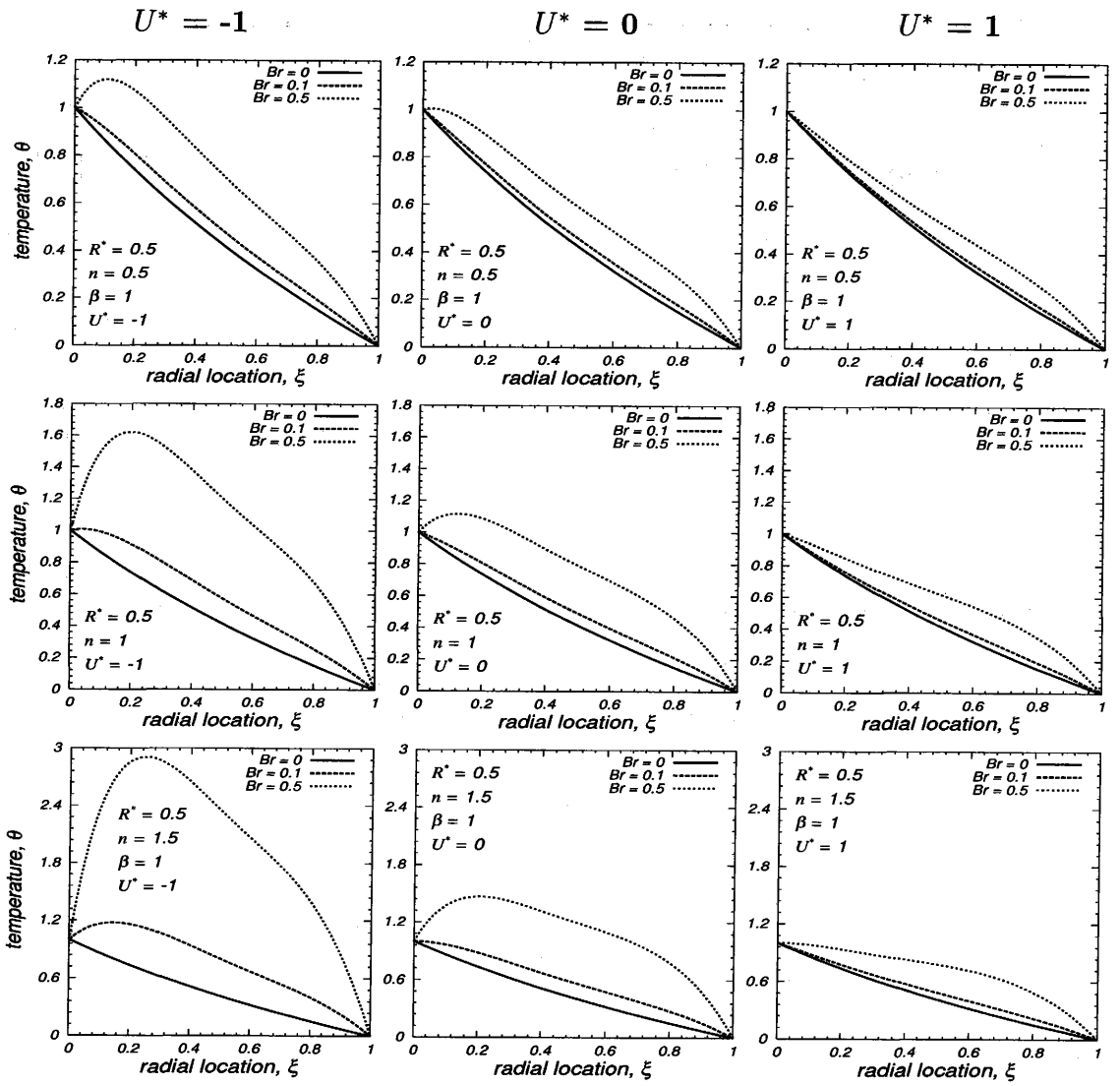

Fig. 3.6: Temperature profiles for different fluids

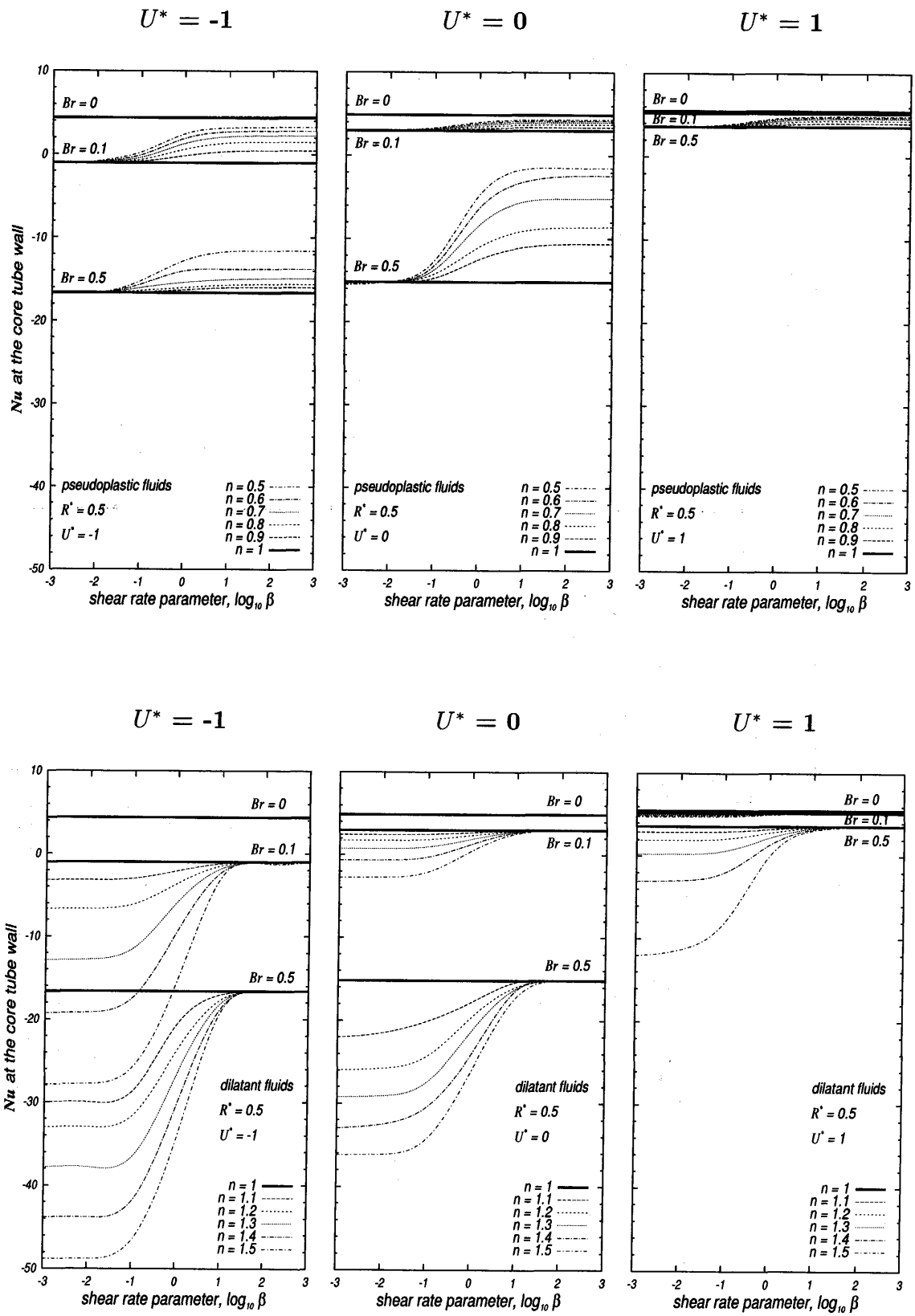

Fig. 3.7: Nusselt number at the inner tube vs β (U^* = -1; 0; 1)

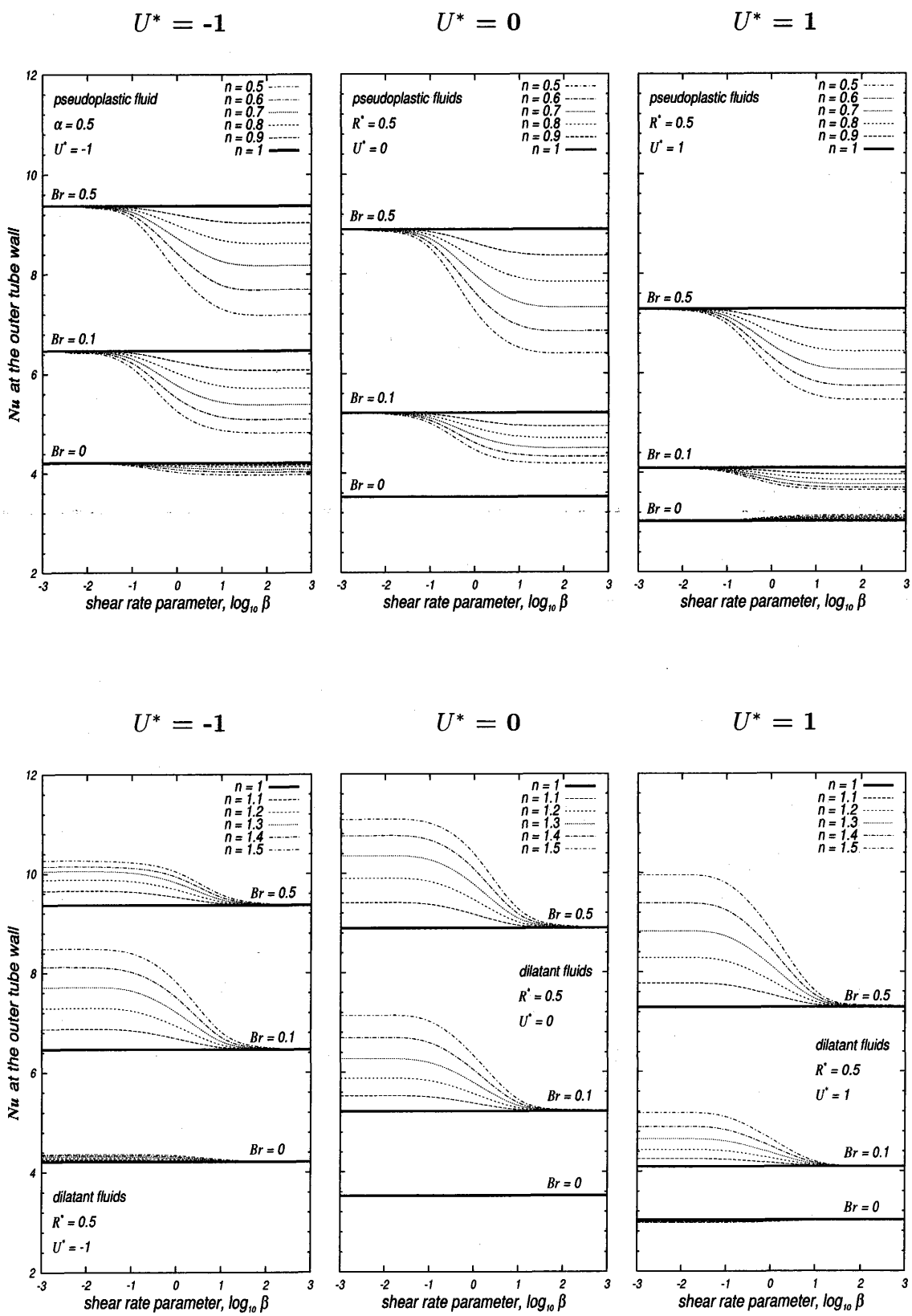

Fig. 3.8: Nusselt number at the outer tube vs β (U^* = -1; 0; 1)

The 2nd kind of T.B.C (solutions for $z \to \infty$)

In Fig.3.9, the solutions are illustrated for an annular duct of the radius ratio, $R^* = 0.5$. The Nusselt number at the core wall, Nu_i defined by Eq.(2.46), is shown in the figure as a function of the dimensionless shear rate parameter β. The relative velocity of the core, U^*, varies in the figures in the vertical direction having the values -1, 0 and 1. The parameter in these figures are the Brinkman number having the values 0; 0.01 and 0.05. The Nusselt number decreases with an increase in Br for U^* = -1 and $U^* = 0$, but increases for $U^* = 1$. The power-law asymptotic values of Nu are tabulated in Appendix (Table 4.2).

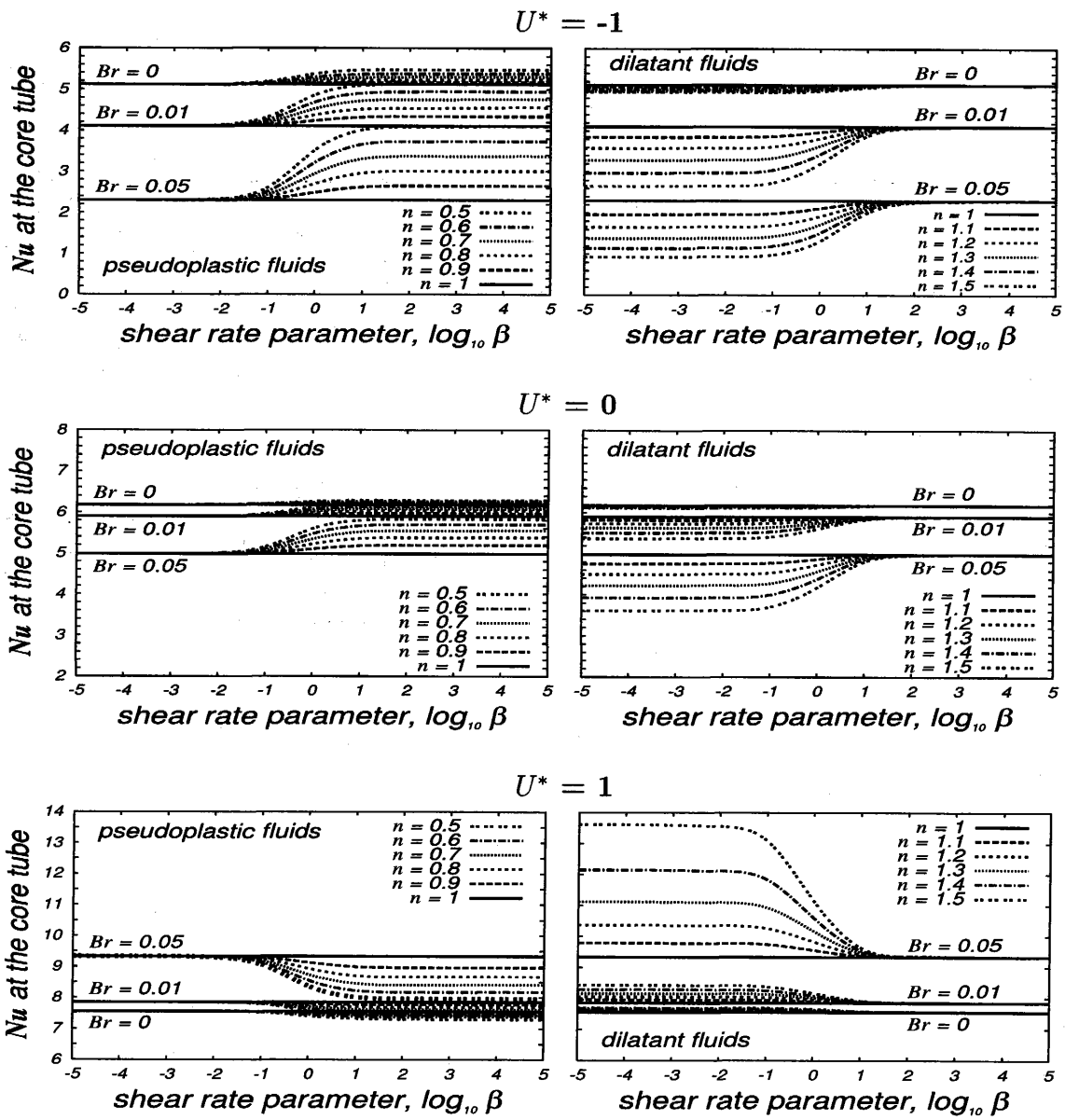

Fig. 3.9: Nusselt number vs. β (U^* = -1; 0; 1)

3.4 Results and Discussions of the 1st Kind of T.B.C

By applying the velocity field in a concentric annular duct consisting of a fixed outer tube and a core tube moving in the stream-wise direction, which was obtained in Section 3.2, the temperature field of the thermally developing flow has been solved numerically. The temperature field under the 1st kind of thermal boundary condition has been obtained by solving the transformed energy equation, Eq.(3.31), with Eq.(3.34).

The objective herein is to display the results and to provide explanations for the solutions. The results are presented in the form of graphs and compared to the available data by other authors. Another objective is to compare the results with the predictions of the results for the stationary annular duct counterpart to show how the effects of viscous dissipation and fluid axial heat conduction will be changed with the core velocity. Thus, the attention is paid how the roles of viscous dissipation and fluid axial heat conduction in heat transfer depend on the core movement.

In order to bring out the effect of the moving core velocity on heat transfer with the viscous dissipation and the fluid axial heat conduction, the values of temperature distributions and the Nusselt numbers at the tube walls are plotted.

The effects of the moving core velocity, U^*, Peclet number, a nondimensional parameter representing the effects of axial heat conduction within the flow, Brinkman number, a nondimensional parameter representing the effects of viscous dissipation, radius ratio, R^*, flow index, n, shear rate parameter, β, on temperature distribution and Nusselt numbers are investigated in this theoretical study.

The notation U^*, which is dimensionless core velocity defined by Eq.(3.7), is used throughout the discussion to describe the core velocity effect. The figures are given in pairs, in order to illustrate the similarities and dissimilarities between the stationary tubes' case ($U^* = 0$) and the moving core's case ($U^* = 1$). The figures on the left are for $U^* = 0$, while the figures on the right are for $U^* = 1$.

The relative importance of the fluid axial heat conduction is established by the magnitude of the Peclet number, Pe defined by Eq.(3.23). From the energy equation Eq.(3.28), it is seen for large values of Pe number the axial heat conduction within the fluid is relatively unimportant. On the other hand, for a flow at a low Peclet number, fluid axial heat conduction is more important.

The relative importance of viscous dissipation is quantified by the Brinkman

number, Br defined by Eq.(3.25). From the energy equation Eq.(3.28), it is seen the heating due to viscous dissipation will be the greatest where the velocity gradient is the highest. Therefore the results displaying the temperature field under the viscous dissipation will be explained with respect to the velocity gradients (See Figs. 3.2 and 3.5).

The results are illustrated for the flows of Newtonian ($n = 1$), pseudoplastic ($n = 0.5$ and $\beta = 1$) and dilatant ($n = 1.5$ and $\beta = 1$) fluids. The values of the radius ratio, R^*, are 0.2, 0.5 and 0.8.

In the following sections, the heat transfer results such as the temperature distribution of the flow and the Nusselt number at the tube walls are given.

3.5 Temperature Distributions of the 1st Kind of T.B.C

The temperature field in an annular duct can be plotted from the results of the numerical calculation for the heat transfer. The dimensionless temperature, θ, shown in the following figures is defined by Eq.(2.30). Then the entering fluid temperature at $z^* \to -\infty$ is 0. The core tube wall is maintained at $\theta = 1$ for $z^* > 0$, but for $z^* \leq 0$ the core tube temperature is 0. The outer wall is kept at the entering fluid temperature or its temperature is 0.

In the following figures, $\xi = 0$ corresponds to the core tube wall and $\xi = 1$ is the outer tube wall and the temperature profiles are illustrated at three different axial locations $z^* = 0$; $z^* = 2.4 \times 10^{-2}$ and $z^* = 1$.

Figures 3.10 - 3.12 contain the radial temperature distributions for large Peclet number values and these plots suggest how the viscous dissipation affects the developing temperature profiles.

Figures 3.13 - 3.15 show the radial temperature distributions for negligible viscous dissipation ($Br = 0$) and these plots suggest how the fluid axial heat conduction affects the developing temperature profiles.

Figure 3.16 contains the radial temperature distributions of, respectively, a Newtonian fluid, a pseudoplastic fluid and a dilatant fluid.

3.5.1 Effect of Br on the temperature distributions

In Figs.3.10 - 3.12, the attention is focused on the viscous dissipation effect on the temperature distribution. Therefore the predictions are presented for the case of negligible fluid axial heat conduction ($Pe \rightarrow \infty$). As stated previously, these results are given for the annular duct of radius ratio, R^* equal 0.5. The temperature profiles of the different fluids, the Newtonian fluid in Fig.3.10; the pseudoplastic fluid in Fig.3.11 and the dilatant in Fig.3.12, bear similar shapes with only difference being quantitative.

In these figures illustrating the temperature field inside the annular duct, the Brinkman number value varies vertically having the values 0 and 0.1. For larger values of Br, it can be seen that the dimensionless temperature of the fluid at $z^* \leq 0$ deviates significantly from zero. Since the tube wall temperatures of the region $z \leq 0$ are set at the same level as the inlet temperature $\theta_e = 0$, the increase of the temperature in this region is due to the viscous dissipation (in this case of $Pe \rightarrow \infty$).

The other relevant parameters are the core velocity, U^*. As throughout in this section, the plots in the left side are for the stationary core case or for $U^* = 0$ and the right hand side ones are for the moving core case of $U^* = 1$. The temperature rise resulting from the viscous dissipation is seen less for $U^* = 1$ than for $U^* = 0$.

Some more information on the effect of Br on the temperature profile may be found in Section 2.10.1.

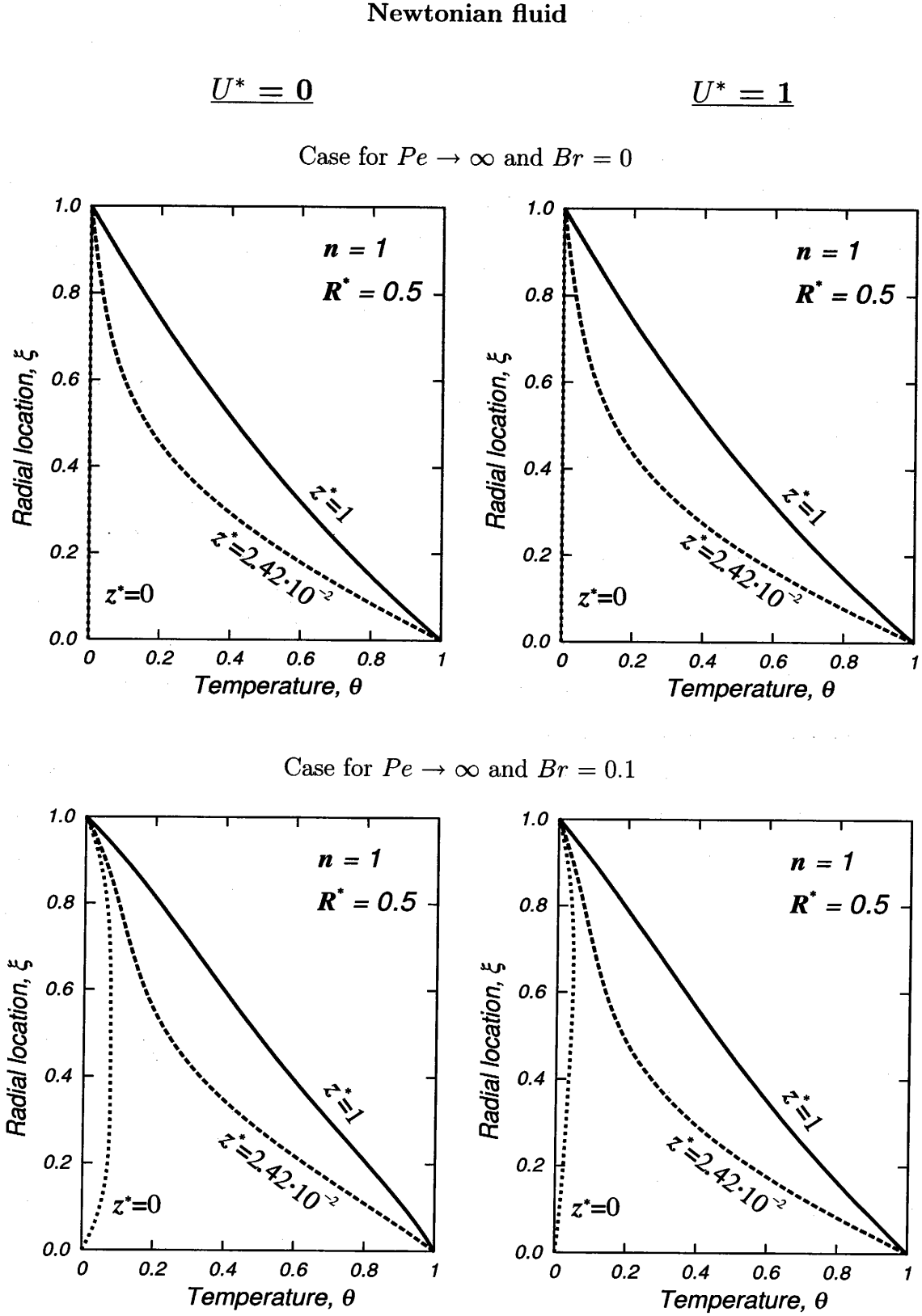

Fig. 3.10: Developing temperature profiles of a Newtonian fluid.
The plots refer to different degrees of viscous dissipation for $U^* = 0$ and 1

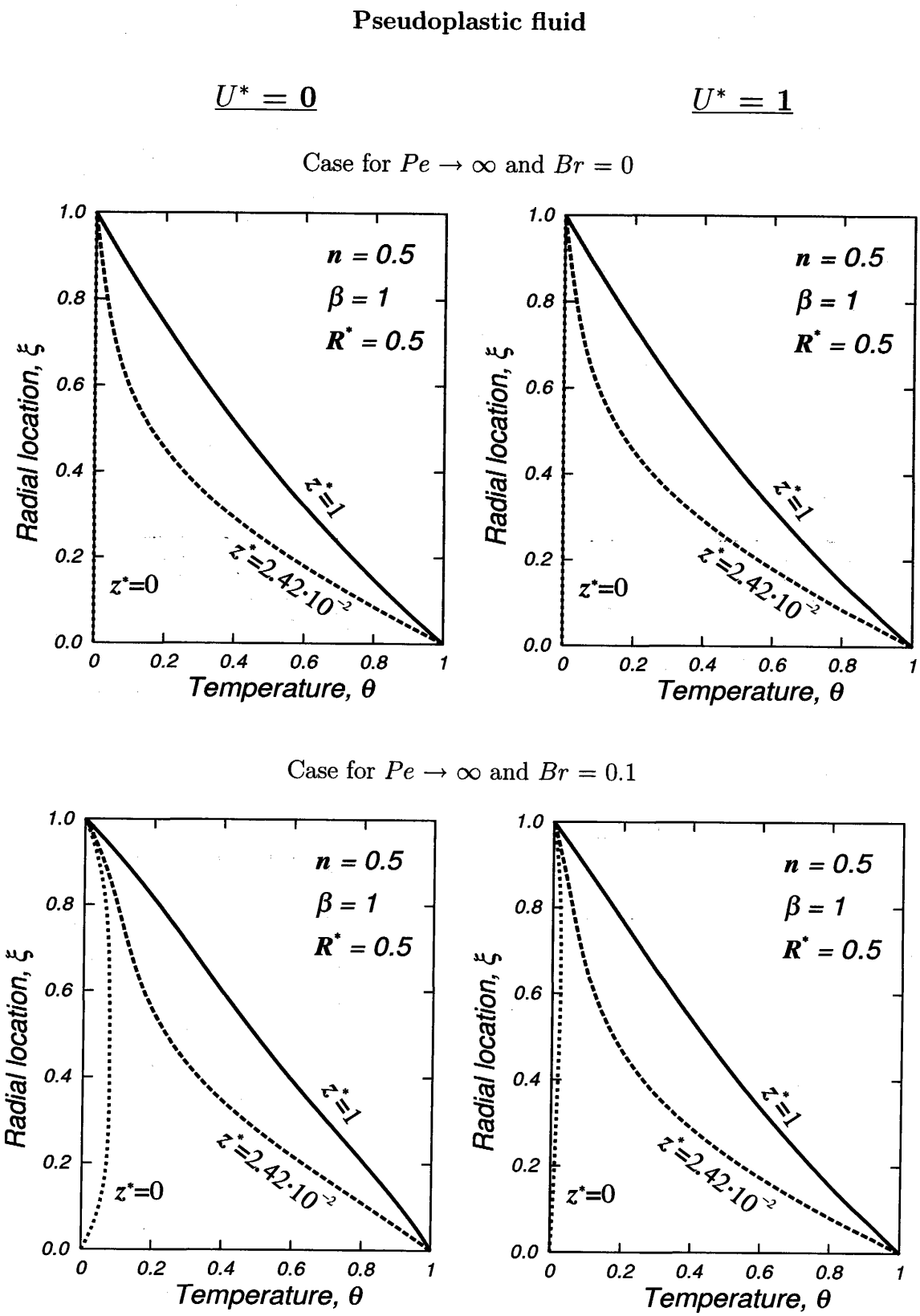

Fig. 3.11: Developing temperature profiles of a pseudoplastic fluid.
The plots refer to different degrees of viscous dissipation for $U^* = 0$ and 1

Dilatant fluid

$\underline{U^* = 0}$ $\underline{U^* = 1}$

Case for $Pe \to \infty$ and $Br = 0$

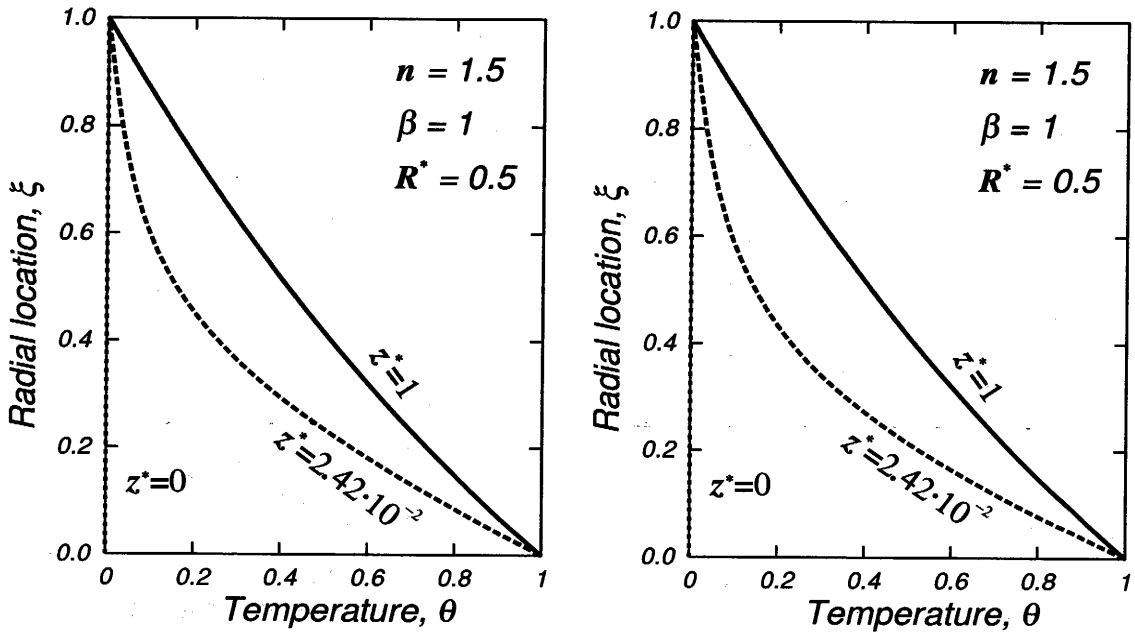

Case for $Pe \to \infty$ and $Br = 0.1$

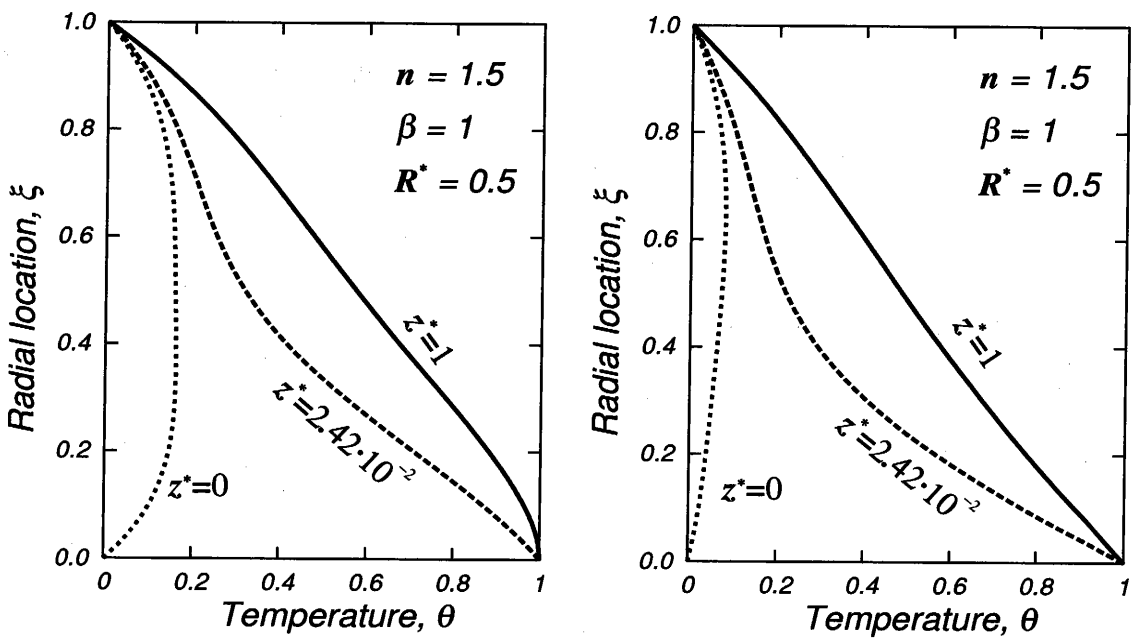

Fig. 3.12: Developing temperature profiles of a dilatant fluid.
The plots refer to different degrees of viscous dissipation for $U^* = 0$ and 1

3.5.2 Effect of Pe on the temperature distributions

Figures 3.13 - 3.15 show the effect of fluid axial heat conduction on the heat transfer in terms of the Peclet number, Pe. These figures display the temperature profiles across the annular duct cross section.

These figures illustrating θ correspond to the flows of Newtonian ($n = 1$), pseudo-plastic ($n = 0.5$ and $\beta = 1$) and dilatant ($n = 1.5$ and $\beta = 1$) fluids, respectively. The plots in each figure are the temperature profiles under the same conditions except for a change in the axial heat conduction term and the core velocity value. These temperature profiles of the different fluids bear similar shapes with only difference being quantitative.

The upper two plots correspond to the negligible fluid axial heat conduction case or $Pe \rightarrow \infty$. The lower ones show the temperature distributions when Pe = 10. If the upper plots are compared with the lower ones, the fluid axial heat conduction effect on the temperature distribution can be observed. As the fluid flows, its temperature rises due to the heat input from the wall and from the fluid axial heat conduction. These results display the expected temperature increase due to the fluid axial heat conduction specially in the region of $z \leq 0$, where the dimensionless temperature θ is 0 at the walls i.e $\xi = 0$ and $\xi = 1$. The location z^* = 0 represents the location of the sudden change in the wall temperature. Since the tubes' wall temperatures of the region $z \leq 0$ are set at the same level as the inlet temperature $\theta_e = 0$, the increase of the temperature in this region is due to the fluid axial heat conduction. It can be observed that the fluid temperature increases in $z \leq 0$ or before the fluid reaches the heated part of the core.

By comparing the pairs of plots in a row, one can observe the core velocity effect on the developing temperature distribution. By comparing the curves in the plots for $U^* = 1$ with the ones for $U^* = 0$, only a slight difference in the radial temperature profile is observed in the heated wall region ($z^* > 0$) and in the unheated wall region ($z^* \leq 0$).

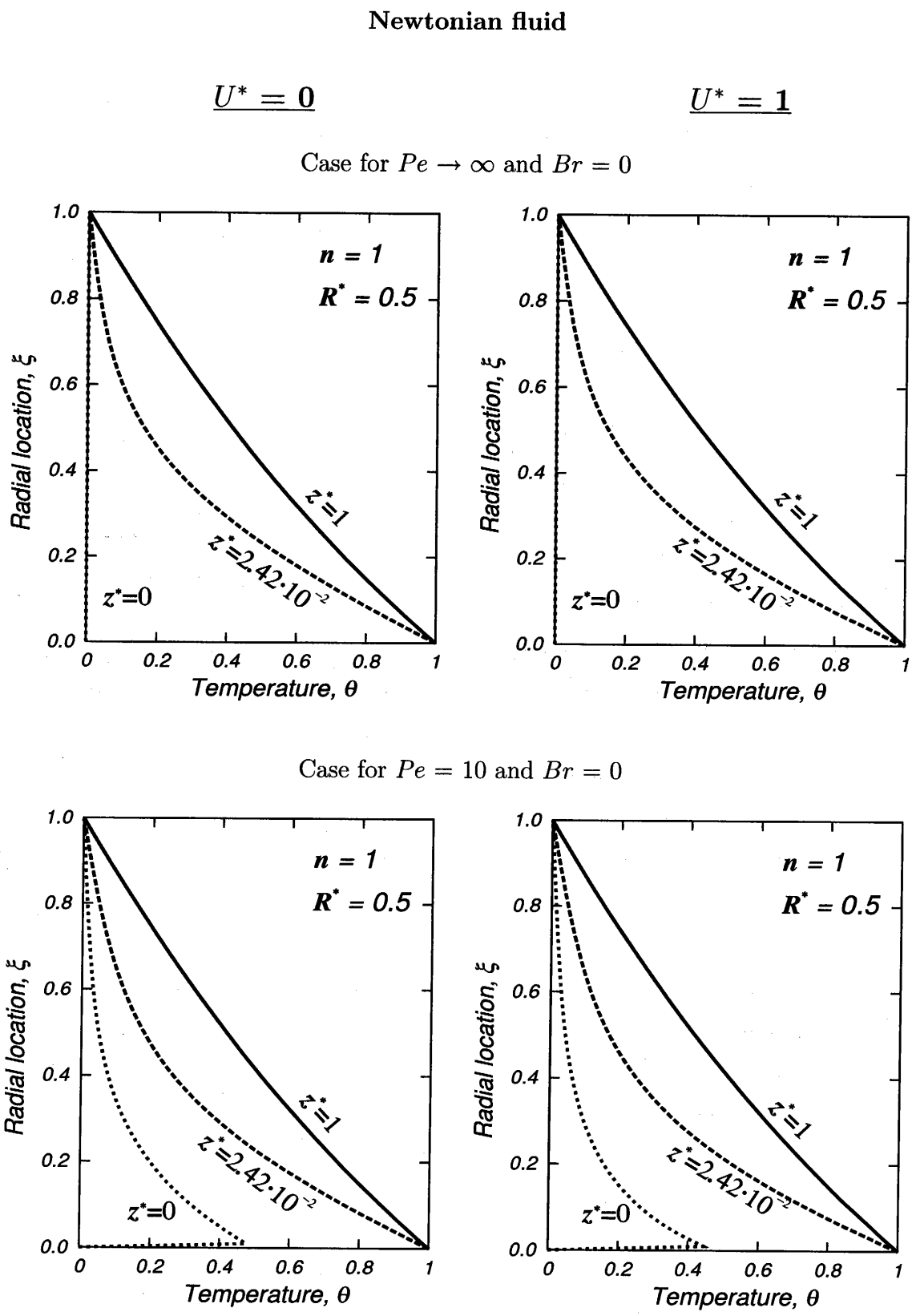

Fig. 3.13: Developing temperature profiles of a Newtonian fluid.
The plots refer to different degrees of fluid axial heat conduction for $U^* = 0$ and 1

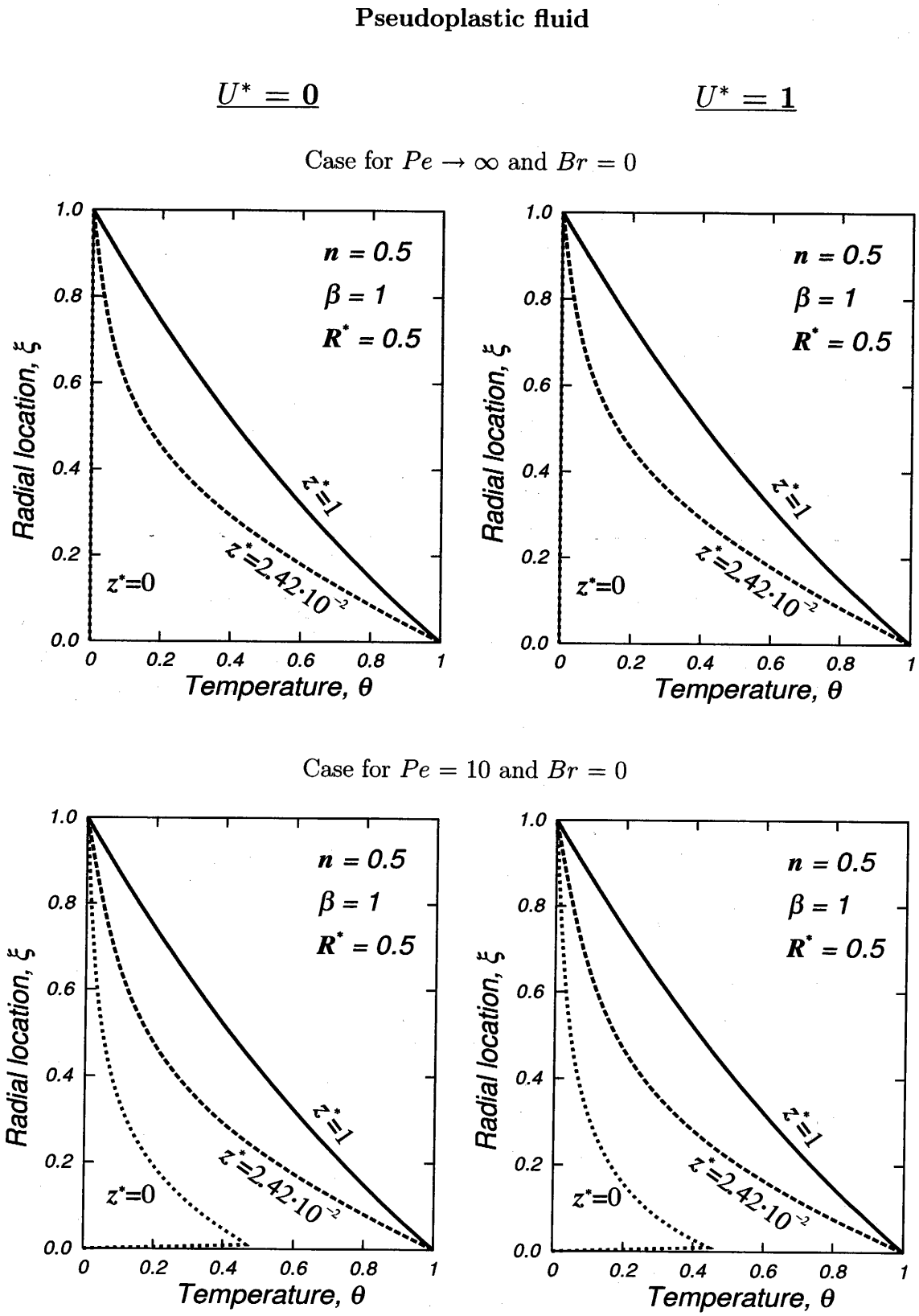

Fig. 3.14: Developing temperature profiles of a pseudoplastic fluid.
The plots refer to different degrees of fluid axial heat conduction for $U^* = 0$ and 1

Dilatant fluid

$\underline{U^* = 0}$ $\underline{U^* = 1}$

Case for $Pe \to \infty$ and $Br = 0$

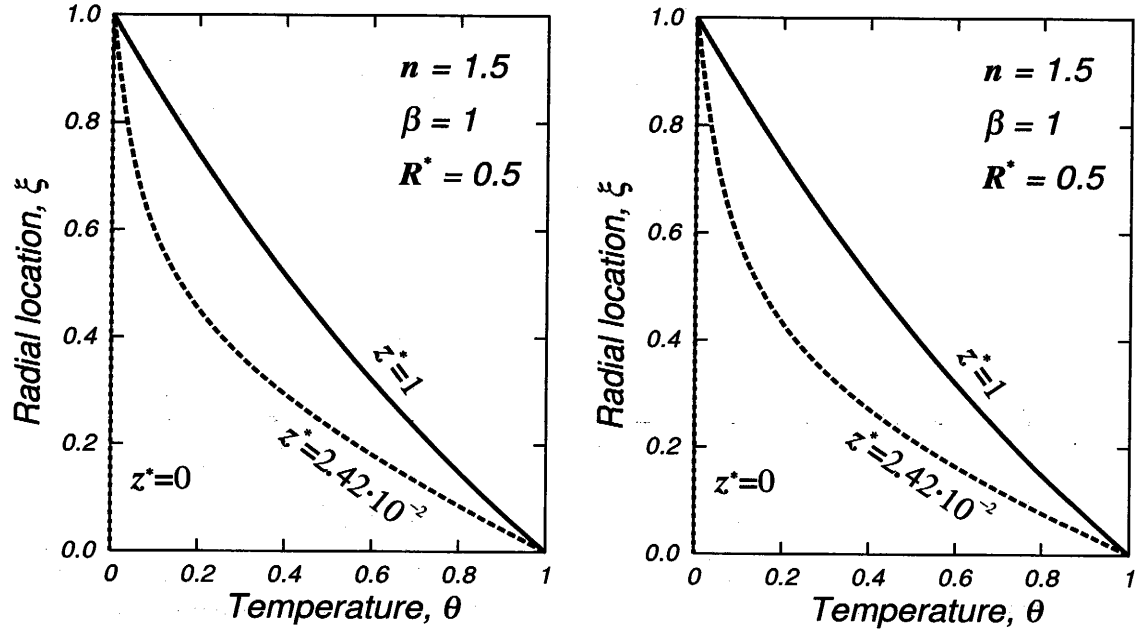

Case for $Pe = 10$ and $Br = 0$

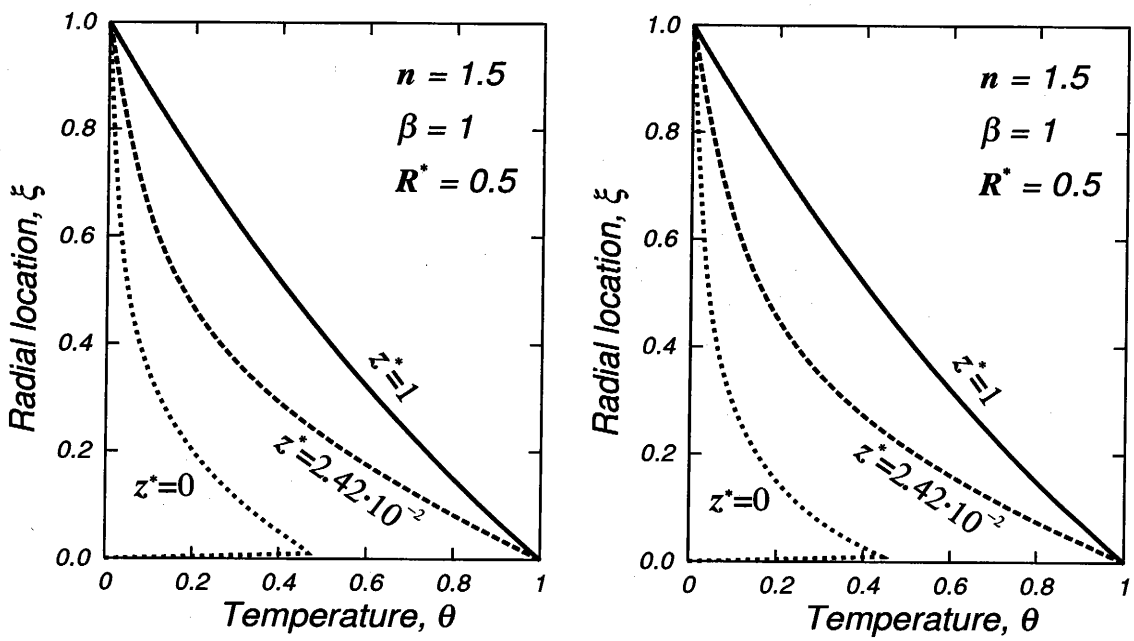

Fig. 3.15: Developing temperature profiles of a dilatant fluid.
The plots refer to different degrees of fluid axial heat conduction for $U^* = 0$ and 1

3.5.3 Effect of n on the temperature distributions

The solutions presented in Fig.3.16 display the effects of n on the temperature distributions. The flow index, n, varies in the figures in a vertical direction having the values of 1, 0.5 and 1.5. The Brinkman number is 0.1 and the Peclet number is 10. By comparing the pairs, it is seen the increase due to the contribution of viscous dissipation and fluid axial heat conduction is greater for the case of the stationary core ($U^* = 0$).

More information on the effect of n on the temperature profile can be found in Section 2.10.3.

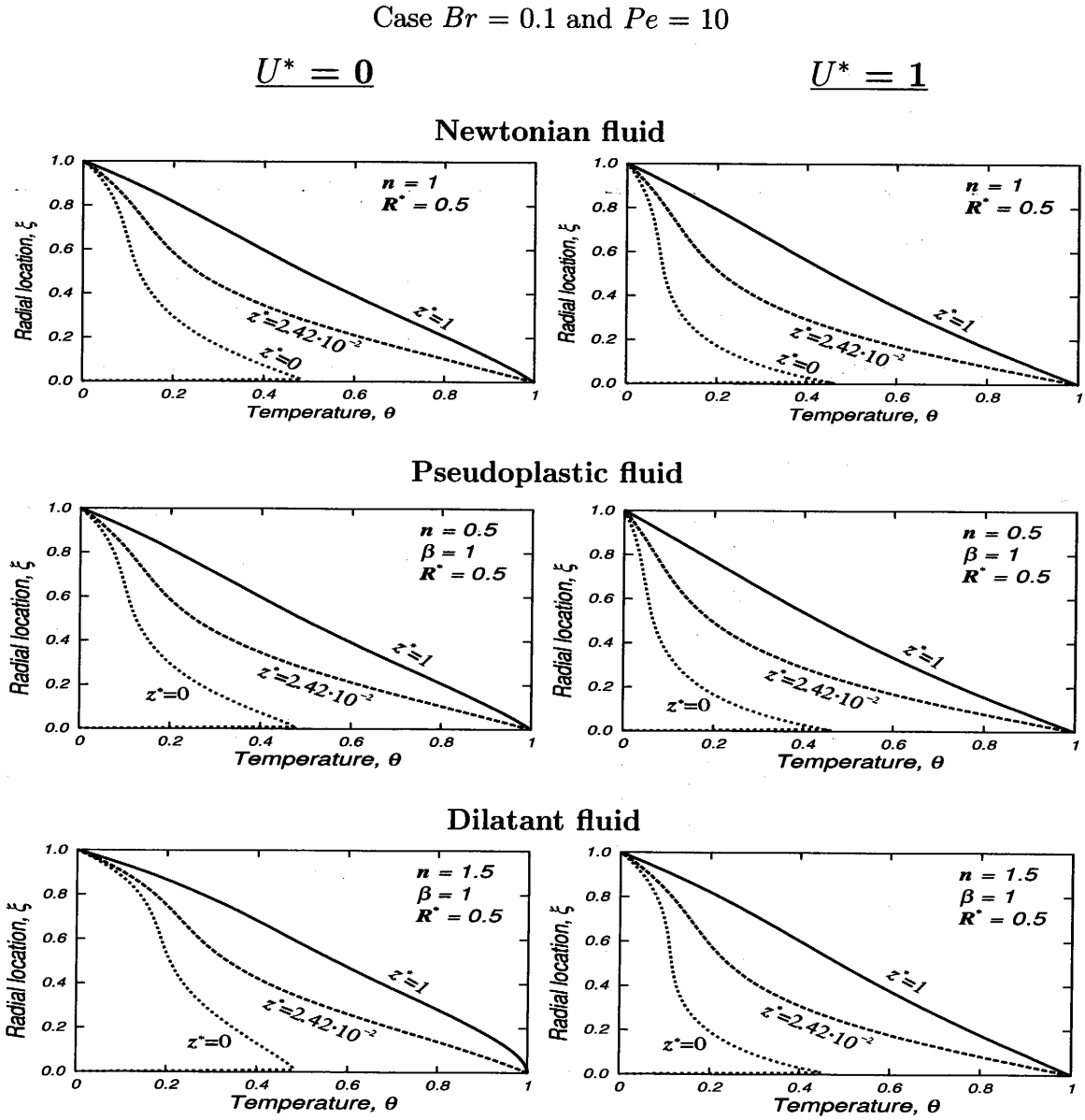

Fig. 3.16: Developing temperature profiles for the different fluids, $Br = 0.1$ and $Pe = 10$ ($U^* = 0$ and 1)

3.6 Nusselt Numbers for the 1st Kind of T.B.C

The Nusselt numbers resulting from the calculations are shown in Figs.3.17 - 3.21. The definition of the Nusselt numbers are given by Eqs.(2.44) - (2.45). The variation of the Nusselt numbers was investigated from the viewpoint of the effects of viscous dissipation and fluid axial heat conduction. The effects of the Brinkman number and the Peclet number on the axial distribution of the local Nusselt number are examined in light of the development of the temperature profiles. Figures 3.17 - 3.19 illustrate the local Nusselt numbers for the different fluids such the Newtonian ($n = 1$), the pseudoplastic ($n = 0.5$ and $\beta = 1$) and the dilatant fluid ($n = 1.5$ and $\beta = 1$).

Also included in these figures is the effect of the core velocity, U^*. Special cases with negligible viscous dissipation and fluid axial heat conduction are given so that the comparison with that of Shah and London [2] for $U^* = 0$ and by Shigechi and Araki [27] for $U^* = 1$ can be made. The agreement between the present solutions with the solutions in Refs.[2] and [27] appears to be excellent.

3.6.1 Effect of Br on the Nusselt numbers

From Figs.3.17 - 3.19, it is seen that for $U^* = 0$ the Nusselt number at the core tube decreases with an increase in the Brinkman number in the fully developed region, whereas for $U^* = 1$ if the fluid is Newtonian or pseudoplastic the Nusselt curves at the core are identical.

For a specified axial position, Nusselt number at the moving core ($U^* = 1$) is larger than the corresponding Nusselt number at the fixed core ($U^* = 0$) with the given Brinkman number and the Peclet number.

For the stationary core case ($U^* = 0$), the viscous dissipation has a strong effect on the local heat transfer rate in the fully developed region. But this effect weakens if the core moves in the direction as the fluid flows.

In the thermal entrance region, viscous dissipation effect ($Br \neq 0$) is strong on the Nusselt number at the outer tube. But Nu curves at the core tube are almost identical in the thermally developing region for different values of Br for the equal Peclet.

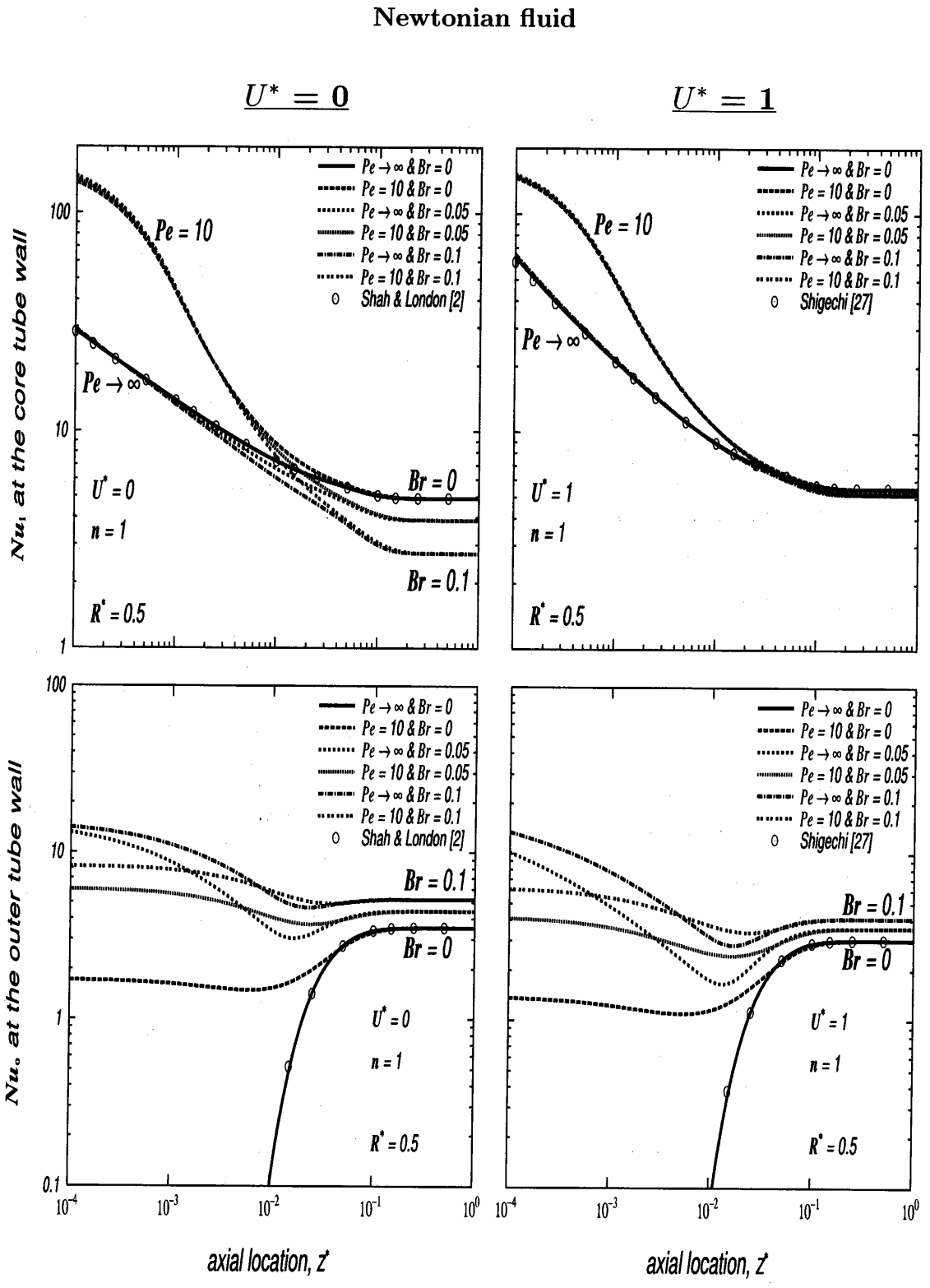

Fig. 3.17: Nu variations for a Newtonian fluid with different degrees of viscous dissipation and fluid axial heat conduction ($U^* = 0$ and $U^* = 1$)

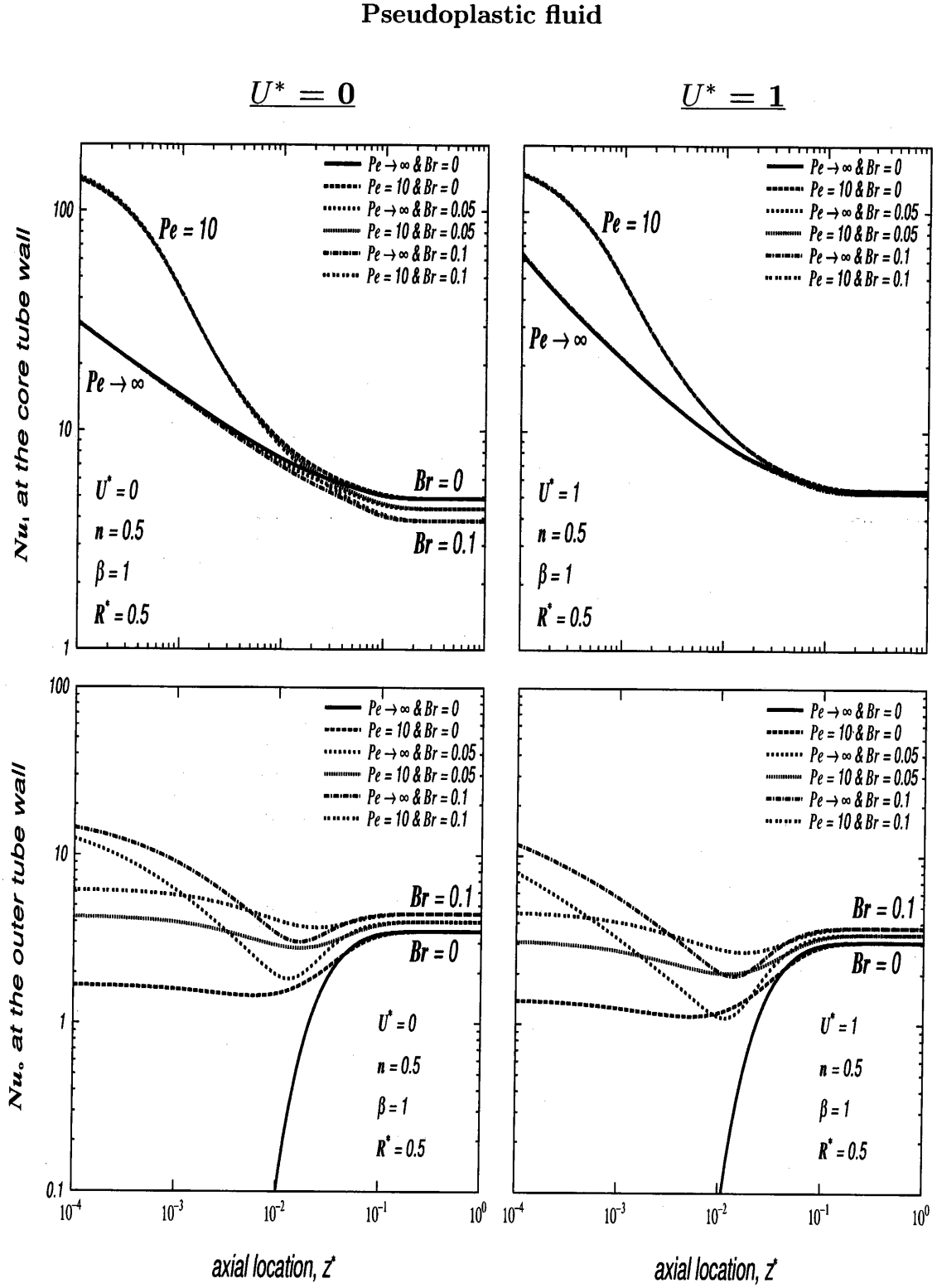

Fig. 3.18: Nu variations for a pseudoplastic fluid with different degrees of viscous dissipation and fluid axial heat conduction ($U^* = 0$ and $U^* = 1$)

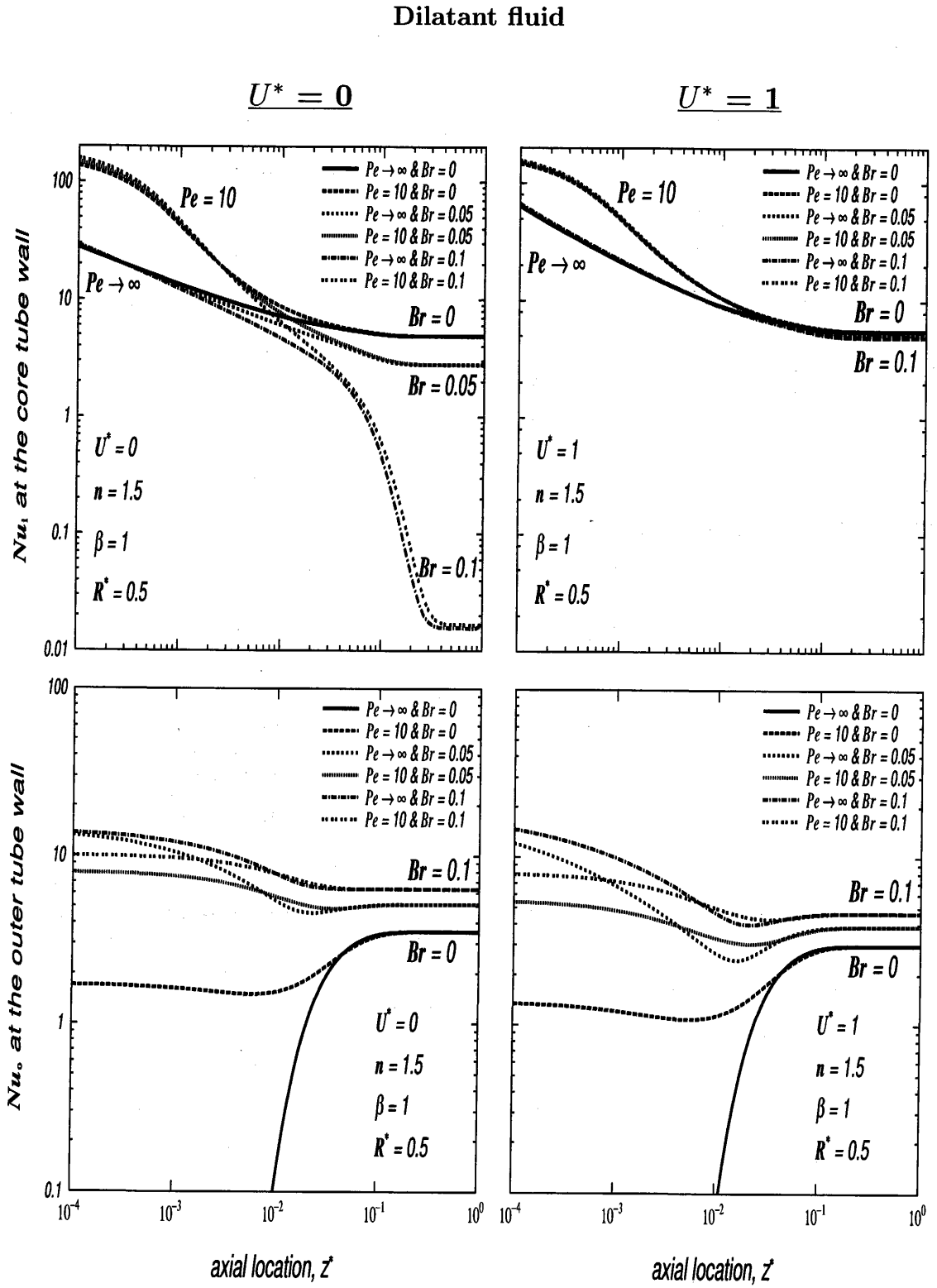

Fig. 3.19: Nu variations for a dilatant fluid with different degrees of viscous dissipation and fluid axial heat conduction ($U^* = 0$ and $U^* = 1$)

3.6.2 Effect of Pe on the Nusselt numbers

From Figs.3.17 - 3.19, the following observations about the effect of Pe number on Nu at the tube walls can be made.

For a given axial position, the Nusselt number at the moving core ($U^* = 1$) is larger than the corresponding Nusselt number at the fixed core ($U^* = 0$) for a specified Peclet number.

The effect of fluid axial heat conduction ($Pe = 10$) accounts for a Nu value increase at the core wall in the thermal entrance region.

3.6.3 Effect of n on the Nusselt numbers

The heat transfer results show quite similar behaviors for different fluids in Figs.3.17 - 3.19. For the non-Newtonian fluids, the Nusselt number increases with decreasing a Peclet number at a given value of z^* in the thermal entrance region just as it does for the Newtonian fluid.

When the viscous dissipation is included in the study, the Nusselt numbers Nu_{i}, for heat transfer to the Newtonian fluid are higher than those to the dilatant fluid but less than those to the pseudoplastic fluid. However, in the fully developed region this effect of n diminishes if U^* is 1.

The response of the Newtonian fluid to viscous heating is more pronounced than that of the pseudoplastic fluid but less remarkable than the dilatant fluid.

3.6.4 Effect of R^* on the Nusselt numbers

In order to study the radius ratio effects, the heat transfer results are shown in Figs.3.20 - 3.21. The general behavior was quite similar for different fluids. Therefore as an example, the calculation results for a pseudoplastic fluid are shown for $Pe \rightarrow \infty$ and $Pe = 10$.

In the sequence of plots in Figs.3.20 - 3.21, the effect of the major parameters of the problem on the Nusselt number is presented. In this section, the attention is focused on the radius ratio.

From these Nusselt curves it can be observed that, for a specified axial position the Nusselt number at the moving core ($U^* = 1$) is larger than the corresponding Nusselt number at the fixed core ($U^* = 0$) with the given Brinkman number and the Peclet number.

The radius ratio $R^* = 0.2$ is superior to $R^* = 0.5$ and $R^* = 0.8$ from the view point of heat transfer at the core under the same conditions.

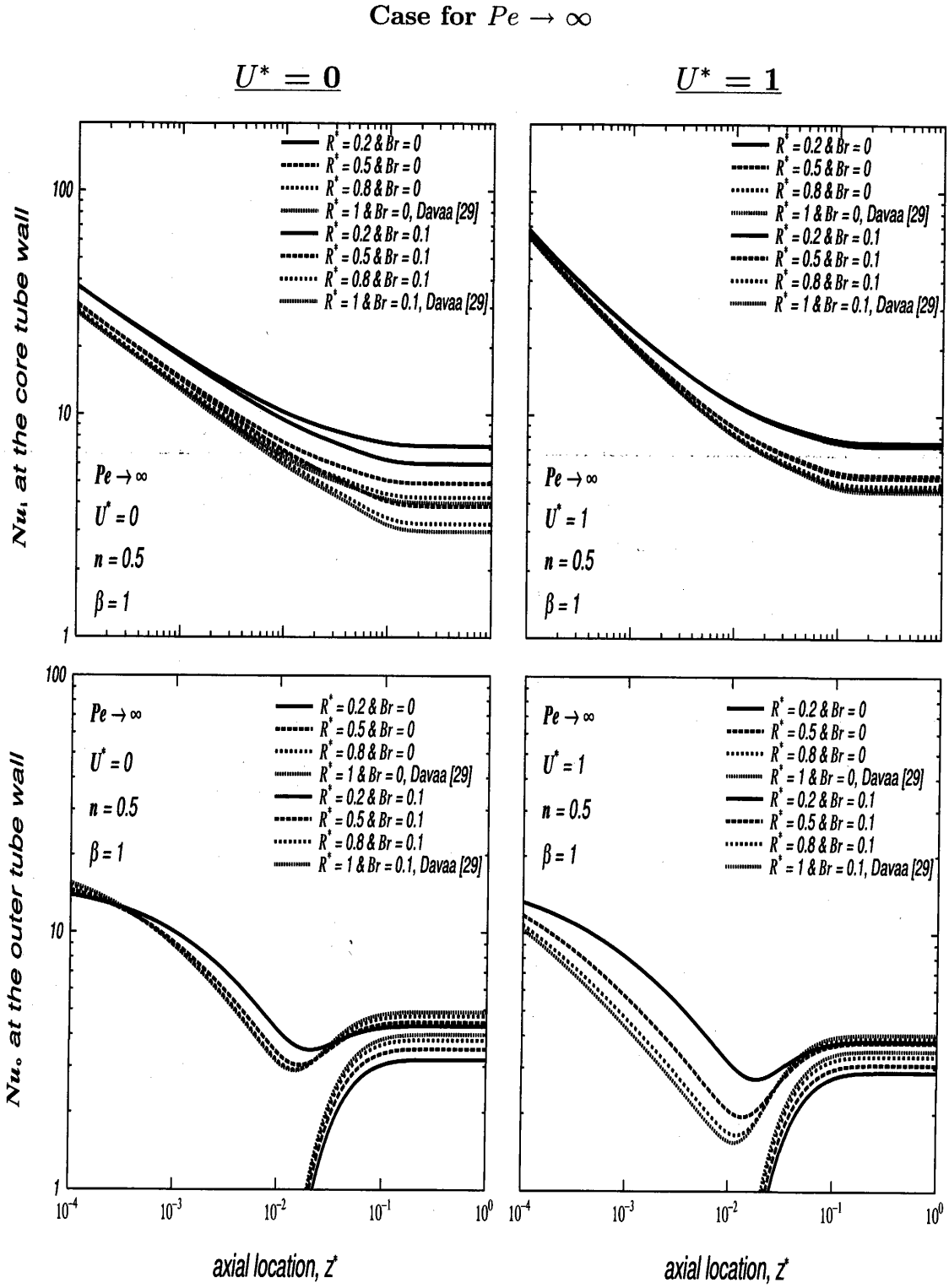

Fig. 3.20: Nu for different R^*, $Pe \to \infty$ ($U^* = 0$ and 1)

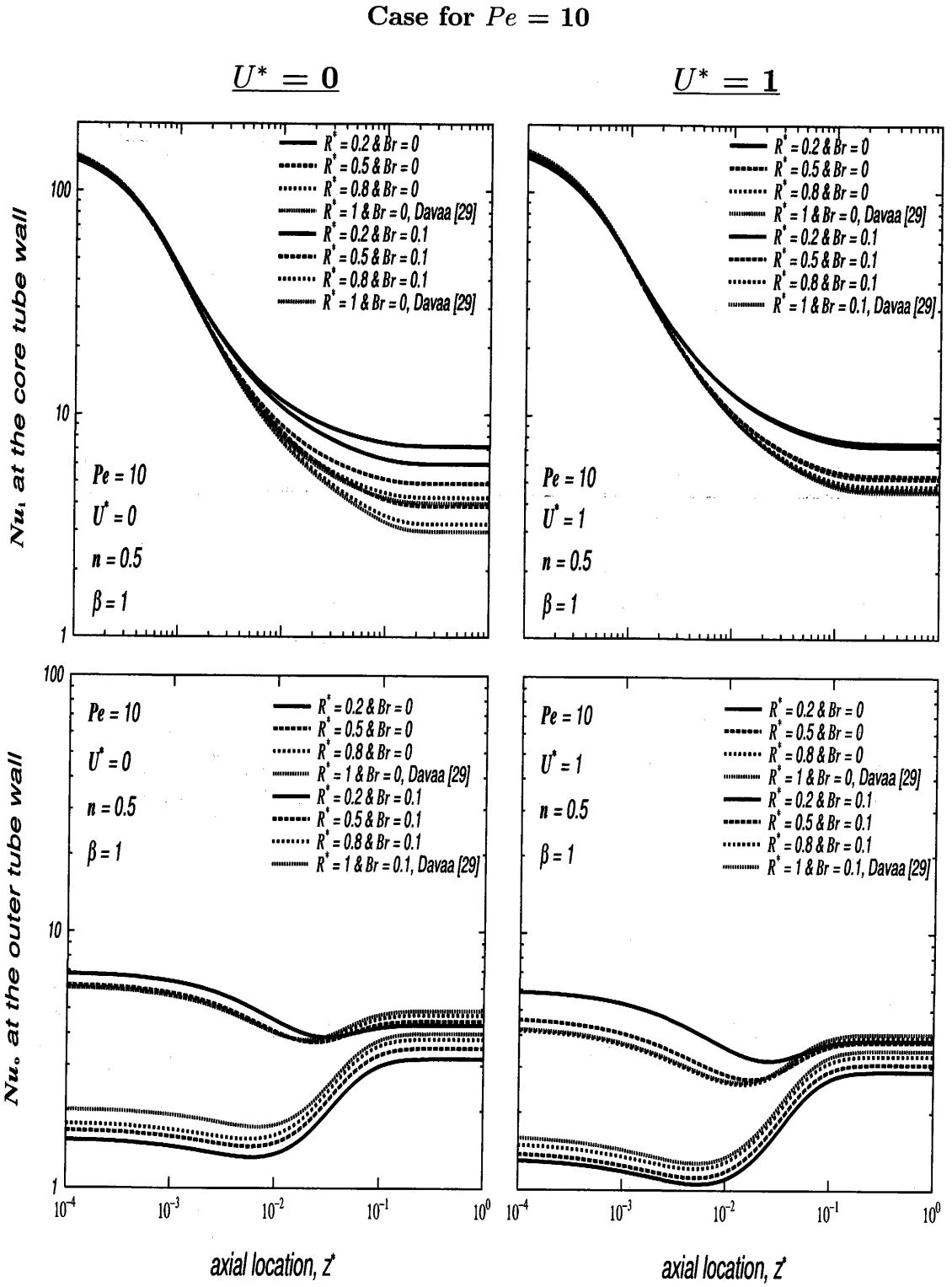

Fig. 3.21: Nu for different R^*, $Pe = 10$ ($U^* = 0$ and 1)

3.7 Results and Discussions of the 2nd Kind of T.B.C

The temperature field under the 2nd kind of thermal boundary condition has been obtained by solving the transformed energy equation, Eq.(3.31), with Eq.(3.35).

The objective herein is to display the results and to provide explanations for the solutions. The results are presented in the form of graphs and compared to the available data by other authors. The discussions will be given in the same way as done for the 1st kind of thermal boundary condition (see Section 3.4).

3.8 Temperature Distributions of the 2nd Kind of T.B.C

The dimensionless temperature, θ, shown in the following figures is defined by Eq.(2.31). Then the entering fluid temperature at $z^* \rightarrow -\infty$ is 0. The core tube wall is heated constantly for $z^* > 0$, whereas for $z^* \leq 0$ the core tube is insulated. The outer tube wall is insulated. At $z^* = 0$, there is a step change in the wall heat flux at the core tube.

In the following figures, $\xi = 0$ corresponds to the core tube wall and $\xi = 1$ is the outer tube wall. The temperature profiles are illustrated at four different axial locations $z^* = 0$; $z^* = 1.04 \times 10^{-1}$; $z^* = 4.2 \times 10^{-1}$ and $z^* = 1$.

The temperature profiles of a thermally developing flow in an annular duct of radius ratio, $R^* = 0.5$ are displayed in Figs.3.22 - 3.24. The considered fluids are Newtonian ($n = 1$), pseudoplastic ($n = 0.5$ and $\beta = 1$) and dilatant ($n = 1.5$ and $\beta = 1$). These figures contain the plots of θ vs ξ for two values Peclet numbers. The solid and dashed lines in these figures stand for the results for negligible ($Pe \rightarrow \infty$) and considerable ($Pe = 10$) fluid axial heat conduction cases, respectively. The upper plots are for $Br = 0$ and the lower ones are for $Br = 0.1$. These results show the combined effects of viscous dissipation and fluid axial heat conduction on the developing temperature profiles with regard to the relative velocity, U^*.

3.8.1 Effect of Br on the temperature distributions

The upper plots in Figs.3.22 - 3.24 refer to the case of negligible viscous dissipation, $Br = 0$. The lower ones are for $Br = 0.1$. From Figs.3.22 - 3.24, the fluid

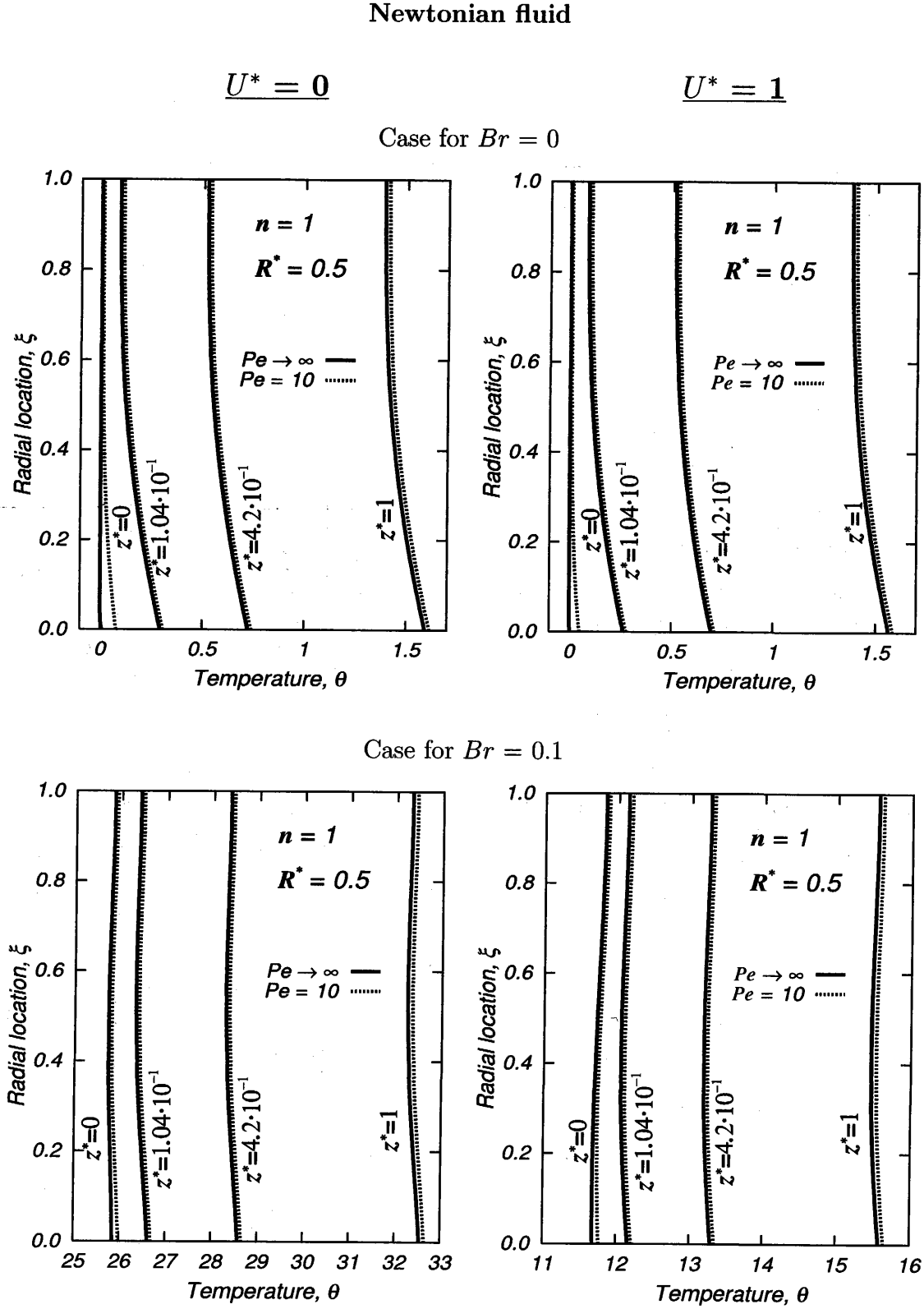

Fig. 3.22: Temperature profiles for a Newtonian fluid ($U^* = 0$ and 1)

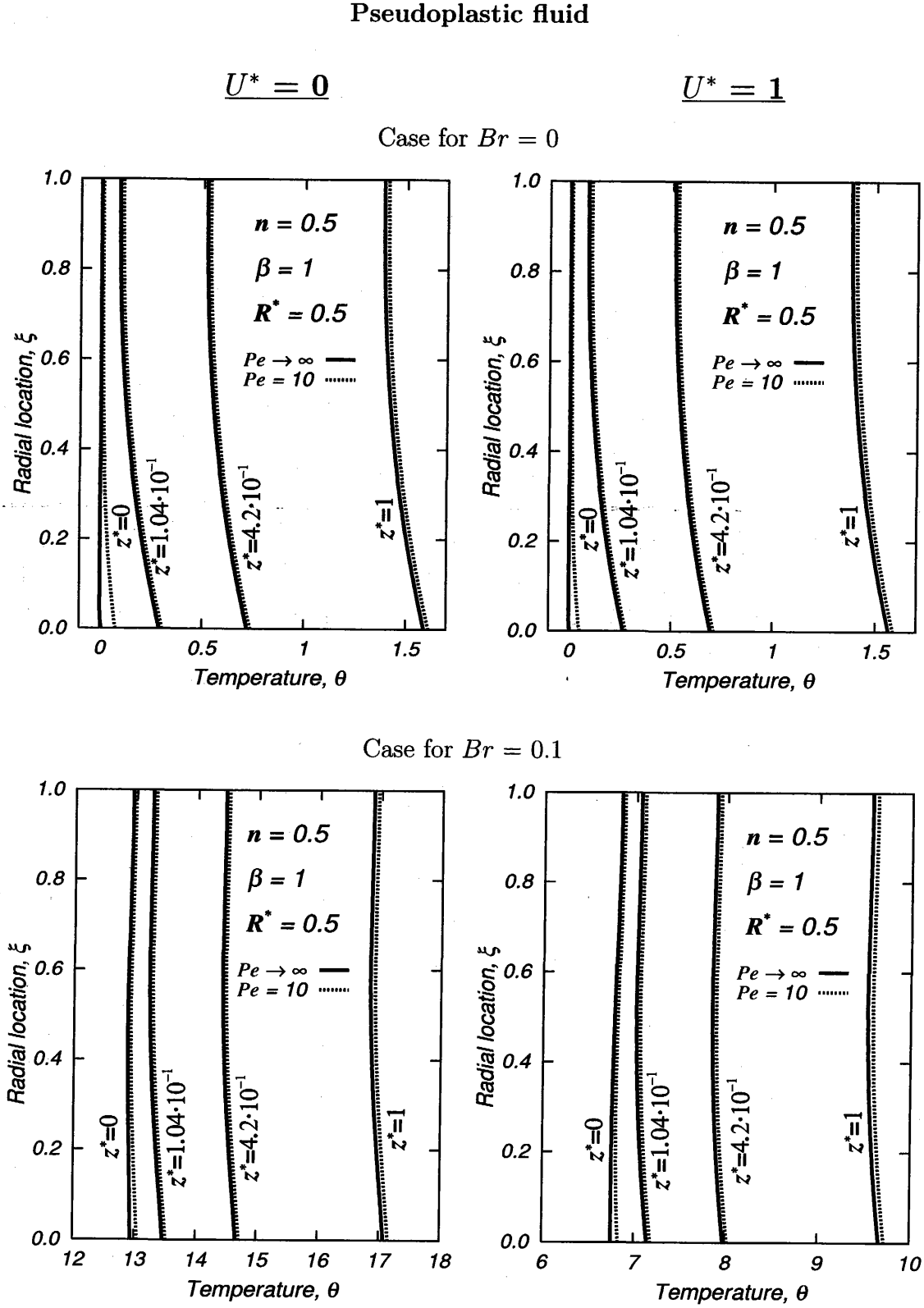

Fig. 3.23: Temperature profiles for a pseudoplastic fluid ($U^* = 0$ and 1)

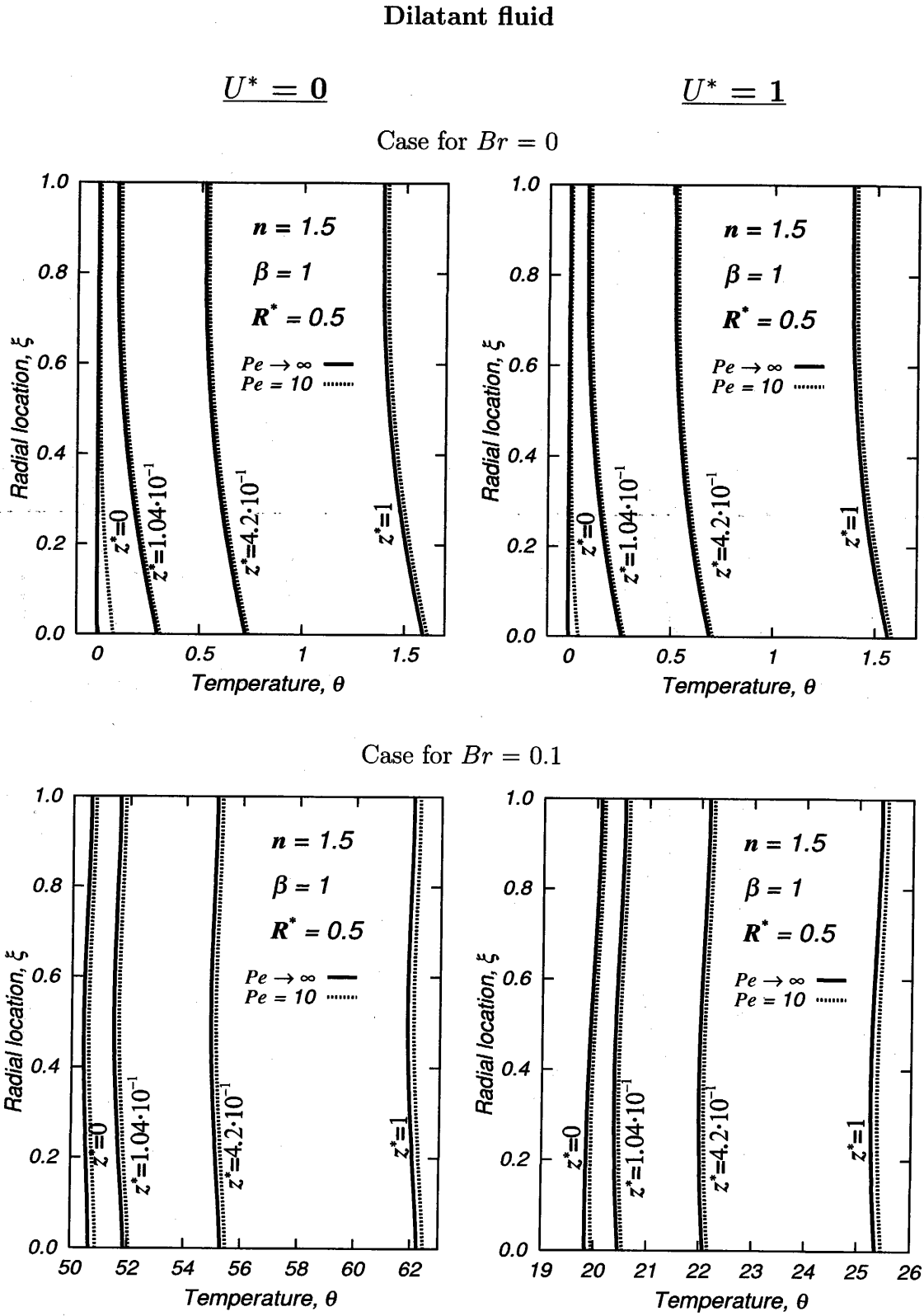

Fig. 3.24: Temperature profiles for a dilatant fluid ($U^* = 0$ and 1)

temperature is seen to be sufficiently large for $Br = 0.1$, before it reaches the heated wall region, specially for $U^* = 0$. This increase is due to the heat generated by viscous dissipation and the heat conducted upstream into the adiabatic wall region. That was not the case for $Pe \rightarrow \infty$ and $Br = 0$ as demonstrated in these plots.

From the developing temperature profiles it is seen that for the 2nd kind of boundary condition, the wall-to-fluid temperature difference is small, whereas the effect of viscous dissipation on heat transfer is more significant. It is also seen that if the channel is infinitely long, there may be generated a significant amount of heat due to viscous shear heating. Thus the value of the fluid temperature increases sufficiently. In these plots, it is clear that the effect of viscous dissipation weakens at $U^* = 1$.

3.8.2 Effect of Pe on the temperature distributions

The effect of fluid axial heat conduction on the fluid temperature is seen as the difference between the dashed and the solid lines in Figs.3.22 - 3.24. These plots demonstrate the fluid axial heat conduction effect as, for $Pe = 10$ the fluid temperature increases before the fluid enters into the heated wall region. However, no appreciable difference is observed in extending the core velocity value from 0 to 1 when only the fluid axial heat conduction is considered.

3.8.3 Effect of n on the temperature distributions

By comparing the temperature profiles in Figs.3.22 - 3.24, the influence of the flow index on the radial temperature profiles can be discerned. For all the fluids, the fluid axial heat conduction raises the temperature of the fluid. The flow index effect on heat transfer with fluid axial heat conduction is seen as insignificant unlike the viscous dissipation included heat transfer. This behavior is the same as in the 1st kind of boundary condition.

The response of the Newtonian fluid to viscous heating is more pronounced than that of the pseudoplastic fluid but less remarkable than the dilatant fluid. The temperature profiles of the different fluids bear similar shapes with the only difference being quantitative.

3.9 Nusselt Numbers for the 2nd Kind of T.B.C

Figure 3.25 presents the calculation results for Nu, defined with respect to the temperature difference of bulk to wall temperature (see Eq.(2.46)) for the different fluids such the Newtonian ($n = 1$), the pseudoplastic ($n = 0.5$ and $\beta = 1$) and the dilatant fluid ($n = 1.5$ and $\beta = 1$). The variation of the Nusselt number was studied in regard to the combined effects of viscous dissipation and fluid axial heat conduction ($Pe = \infty$; 10 and $Br = 0.01$; 0.05; 0.1). These curves clearly exhibit the trend of Nu in the thermal entrance region by comparing them with the relative velocity, U^*. The circles show the results from Ref.[2] and Ref.[27] for a Newtonian fluid when $Br = 0$ and $Pe \rightarrow \infty$. The solid diamonds are the results by Hsu [13] who studied the laminar heat transfer by including the fluid axial heat conduction for a Newtonian fluid by neglecting the viscous dissipation. It is seen even at small values of z^*, the agreement is excellent.

3.9.1 Effect of Br on the Nusselt numbers

From Fig.3.25 it is seen that Br has a strong effect on Nu in both thermally developing and developed regions.

For $U^* = 0$, the Nusselt number at the core decreases with an increase in Brinkman number in the fully developed region. For $U^* = 1$ these are opposite.

3.9.2 Effect of Pe on the Nusselt numbers

The effect of axial fluid heat conduction is considerable for small values of Pe. Unlike the case of the 1st kind of thermal boundary condition, Nusselt number at the heated core tube decreases with a decrease in Peclet number in the thermal entrance region.

It is also seen that the local Nusselt number remains almost constant throughout the thermal entrance region if Pe is small. The same trend is observed for Newtonian and non-Newtonian fluids.

For a specified axial position with a given Peclet number, the Nusselt number at the core tube wall is larger for $U^* = 1$ than for $U^* = 0$.

Nu tends to decrease near $z^* = 0$ as Pe reduces. It can also be noted that, for a fixed value of z^*, Nu at the moving core is larger than the corresponding Nu at the stationary core.

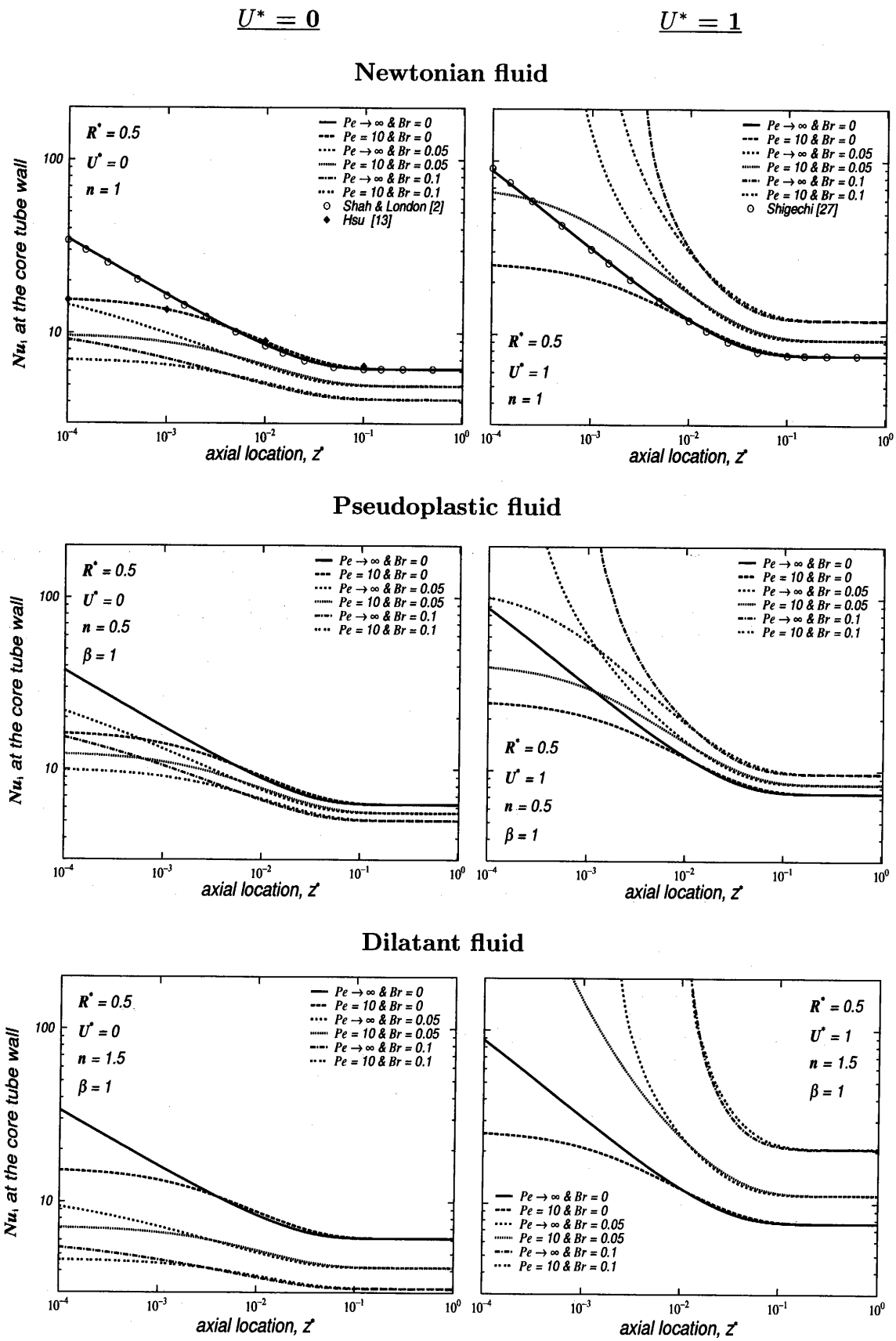

Fig. 3.25: Nu variations for different fluids with different degrees of viscous dissipation and fluid axial heat conduction ($U^* = 0$ and $U^* = 1$)

3.9.3 Effect of n on the Nusselt numbers

The heat transfer results show quite similar behaviors for different fluids as shown in Fig.3.25. For the non-Newtonian fluids, the Nusselt number remains almost constant throughout the thermal entrance region if Pe is small. The same trend is observed for Newtonian and non-Newtonian fluids.

When $U^* = 0$, if the viscous dissipation is included in the study, the Nusselt numbers for heat transfer to the Newtonian fluid are higher than those to the dilatant fluid but less than those to the pseudoplastic fluid. However, when $U^* = 1$ the Nusselt number for the dilatant fluid show higher values if the viscous dissipation is included in the study.

The response of the Newtonian fluid to viscous heating is more pronounced than that of the pseudoplastic fluid but less remarkable than the dilatant fluid.

3.9.4 Effect of R^* on the Nusselt numbers

In order to show the radius ratio effects, the heat transfer results are given in Fig.3.26 for $Pe \to \infty$ and $Pe = 10$. The general behavior is quite similar for different values of Pe and the results show that the radius ratio $R^* = 0.2$ is superior to $R^* = 0.5$ and $R^* = 0.8$ from the view point of heat transfer at the core under the same conditions. Also shown in Fig.3.26 is that the decrease of Nusselt number tends to slightly change with R^* if R^* approaches 1.

In the plots of Fig.3.26, the effect of the major governing parameters of the problem on the Nusselt number may be observed. From these Nusselt curves it can be observed that, for a specified axial position the Nusselt number at the moving core ($U^* = 1$) is larger than the corresponding Nusselt number at the fixed core ($U^* = 0$) with the given Brinkman number and the Peclet number.

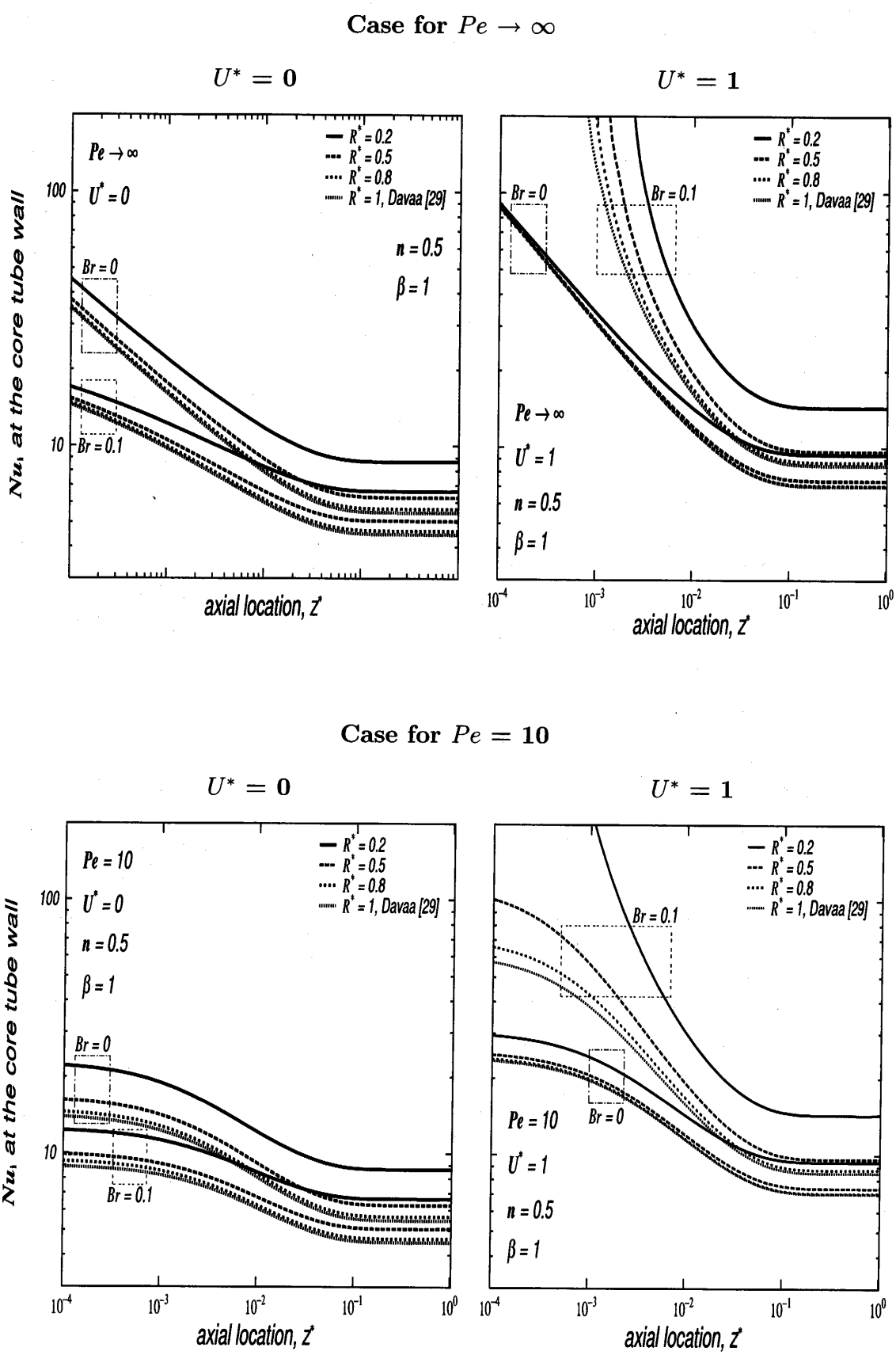

Fig. 3.26: Nusselt number for $R^* = 0.2$, 0.5, 0.8 ($U^* = 0$ and $U^* = 1$)

3.10 Concluding Remarks

The heat transfer to a laminar flow has been investigated for an annular duct consisting of an axially moving core and a stationary outer tube. In the study both the viscous dissipation and the fluid axial heat conduction were included. The ducts are considered to be under a step jump in the wall temperature or in the wall heat flux. The obtained numerical solutions were compared with the available data by the previous researchers and the agreement was excellent.

The numerical results are given graphically in terms of the temperature distributions and the conventional Nusselt number showing the effects of the core velocity, the Brinkman number and the Peclet number.

For the 1st kind of thermal boundary condition, for a specified axial position with a given Peclet number and a Brinkman number, the Nusselt number at the core tube wall is larger for $U^* = 1$ than for $U^* = 0$. For $U^* = 0$ the Nusselt number at the core tube decreases with an increase in the Brinkman number in the fully developed region, whereas for $U^* = 1$ the Nusselt curves at the core are almost identical for different Brinkman number values.

For the 2nd kind of thermal boundary condition, at a specified axial position with a given Peclet number, the Nusselt number at the core tube wall is larger for $U^* = 1$ than for $U^* = 0$. For $U^* = 0$, the Nusselt number at the core decreases with an increase in the Brinkman number in the fully developed region. For $U^* = 1$ these are opposite. As the calculations show, the core velocity direction is essential for the viscous dissipation effects on the heat transfer.

Chapter 4

Conclusions

This thesis has dealt with the theoretical study of the hydrodynamically fully developed but thermally developing laminar flow in annular ducts. As a part of the present research a comprehensive literature survey on heat transfer for laminar duct flows has been compiled. The survey revealed that such analysis are mostly concerned the heat transfer by neglecting the viscous dissipation and the fluid axial heat conduction. The present study made a step toward solving the heat transfer problem without making a simplifying assumption of negligible viscous dissipation and/or fluid axial heat conduction.

A finite-difference program has been developed that is capable of solving flow and heat transfer of Newtonian and non-Newtonian fluids in annular ducts under a variety of thermal boundary conditions. In this thesis it has been used to solve the heat transfer problem for Ⓣ, 1st kind and 2nd kind of thermal boundary conditions.

The research has yielded some new results that lead to a better understanding of the flow and heat transfer characteristics in annular ducts. The results have been illustrated in the form of friction factor, dimensionless temperature distribution and conventional Nusselt number. The study has been carried out for stationary annular ducts and for annular ducts with an axially moving core.

It was found that, for stationary annular ducts: in the case of the Ⓣ thermal boundary condition, there is a fixed point on the plot of Nu curves. This fixed point appears because of the inclusion of the viscous dissipation of the incoming flow at the unheated wall region. The asymptotic Nusselt numbers in the fully developed region decrease as the flow index increases. The Nusselt numbers for heat transfer to a Newtonian fluid are higher than those to dilatant fluids but less than those to

pseudoplastic fluids. In the case of the 1st kind of thermal boundary condition, the effect of fluid axial heat conduction on heat transfer rate is strong in the thermal entrance region. Including the fluid axial heat conduction and viscous dissipation causes a higher Nusselt number at the outer cylinder wall (which is maintained at a constant temperature value equal to the entering fluid temperature). For the Ⓣ and 1st kind of thermal boundary conditions, the Nusselt number at the inner core wall is greater for small radius ratios and that the Nusselt number at the outer cylinder wall is greater for large radius ratios. In the case of the 2nd kind of thermal boundary condition, the Nusselt number at the heated core tube decreases with a decrease in Peclet number in the thermal entrance region. As the radius ratio value decreases the Nusselt number at the core tube wall increases. Br has a strong effect on Nu in both thermally developing and developed regions. It was found for each considered thermal boundary condition, the response of the Newtonian fluid to viscous heating is more pronounced than that of the pseudoplastic fluid but less remarkable than the dilatant fluid.

The effect of an axially moving core velocity on heat transfer has been analyzed and the results are: for the 1st kind of thermal boundary condition, for a specified axial position the Nusselt number at the moving core ($U^* = 1$) is larger than the corresponding Nusselt number at the fixed core ($U^* = 0$) with the given Brinkman number and Peclet number. Also it was shown that the viscous dissipation effect weakens if the core moves in the direction of the flow. For the 2nd kind of thermal boundary condition, unlike the case of the stationary core, the Nusselt number at the core increases with an increase in the Brinkman number in the fully developed region. An additional observation from the results is that the effect of viscous dissipation on the heat transfer becomes more important as the core moves to the opposite direction of the flow. These effects hold true over all the range of the core velocity investigated.

Solutions obtained in this thesis may serve as a reliable reference to check the techniques developed for the treatment of more complicated problems associated laminar heat transfer of Newtonian and non-Newtonian fluids.

Acknowledgements

It is a pleasure to express my thanks to a number of people who lent their support, expertise, patience, and guidance to me during this study.

I am grateful to my supervisor Professor Toru SHICECHI who gave me the opportunity to take part at an exciting time in Nagasaki University. I would also like to thank for his extensive supervision, steady preparedness to through discussions, for his active support and encouragement throughout the research.

I would like to warmly thank the doctoral committee members, Associate Professor Satoru MOMOKI, Professor Yoshio KODAMA, Professor Masahiro ISHIDA, for their helpful comments and valuable suggestions to improve the thesis.

To my husband, GANBAT Davaa, I owe special thanks for his strength, love and care were integral to completion of this thesis. I extend my deep appreciation to my children BAYASGALAN Ganbat and JAVKHLAN Ganbat, for their love, patience and, endless support and encouragement of my dream.

I would like to use this opportunity to thank my parents JAMBAL Dorj and SHAALAI Natsagdorj, other family members and friends. My sincerest thanks extend to DELORES Stolberg and EUGENE Stolberg, KYOKO Hart and Nicolaas HART, VERA Hankins and DANIEL Hankins and the daughters, CHRIS Hankins and LAVERN Hankins, Masanobu ITOH, Sadeko ITOH, Seiko ITOH, RON Davies, Keiko MORIYAMA, BILL Hollier, GRANDMA and GRANDPA (Bill and Iola Hinkle), AMRAA Banzragch, ROB Forbes and BRIDGET Forbes, LYDIA Kim, SARAH Jun, YO Kim and their families, Kazumi SAKAI, OPHELIA Raner and many others in Bonanza and Portland, Oregon for their prayers, assistance, faith and support.

Furthermore, special thanks to the graduate and undergraduate students in our

laboratory who created a very pleasant working environment. I would like to thank to many laboratory colleagues for supporting me in different ways. I am also indebted to TAKITA sensei for her helpfulness and kind friendship. There are many people including the ROTARIANS and the members of NIK and Soroptomist International of Nagasaki Garland that I have not mentioned but whose debt I am in for they made my time in Nagasaki most memorable.

Realizing that it would be meaningless without the acknowledgement of God who made it all possible, most of all I am grateful to the LORD: "My help comes from the Lord, who made heaven and earth." (Psalm 121)

Nomenclature

Br	: Brinkman number	
c_p	: specific heat at constant pressure	[kJ/(kg·K)]
D_h	: hydraulic diameter $= 2(R_\mathrm{o} - R_\mathrm{i})$ for annular ducts, or $= 2L$ for parallel-plates ducts, or $= 2R$ for circular ducts	[m]
E	: constant of the axial transformation in Eq.(2.64)	
f	: friction factor	
h	: heat transfer coefficient	[W/(m^2·K)]
k	: thermal conductivity	[W/(m·K)]
m	: consistency index	[N·s^n/m^2]
n	: flow index	
Nu	: Nusselt number	
P	: pressure	[Pa]
Pe	: Peclet number $= RePr$, or $= Re_\mathrm{M}Pr_\mathrm{M}$	
Pr	: Prandtl number $= c_\mathrm{p}\mu/k$	
Pr_M	: modified Prandtl number $= c_\mathrm{p}\eta^*/k$	
q	: wall heat flux	[W/m^2]
r	: radial coordinate	[m]
r^*	: dimensionless radial coordinate $= r/D_\mathrm{h}$	
R	: radius	[m]
R^*	: radius ratio $= R_\mathrm{i}/R_\mathrm{o}$	
Re	: Reynolds number $= \rho u_\mathrm{m} D_\mathrm{h}/\nu$	
Re_M	: modified Reynolds number $= \rho u_\mathrm{m} D_\mathrm{h}/\eta^*$	
T	: temperature	[K]
u	: axial velocity of the flow	[m/s]
u_m	: average velocity of the flow	[m/s]
u^*	: dimensionless velocity $= u/u_\mathrm{m}$	
U	: axial velocity of the moving core	[m/s]
U^*	: dimensionless relative velocity of the core $= U/u_\mathrm{m}$	
V	: dimensionless parameter in Eq.(2.57)	
z	: axial coordinate	[m]
z^*	: dimensionless axial coordinate $= z/(PeD_\mathrm{h})$	
z_t	: transformed axial coordinate	

Greek symbols

β	: dimensionless shear rate parameter	
η	: reference viscosity based on D_h	[N·s/m^2]
η_a	: apparent viscosity	[N·s/m^2]
η_a^*	: dimensionless apparent viscosity $= \eta_a/\eta$	
η_0	: viscosity at zero shear rate	[N·s/m^2]
μ	: dynamic viscosity	[N·s/m^2]
ν	: kinematic viscosity $= \mu/\rho$	[m^2 / s]
ρ	: density	[kg/m^3]
τ	: shear stress	[Pa]
θ	: dimensionless temperature	
ξ	: dimensionless radial coordinate $= [2(1-R^*)r^* - R^*]/(1-R^*)$	

Subscripts

b	: bulk
e	: entrance or inlet
fd	: fully developed
i	: inner tube
o	: outer tube

Abbreviation words

PL	power-law
T.B.C.	thermal boundary condition

Bibliography

[1] Y. Jaluria, *Thermal processing of materials: From basic research to engineering*, 2002 Max Jacob Memorial Award Lecture, J. of Heat Transfer, Vol. 125, 957-979 (2003)

[2] R.K. Shah and A.L. London, *Laminar flow forced convection in ducts*, Advances in Heat Transfer, Supplement 1, Academic Press, New York (1978)

[3] S. Kakac, R.K. Shah, and W. Aung, *Handbook of Single phase Convective Heat Transfer*, Wiley Interscience, New York (1987)

[4] A.P. Hatton, and A. Quarmby, *Heat transfer in the thermal entry length with laminar flow in an annulus*, Int. J. Heat Mass Transfer, Vol. 5, 973-980 (1962)

[5] R.E. Lundberg, W.C. Reynolds, and W.M. Kays, *Heat transfer with laminar flow in concentric annuli with constant and variable wall temperature with heat flux*, NASA TN D-1972, 1-194 (1963)

[6] R.E. Lundberg, P.A. McCuen, and W.C. Reynolds, *Heat transfer in annular passages. Hydrodynamically developed laminar flow with arbitrarily prescribed wall temperatures or heat fluxes*, Int. J. Heat Mass Transfer, Vol. 6, 495-529 (1963)

[7] P.M. Worsøe-Schmidt, *Heat transfer in the thermal entrance region of circular tubes and annular passages with fully developed laminar flow*, Int. J. Heat Mass Transfer, Vol. 10, 541-551 (1967)

[8] Y.M. Lee and Y.M. Kuo, *Laminar flow in annuli ducts with constant wall temperature* Int. Comm. Heat Mass Transfer, Vol. 25, 227-236 (1998)

[9] E. Buyruk, H. Barrow, and I. Owen, *Heat transfer in laminar flow in a concentric annulus with peripherally varying heat transfer* Int. J. Heat Mass Transfer, Vol. 42, 487-496 (1999)

[10] S.N. Hong and J.C. Matthews, *Heat transfer to non-Newtonian fluids in laminar flow through concentric annuli*, Int. J. Heat Mass Transfer, Vol. 12, 1699-1703 (1969)

[11] U.C.S. Nascimento, E.N. Macedo, and J.N. Quaresma, *Thermal entry region analysis through the finite integral transform technique in laminar flow of Bingham fluids within concentric annular ducts*, Int. J. Heat Mass Transfer, Vol. 45, 923-929 (2002)

[12] E.J. Soares, M.F. Naccache, and P.R. S. Mendes, *Heat transfer to viscoplastic materials flowing axially through concentric annuli*, Int. J. Heat Fluid Transfer, Vol. 24, 762-773 (2003)

[13] C.J.Hsu, *Theoretical solutions for low Peclet number thermal entry region heat transfer in laminar flow through concentric annuli*, Int.J.Heat and Mass Transfer, Vol.13, 1907-1924 (1970)

[14] B. Weigand, M. Wolf, and H. Beer, *Heat transfer in laminar and turbulent flows in the thermal entrance region of concentric annuli: Axial heat conduction effects in the fluid* Heat and Mass Transfer, Vol. 33, 67-80 (1997)

[15] A.S. Telles, E.M. Queiroz, and G.E. Filho, *Solutions to the extended Graetz problem* Int. J. Heat Mass Transfer, Vol. 44, 471-483 (2001)

[16] B. Weigand, and F. Wrona, *The extended Graetz problem with piecewise constant wall heat flux for laminar and turbulent flows inside concentric annuli* Heat and Mass Transfer, Vol. 39, 313-320 (2003)

[17] H.W. Cox and C.W. Macosko, *Viscous dissipation in die flows*, AIChE Journal, Vol. 20, 785-795 (1974)

[18] H.H. Winter, *Temperature fields in extruder dies with circular, annular, or slit cross-section*, Polymer Engineering and Science, Vol. 15, 84-89 (1975)

[19] H.H. Winter, *Viscous dissipation in shear flows of molten polymers*, Advances in Heat Transfer, Academic Press, New York, 205-267 (1977)

[20] M. Capobianchi and T.F. Irvine, *Predictions of pressure drop and heat transfer in concentric annular ducts with modified power-law fluids*, Wärme-und Stoffübertragung, Vol. 27, 209-215 (1992)

[21] H.S. Heaton, W.C. Reynolds, and W.M. Kays, *Heat transfer in annular passages. Simultaneous development of velocity and temperature fields in laminar flow*, Int. J. Heat Mass Transfer, Vol. 7, 763-781 (1964)

[22] R.E. Fuller, and M.R. Samuels, *Simultaneous development of the velocity and temperature fields in the entry region of an annulus*, Chemical Engineering Progress Symposium Series, Vol. 67, 71-77 (1971)

[23] R.M. Manglik, and P. Fang, *Thermal processing of viscous non-Newtonian fluids in annular ducts: effects of power-law rheology, duct eccentricity, and thermal boundary conditions*, Int. J. Heat Mass Transfer, Vol. 45, 803-814 (2002)

[24] T. Shigechi, N. Kawae and Y. Lee, *Turbulent fluid flow and heat transfer in concentric annuli with moving cores*, Int.J.Heat Mass Transfer, Vol.33, No.9, 2029-2037 (1990)

[25] Y. Lee and T. Shigechi, *Heat transfer in concentric annuli with moving cores - fully developed turbulent flow with arbitrarily prescribed heat flux*, Int.J.Heat Mass Transfer, Vol.35, No.12, 3488-3493 (1992)

[26] T. Shigechi and Y. Lee, *An analysis on fully developed laminar fluid flow and heat transfer in concentric annuli with moving cores*, Int.J.Heat Mass Transfer, Vol.34, No.10, 2593-2601 (1991)

[27] T. Shigechi, K. Araki and Y. Lee, *Laminar heat transfer in the thermal entrance regions of concentric annuli with moving heated cores*, Trans. ASME, J.Heat Transfer, Vol.115, No.4, 1061-1064 (1993);
K.Araki, *Laminar heat transfer in annuli*, Department of Mechanical Systems Engineering, Nagasaki University, Master Thesis (1991)

[28] T. Shigechi, S. Momoki and Y. Lee, *Fully developed laminar flow and heat transfer in an eccentric annulus with an axially moving core*, Trans. ASME, J.Heat Transfer, Vol.118, No.1, 205-209 (1996)

[29] G. Davaa, *Ph.D Thesis, "Laminar heat transfer in non-Newtonian plane Poiseuille-Couette flow"*, Nagasaki University, Graduate School Science and Technology (2003)

[30] S.H. Lin and D.M. Hsieh, *Heat transfer to generalized Couette flow of non-Newtonian fluid in annuli with moving inner cylinder*, J. Heat Transfer, Vol. 102, 786-789 (1980)

[31] S. Lin, *Heat transfer to generalized non-Newtonian Couette flow in annuli with moving outer cylinder*, Int. J. Heat Mass Transfer, Vol. 35, 3069-3075 (1992)

[32] S. Choudhury and Y. Jaluria, *Forced convective heat transfer from a continuously moving cylindrical rod undergoing thermal processing*, HTD-224, Heat Transfer in Materials Processing, ASME, California, Nov.8-13, 43-50 (1992)

[33] S. Choudhury, Y. Jaluria, T. Vaskopoulos and C. Polymeropoulos, *Forced convective cooling of optical fiber during drawing processes* J. Heat Transfer, Vol. 116, 790-794 (1994)

[34] T. Vaskopulos, C. Polymeropoulos and A. Zebib, *Cooling of optical fiber in aiding and opposing forced gas flow*, Int. J. Heat Mass Transfer, Vol. 38, 1933-1944 (1995)

[35] S.N. Singh, *Heat transfer by laminar flow in a cylindrical tube* Appl. sci. Res., Section A, Vol. 7, 325-340 (1958)

[36] C. A. Deavours, *An exact solution for the temperature distribution in parallel plate Poiseuille flow*, Trans. ASME, J. of Heat Transfer, Vol. 96, 489-495 (1974)

[37] D. Wei, and Z. Zhang, *Decay estimates of heat transfer to molten polymer flow in pipes with viscous dissipation*, Electronic J. of Differential Equations, Vol. 39, 1-14 (2001)

[38] V.D. Dang, *Heat transfer of power-law fluid at low Peclet number flow*, Trans. ASME, J. of Heat Transfer, Vol. 105, 542-549 (1983)

[39] R.C. LeCroy, and A.H. Eraslan, *The solution of temperature development in the entrance region of an MHD channel by the B.G. Galerkin method*, Trans. ASME, J. of Heat Transfer, Vol. 91, 212-220 (1969)

[40] J. Lahjomri, A. Oubarra, and A. Alemany, *Heat transfer by laminar Hartmann flow in thermal entrance region with a step change in wall temperatures: the Graetz problem extended*, Int. J. Heat Mass Transfer, Vol. 45, 1127-1148 (2002)

[41] T. Min, J. Y. Yoo, and H. Choi, *Laminar convective heat transfer of a Bingham plastic in a circular pipe-I. Analytical approach thermally fully developed flow and thermally developing flow (the Graetz problem extended)*, Int. J. Heat Mass Transfer, Vol. 40, 3025-3037 (1997)

[42] D.A. Nield, A.V. Kuznetsov, and Ming Xiong, *Thermally developing forced convection in a porous medium: parallel plate channel with walls at uniform temperature, with axial conduction and viscous dissipation effects*, Int. J. Heat Mass Transfer, Vol. 46, 643-651 (2003)

[43] M. Akiyama and K.C. Cheng, *Boundary vorticity method for laminar forced convection heat transfer in curved pipes*, Int. J. Heat Mass Transfer, Vol. 14, 1659-1675 (1971)

[44] A.S. Jones, *Extensions to the solution of the Graetz problem*, Int. J. Heat Mass Transfer, Vol. 14, 619-623 (1971)

[45] J. Lahjomri, and A. Oubarra, *Analytical solution of the Graetz problem with axial conduction*, Trans. ASME, J. of Heat Transfer, Vol. 121, 1078-1083 (1999)

[46] A. Goldman and Y.C. Kao, *Numerical solution to a two-dimensional conduction problem using rectangular and cylindrical body-fitted coordinate systems*, J. Heat Transfer, Transactions of the ASME, Vol. 103, 753-758 (1981)

[47] D. K. Hennecke, *Heat transfer by Hagen-Poiseuille flow in the thermal development region with axial conduction*, Wärme-und Stoffübertragung, Vol. 1, 177-184 (1968)

[48] F.T. Pinho and P.J. Oliveira, *Axial annular flow of a nonlinear viscoelastic fluid - an analytical solution*, J. Non-Newtonian Fluid Mechanics, Vol. 93, 325-337 (2000)

[49] R.B. Bird, W.E. Steward, E.N. Lightfoot, *Transport Phenomena*, Wiley, New York (1960)

[50] M. Biermann, *Calculation of steady temperature fields in generalized Couette flows of simple fluids*, Int. J. Heat Mass Transfer, Vol. 18, 1015-1030 (1975)

[51] C.P. Tso and S.P. Mahulikar, *The use of the Brinkman number for single phase forced convective heat transfer in microchannels*, Int. J. Heat Mass Transfer, Vol. 41, 1759-1769 (1998)

[52] K.C. Cheng and R.S. Wu, *Axial heat conduction effects on thermal instability of horizontal plane Poiseuille flows heated from below*, J. Heat Transfer, Transactions of the ASME, 564-569 (November 1976)

[53] J.H. Rao, D.R. Jeng and K.J. Witt, *Momentum and heat transfer in power-law fluid with arbitrary injection/suction at a moving wall*, Int. J. Heat Mass Transfer, Vol. 42, 2837-2847 (1999)

[54] R.P. Chhabra and J.F. Richardson, *Non-Newtonian flow in the process industries*
Fundamentals and engineering applications, Butterworth-Heinemann, Oxford (1999)

[55] S. Rajasekharan, V.G. Kubair and N.R. Kuloor, *Heat transfer to non-Newtonian fluids in coiled pipes in laminar flow*, Int. J. Heat Mass Transfer, Vol. 13, 1583-1594 (1970)

[56] C.P. Tso and S.P. Mahulikar, *The role of the Brinkman number in analysing flow transitions in microchannels*, Int. J. Heat and Mass Transfer, Vol. 42, 1813-1833 (1999)

[57] C.P. Tso and S.P. Mahulikar, *Experimental verification of the role of Brinkman number in microchannels using local parameters*, Int. J. Heat and Mass Transfer, Vol. 43, 1837-1849 (2000)

[58] Yunus A. Çengel and Robert H. Turner, *Fundamentals of thermal-fluid sciences*, 2nd edition, McGraw-Hill (2005)

[59] F.H. Verhoff and D.P. Fisher, *A numerical solution of the Graetz problem with axial conduction included*, Trans. ASME, Journal of Heat Transfer, Vol. 95, 132-134 (1973)

[60] H.C. Ku, and D. Hatziavramidis, *Chebyshev expansion methods for the solution of the extended Graetz problem*, J. of Computational Physics, Vol. 56, 495-512 (1984)

[61] A. Campo, and J.C. Auguste, *Axial conduction in laminar pipe flows with nonlinear wall heat fluxes*, Int. J. Heat Mass Transfer, Vol. 21, 1597-1607 (1978)

[62] R.M. Cotta, and M.N. Özisik, *Laminar forced convection of power-law non-Newtonian fluids inside ducts*, Wärme-und Stoffübertragung, Vol. 20, 211-218 (1986)

[63] J.W. Ou, and K.C. Cheng, *Viscous dissipation effects on thermal entrance heat transfer in laminar and turbulent pipe flows with uniform wall temperature*, Thermophysics and Heat Transfer Conference, ASME, 74-HT-51, 1-6 (1974)

[64] T. Basu, and B.N. Roy, *Laminar heat transfer in a tube with viscous dissipation*, I. J. Heat Mass Transfer, Vol. 28, 699-701 (1985)

[65] A. Lawal, and A.S. Mujumdar, *The effects of viscous dissipation on heat transfer to power law fluids in arbitrary cross-sectional ducts*, Wärme-und Stoffübertragung, Vol. 27, 437-446 (1992)

[66] R.M. Manglik, and J. Prusa, *Viscous dissipation in non-Newtonian flows: Implications for the Nusselt number*, J. Thermophysics and Heat Transfer, Vol. 9, 733-741 (1995)

[67] G.C. Vradis, J. Dougher, and S. Kumar, *Entrance pipe flow and heat transfer for a Bingham plastic*, Int. J. Heat Mass Transfer, Vol. 36, 543-552 (1993)

[68] T. Min, H.G. Choi, J.Y. Yoo, and H. Choi, *Laminar convective heat transfer of a Bingham plastic in a circular pipe-II. Numerical approach hydrodynamically developing flow and simultaneously developing flow*, Int. J. Heat Mass Transfer, Vol. 40, 3689-3701 (1997)

[69] P.M. Coelho, F.T. Pinho, and P.J. Oliveira, *Thermal entry flow for a viscoelastic fluid: the Graetz problem for the PTT model*, Int. J. Heat Mass Transfer, Vol. 46, 3865-3880 (2003)

[70] S. Olek, *Heat transfer in duct flow of non-Newtonian fluids with axial conduction*, Int. Comm. Heat Mass Transfer, Vol. 25, 929-938 (1998)

[71] T. F. Lin, K. H. Hawks, and W. Leidenfrost, *Analysis of viscous dissipation effect on thermal entrance heat transfer in laminar pipe flows with convective boundary conditions*, Wärme-und Stoffübertragung, Vol. 17, 97-105 (1983)

[72] J. Prusa, and R.M. Manglik, *Asymptotic and numerical solutions for thermally developing flows of Newtonian and non-Newtonian fluids in circular tubes with uniform wall temperature*, Fundamentals of Forced Convection Heat Transfer, ASME, HTD 210, 1-10 (1992)

[73] A.A. McKillop, *Heat transfer for laminar flow of non-Newtonian fluids in entrance region of a tube* Int. J. Heat Mass Transfer, Vol. 7, 853-862 (1964)

[74] T.V. Nguyen, *Laminar heat transfer for thermally developing flow in ducts*, Int. J. Heat Mass Transfer, Vol. 35, 1733-1741 (1992)

[75] O. Jambal, T. Shigechi, G. Davaa and S. Momoki, *Effects of viscous dissipation and fluid axial heat conduction on laminar heat transfer in ducts with constant wall temperature (Part III: Annular ducts)*, Reports of the Faculty of Engineering, Nagasaki University, Vol.34, No.62, 41-53 (2004)

[76] B.H. Kang and Y. Jaluria, *Heat transfer from continuously moving material in channel flow for thermal processing*, J. Thermophysics and Heat Transfer, Vol. 8, 546-554 (1994)

[77] H.S. Seo and U.C. Paek *Melt coating of tin on silica optical fiber*, J. Lightwave Technology, Vol. 16, 2355-2364 (1998)

[78] U.C. Paek, *Free drawing and polymer coating of silica glass optical fibers*, J. Heat Transfer, Vol. 121, 774-788 (1999)

[79] T. Shigechi, K. Araki and Y. Lee, *Laminar heat transfer in the thermal entrance regions of concentric annuli with moving heated cores*, Fundamentals of Forced Convection Heat Transfer, HTD-Vol. 210, 19-26 (1992)

[80] T. Shigechi, S. Momoki, T. Yamaguchi, S. Higasiiue and Y. Lee, *Fully developed non-Newtonian fluid flow and heat transfer in a concentric annulus with an axially moving core*, Proceedings of 11th IHTC, Vol. 3, 151-156 (1998)

[81] S.R. Lee and T.F. Irvine, *A computational analysis of natural convection in a vertical channel with a modified power law non-Newtonian fluid*, Proceedings of 11th IHTC, Vol. 3, 367-372 (1998)

[82] J. Ŝestâk and F. Rieger, *Laminar heat transfer to a steady Couette flow between parallel plates*, Int. J. Heat Mass Transfer, Vol. 12, 71-80 (1969)

Appendices

Table 4.1: Numerical values of fRe_{M} for PL fluids in concentric annular ducts

		fRe_{M}										
U^*	R^*	n										
		0.5	0.6	0.7	0.8	0.9	1.0	1.1	1.2	1.3	1.4	1.5
	0.1	8.497	11.047	14.362	18.675	24.290	31.595	41.120	53.510	69.641	90.634	117.934
	0.2	9.193	12.066	15.817	20.721	27.132	35.510	46.473	60.797	79.521	103.988	135.931
	0.3	9.664	12.761	16.822	22.149	29.139	38.307	50.344	66.129	86.830	113.974	149.527
	0.4	10.017	13.288	17.590	23.250	30.700	40.500	53.404	70.376	92.697	122.040	160.583
-2	0.5	10.296	13.707	18.205	24.138	31.967	42.292	55.921	73.890	97.581	128.800	169.942
	0.6	10.523	14.051	18.712	24.875	33.024	43.794	58.042	76.865	101.735	134.580	177.923
	0.7	10.712	14.338	19.138	25.497	33.921	45.075	59.858	79.425	105.318	139.574	184.830
	0.8	10.871	14.581	19.501	26.030	34.693	46.183	61.434	81.653	108.457	143.960	191.009
	0.9	11.008	14.790	19.815	26.492	35.364	47.149	62.814	83.612	111.218	147.852	196.443
	1	11.132	14.975	20.089	26.893	35.949	48.000	64.034	85.364	113.734	151.462	201.627
	0.1	8.040	10.265	13.085	16.664	21.206	26.969	34.296	43.591	55.388	70.358	89.345
	0.2	8.523	10.948	14.030	17.952	22.945	29.299	37.395	47.698	60.809	77.492	98.714
	0.3	8.833	11.391	14.651	18.809	24.115	30.884	39.529	50.556	64.624	82.566	105.429
	0.4	9.059	11.716	15.111	19.449	24.997	32.089	41.164	52.764	67.591	86.541	110.743
-1	0.5	9.232	11.969	15.471	19.954	25.698	33.052	42.480	54.550	70.005	89.784	115.104
	0.6	9.371	12.172	15.762	20.366	26.272	33.846	43.569	56.036	72.020	92.516	118.767
	0.7	9.484	12.339	16.003	20.708	26.752	34.512	44.488	57.295	73.739	94.838	121.919
	0.8	9.578	12.479	16.206	20.997	27.160	35.081	45.276	58.378	75.218	96.862	124.651
	0.9	9.657	12.597	16.379	21.245	27.510	35.572	45.958	59.319	76.509	98.617	127.044
	1	9.723	12.701	16.527	21.457	27.811	36.000	46.554	60.154	77.676	100.249	129.325

(continued)

		fRe_M										
U^*	R^*	n										
		0.5	0.6	0.7	0.8	0.9	1.0	1.1	1.2	1.3	1.4	1.5
0	0.1	7.489	9.360	11.666	14.509	18.018	22.343	27.689	34.281	42.413	52.444	64.813
	0.2	7.714	9.653	12.041	14.984	18.614	23.088	28.614	35.427	43.830	54.193	66.972
	0.3	7.828	9.801	12.230	15.223	18.912	23.461	29.078	36.002	44.542	55.071	68.055
	0.4	7.895	9.889	12.340	15.362	19.087	23.678	29.347	36.336	44.955	55.583	68.687
	0.5	7.937	9.942	12.408	15.448	19.194	23.813	29.514	36.543	45.211	55.900	69.078
	0.6	7.963	9.975	12.451	15.502	19.262	23.897	29.619	36.673	45.372	56.099	69.319
	0.7	7.979	9.997	12.478	15.535	19.304	23.950	29.684	36.754	45.472	56.222	69.476
	0.8	7.989	10.009	12.494	15.555	19.329	23.980	29.722	36.801	45.531	56.294	69.563
	0.9	7.994	10.015	12.502	15.565	19.341	23.996	29.741	36.825	45.560	56.331	69.607
	1	8.000	10.019	12.504	15.566	19.342	24.000	29.746	36.835	45.580	56.368	69.674
1	0.1	6.707	8.184	9.957	12.085	14.644	17.717	21.419	25.868	31.218	37.652	45.389
	0.2	6.549	7.952	9.627	11.627	14.018	16.877	20.304	24.402	29.307	35.177	42.204
	0.3	6.359	7.688	9.266	11.143	13.378	16.038	19.213	22.995	27.504	32.879	39.285
	0.4	6.169	7.429	8.920	10.687	12.782	15.268	18.223	21.732	25.899	30.850	36.731
	0.5	5.988	7.186	8.599	10.267	12.240	14.573	17.338	20.610	24.485	29.073	34.507
	0.6	5.818	6.960	8.303	9.885	11.750	13.949	16.548	19.615	23.237	27.514	32.566
	0.7	5.658	6.751	8.032	9.536	11.305	13.387	15.840	18.728	22.131	26.140	30.862
	0.8	5.510	6.557	7.782	9.218	10.902	12.879	15.205	17.936	21.146	24.921	29.358
	0.9	5.371	6.377	7.552	8.926	10.535	12.419	14.631	17.223	20.265	23.834	28.021
	1	5.260	6.223	7.347	8.662	10.200	12.000	14.109	16.578	19.471	22.860	26.831
2	0.1	4.876	5.976	7.303	8.897	10.809	13.091	15.809	19.028	22.839	27.354	32.715
	0.2	3.970	4.871	5.955	7.255	8.810	10.667	12.882	15.513	18.628	22.306	26.639
	0.3	3.212	3.941	4.816	5.865	7.119	8.615	10.401	12.524	15.045	18.035	21.574
	0.4	2.561	3.141	3.837	4.671	5.668	6.857	8.276	9.963	11.968	14.347	17.166
	0.5	1.995	2.446	2.987	3.635	4.410	5.333	6.436	7.747	9.305	11.154	13.346
	0.6	1.498	1.836	2.242	2.727	3.308	4.000	4.826	5.809	6.976	8.362	10.006
	0.7	1.058	1.297	1.583	1.926	2.335	2.824	3.406	4.100	4.923	5.901	7.061
	0.8	0.667	0.817	0.997	1.213	1.470	1.778	2.145	2.581	3.100	3.715	4.445
	0.9	0.316	0.387	0.472	0.574	0.697	0.842	1.016	1.223	1.468	1.760	2.106
	1	0.000	0.000	0.000	0.000	0.000	0.000	0.000	0.000	0.000	0.000	0.000

Table 4.2: Nusselt number at the core tube for fully developed flow of PL fluids for the 2nd kind of T.B.C

$U^* = -1$

R^*	Br		Flow index, n										
			0.5	0.6	0.7	0.8	0.9	1.0	1.1	1.2	1.3	1.4	1.5
0.2	0	present work	8.061	7.964	7.875	7.796	7.725	7.655	7.605	7.555	7.509	7.467	7.43
		[26]						7.667					
	0.01	present work	7.446	7.178	6.885	6.566	6.215	5.828	5.415	4.97	4.503	4.025	3.546
	0.05	present work	5.707	5.146	4.582	4.025	3.488	2.982	2.516	2.099	1.731	1.415	1.147
	0.1	present work	4.417	3.802	3.231	2.713	2.252	1.852	1.508	1.219	0.979	0.782	0.622
0.5	0	present work	5.475	5.377	5.296	5.227	5.168	5.114	5.072	5.033	4.999	4.969	4.94
		[26]						5.117					
	0.01	present work	5.128	4.942	4.752	4.554	4.34	4.106	3.853	3.578	3.283	2.974	2.655
	0.05	present work	4.09	3.732	3.37	3.005	2.645	2.296	1.965	1.659	1.384	1.141	0.932
	0.1	present work	3.265	2.858	2.471	2.109	1.777	1.48	1.219	0.994	0.803	0.645	0.514
0.8	0	present work	4.716	4.619	4.541	4.477	4.423	4.375	4.337	4.303	4.272	4.246	4.222
		[26]						4.377					
	0.01	present work	4.433	4.266	4.102	3.933	3.753	3.557	3.345	3.114	2.865	2.601	2.329
	0.05	present work	3.575	3.267	2.957	2.646	2.337	2.035	1.747	1.479	1.236	1.02	0.834
	0.1	present work	2.878	2.527	2.193	1.878	1.588	1.326	1.094	0.893	0.723	0.58	0.462

$U^* = 0$

R^*	Br		Flow index, n										
			0.5	0.6	0.7	0.8	0.9	1.0	1.1	1.2	1.3	1.4	1.5
0.2	0	present work	8.602	8.581	8.558	8.535	8.513	8.485	8.473	8.454	8.437	8.422	8.407
		[20]	8.618	8.598	8.576	8.553	8.531	8.509	8.49	8.471	8.455	8.439	8.424
	0.01	present work	8.446	8.374	8.291	8.194	8.084	7.951	7.81	7.64	7.445	7.22	6.963
	0.05	present work	7.875	7.639	7.370	7.066	6.728	6.353	5.949	5.516	5.063	4.596	4.126
	0.1	present work	7.262	6.884	6.472	6.029	5.561	5.078	4.584	4.094	3.616	3.16	2.734
0.5	0	present work	6.286	6.259	6.236	6.215	6.196	6.177	6.165	6.152	6.139	6.128	6.119
		[20]	6.293	6.266	6.242	6.22	6.202	6.185	6.17	6.156	6.144	6.134	6.124
	0.01	present work	6.189	6.138	6.085	6.028	5.966	5.895	5.819	5.73	5.627	5.508	5.371
	0.05	present work	5.829	5.696	5.548	5.382	5.196	4.986	4.754	4.498	4.219	3.921	3.608
	0.1	present work	5.433	5.226	4.997	4.746	4.473	4.18	3.868	3.545	3.214	2.883	2.558
0.8	0	present work	5.683	5.654	5.63	5.61	5.593	5.576	5.565	5.554	5.544	5.535	5.527
		[20]	5.689	5.659	5.634	5.613	5.596	5.581	5.568	5.556	5.546	5.536	5.528
	0.01	present work	5.599	5.551	5.504	5.456	5.404	5.346	5.285	5.214	5.131	5.036	4.927
	0.05	present work	5.286	5.174	5.051	4.915	4.763	4.591	4.4	4.188	3.955	3.703	3.435
	0.1	present work	4.942	4.769	4.58	4.373	4.147	3.902	3.639	3.362	3.074	2.782	2.492

$U^* = 1$

R^*	Br		Flow index, n										
			0.5	0.6	0.7	0.8	0.9	1.0	1.1	1.2	1.3	1.4	1.5
0.2	0	present work	9.217	9.281	9.332	9.375	9.409	9.432	9.463	9.484	9.502	9.518	9.532
		[26]						9.447					
	0.01	present work	9.45	9.559	9.664	9.771	9.884	10	10.15	10.31	10.5	10.73	11.01
	0.05	present work	10.51	10.86	11.27	11.76	12.38	13.18	14.28	15.82	18.13	21.9	29.1
	0.1	present work	12.23	13.09	14.21	15.78	18.11	21.89	29.12	47.7	196.3	-72.66	-27.64
0.5	0	present work	7.289	7.363	7.424	7.476	7.519	7.554	7.59	7.618	7.643	7.666	7.686
		[26]						7.559					
	0.01	present work	7.413	7.511	7.601	7.686	7.77	7.853	7.946	8.044	8.153	8.276	8.419
	0.05	present work	7.954	8.168	8.399	8.66	8.966	9.328	9.785	10.36	11.12	12.14	13.62
	0.1	present work	8.753	9.17	9.669	10.29	11.1	12.19	13.77	16.19	20.38	29.22	59.61
0.8	0	present work	6.96	7.042	7.113	7.172	7.224	7.266	7.308	7.342	7.373	7.4	7.425
		[26]						7.269					
	0.01	present work	7.057	7.158	7.25	7.336	7.418	7.496	7.58	7.666	7.757	7.857	7.969
	0.05	present work	7.474	7.662	7.859	8.071	8.31	8.582	8.911	9.307	9.800	10.43	11.27
	0.1	present work	8.071	8.402	8.78	9.228	9.78	10.48	11.42	12.71	14.61	17.68	23.36